Intercollegiate Faculty of Biotechnology
University of Gdańsk and Medical University of Gdańsk

M.Eng. Sara Mikac

Identification of a novel, transcription-independent role of Nrf2 in lung cells

Identyfikacja nowej roli białka Nrf2, niezależnej od regulacji transkrypcji, w komórkach płuca

Thesis submitted to the Board of the Discipline of Biological Sciences of the University of Gdańsk in order to be awarded a doctoral degree in the field of exact and natural sciences in the discipline of biological sciences.

Promotor: Prof. Robin Fahraeus
Assistant promotor: Dr Alicja Sznarkowska

PhD thesis completed in the International Centre for Cancer Vaccine Science

Gdańsk 2022

This research was funded by the International Research Agenda's Program of the Foundation for Polish Science (MAB/2017/03), the Polish National Science Center PRELUDIUM9 grant No. 2015/17/N/NZ3/03773 and UGrants Advanced nr 533-0B00-GA08-22.

The data presented in this PhD thesis was published in the following scientific articles:

- Mikac S., Rychłowski M., Dziadosz A., Szabelska-Beresewicz A., Fahraeus R., Hupp T., Sznarkowska A. Identification of a Stable, Non-Canonically Regulated Nrf2 Form in Lung Cancer Cells. Antioxidants 2021; 10(5): 786. DOI: 10.3390/antiox10050786.

- Mikac S., Dziadosz A., Padariya M., Kalathiya U., Fahraeus R., Marek-Trzonkowska N., Chruściel E., Urban-Wójciuk Z., Papak I., Arcimowicz Ł., Marjanski T., Rzyman W., Sznarkowska A. Keap1-resistant ΔN-Nrf2 isoform does not translocate to the nucleus upon electrophilic stress (submitted; preprint https://doi.org/10.1101/2022.06.10.495609)

Acknowledgements

At the end of this PhD adventure, I would like to thank my supervisors Prof. Robin Fahraeus and Dr Alicja Sznarkowska for all the support and the knowledge they shared with me. I am profoundly thankful on their encouragement and everyday motivation.

I am very thankful to all the collaborators (Cancer Immunology group at ICCVS, Dr Michał Rychłowski, Dr Alicja Szabelska-Beresewicz, Dr Monikaben Padariya, Dr Umesh Kalathiya, Prof Eric Kmiec and Pawel Bialk from Christiana Care Health System and Dr Andrea Lipinska and Magda Wachalska from the Department of Virus Molecular Biology) and to the ICCVS staff, for the help and support during these challenging four years.

I would also like to thank my colleagues in the lab for every advice, scientific and non-scientific discussion. It was great to have so many young and inspiring people around me on everyday basis.

Finally, I would like to thank my fiancé, family and friends for always believing in me, for their unconditional love and support, which always led me forward.

TABLE OF CONTENTS

Abstract

The transcription factor Nrf2 is recognized for its pro-survival and cell-protective role upon exposure to different types of extrinsic and intrinsic insults. It controls a number of cellular processes such as proliferation, differentiation, apoptosis, autophagy, protein homeostasis and amino acids metabolism. Under no-stress conditions, the level of Nrf2 is low since it is constantly degraded by Keap1-Cul3-E3 ubiquitin ligase pathway. However, when the regulation of Nrf2 is imbalanced (e.g. via oncogene activation or mutations), it becomes constitutively active promoting carcinogenesis, metastasis and radio- and chemoresistance. Transient activation of Nrf2 in normal cells is protective, however, constitutive activation as seen in cancer, enhances the survival and progression of cancer cells. Since oncogenic and immune pathways are interconnected, my PhD project investigated the impact of Nrf2 on the expression of major histocompatibility complex class I (MHC-I) molecules, which present self and non-self peptides to the immune cells. In the course of the project we have also identified the stable, non-canonically regulated Nrf2 which does not play a transcription factor role.

In the first part of the project, we have shown that Nrf2 knockdown in both, normal lung fibroblasts and the non-small cell lung cancer cell line A549, reduced intracellular and cell surface MHC-I molecules levels, but not their transcript levels. Inhibition of translation with emetine revealed that Nrf2 stabilizes MHC-I in cells, while labeling of freshly synthesized proteins with Click-iT chemistry indicated that Nrf2 could also affect their synthesis. Immunoprecipitation studies together with molecular modeling and molecular dynamics simulations showed that Nrf2 binds to MHC-I and stabilizes it in cells.

The second part of the thesis focuses on the identification and characterization of the stable, non-canonically regulated Nrf2 isoform (named ΔN-Nrf2) that is abundantly expressed in the lung cells. This form originates from the alternatively transcribed *NFE2L2* transcripts and is not degraded via Keap1-Cul3-mediated pathway. Compared to the full-length Nrf2, ΔN-Nrf2 has a deletion of the first 16 amino acids causing the impairment of the Keap1 binding. ΔN-Nrf2 is localized in the cytoplasm under homeostatic conditions and upon exposure to electrophilic stress, therefore it does not play a transcription factor role.

Altogether these results point to the new function of Nrf2 in cells, which relies on the protein-protein interaction.

Streszczenie

Czynnik transkrypcyjny Nrf2 pełni rolę pro-przyżyciową i ochronną po ekspozycji komórek na bodźce stresowe wewnątrz- i zewnątrzkomórkowe. Nrf2 zawiaduje szeregiem komórkowych procesów takich jak proliferacja, różnicowanie, apoptoza, autofagia, homeostaza czy metabolizm aminokwasów. W warunkach braku stresu, poziom Nrf2 w komórkach jest niski ze względu na konstytutywną degradację przez kompleks E3 ligazy ubikwityny Keap1-Cul3. Jednak jeśli ścieżka Nrf2 ulega rozregulowaniu (w przypadku aktywacji onkogenów albo mutacji), czynnik transkrypcyjny staje się konstytutywnie aktywny i promuje kancerogenezę, przerzutowanie oraz chemowrażliwość nowotworów. Przejściowa aktywacja Nrf2 w komórkach prawidłowych działa więc protekcyjnie, podczas gdy ciągła aktywność podtrzymuje proliferację komórek nowotworowych. Ze względu na to, że ścieżki onkogenne oraz odpowiedzi immunologicznej są ze sobą powiązane, w projekcie doktorskim badałam czy Nrf2 ma wpływ na ekspresję cząsteczek głównego układu zgodności tkankowej klasy I (ang. Major Histocompatibility Complex class I, MHC-I), które prezentują ‘swoje’ i ‘obce’ antygeny komórkom układu immunologicznego. Projekt doprowadził również do identyfikacji stabilnej izoformy Nrf2, regulowanej na drodze nie-kanonicznej, która nie pełni roli czynnika transkrypcyjnego.

W pierwszej części projektu pokazaliśmy że knockdown Nrf2 w normalnych fibroblastach płuca oraz w linii niedrobnokomórkowego raka płuca A549 zredukował zarówno całkowitą ilość MHC-I, jak i poziom MHC-I na powierzchni komórek. Ilość transkryptów MHC-I nie uległa jednak obniżeniu. Inhibicja translacji przy użyciu emetyny wykazała, że Nrf2 stabilizuje MHC-I w komórkach, natomiast znakowanie świeżo syntetyzowanych białek w reakcji ‘Click chemistry’ wskazuje że Nrf2 może również promować translację MHC-I. Immunoprecypitacja wraz z modelowaniem molekularnym i dynamiką molekularną wskazują że Nrf2 wiąże się do cząsteczek MHC-I i stabilizuje je w komórce.

Druga część pracy koncentruje się na identyfikacji i charakterystyce stabilnej i niekanonicznie regulowanej izoformy Nrf2, nazwanej ΔN-Nrf2, która ulega ekspresji w komórkach prawidłowych i nowotworowych. Forma ta powstaje na skutek transkrypcji z alternatywnego promotora i nie ulega konstytutywnej degradacji przez kompleks Keap1-Cul3. W porównaniu do białka Nrf2 o pełniej długości, ΔN-Nrf2 jest pozbawiona pierwszych szesnastu aminokwasów, co zaburza wiązanie z Keap1. ΔN-Nrf2 lokalizuje się w cytoplazmie zarówno w warunkach homeostazy, jak i w odpowiedzi na stres elektrofilowy, co wskazuje na to, że nie pełni funkcji czynnika transkrypcyjnego.

Podsumowując, uzyskane w pracy wyniki wskazują na nową funkcję Nrf2 w komórkach, która nie zależy od regulacji transkrypcji i opiera się na interakcji białko-białko.

ABBREVIATIONS

ABCG5	ATP-binding cassette g5
ABCG8	ATP-binding cassette g8
AKRs	Aldo-keto reductases
ALDH1	Aldehyde dehydrogenase 1
AMPK	AMP-activated protein kinase
ARE	Antioxidant response elements
ATF6	Activating transcription factor 6
ATG	Autophagy-related
BCRP	Breast cancer resistant protein
B-Raf	V-raf murine sarcoma viral oncogene homolog B1
BRCA1	Breast Cancer Type 1 Susceptibility Protein
BTB	Broad Complex/Tramtrack/Bric-a-brac
bZIP	Basic leucine zipper
CALCOCO2	Calcium-binding and coiled-coil domain-containing protein 2
CAT	Catalase
CBRs	Carbonyl reductases
C-MYC	C-myelocytomatosis oncogene
CNC	Cap ‘N’ Collar
CTR	C-terminal region
CYPs	Cytochrome P450 oxidoreductases
Cul3	Cullin 3
Cys	Cysteine
DGR	Double-glycine repeat
DPP3	Dipeptidyl peptidase 3
EGFR	Epidermal Growth Factor Receptor
EpRE	Electrophile response elements
ER	Endoplasmic reticulum
ERK	Extracellular signal-regulated kinase
G6PD	Glucose-6-phosphate dehydrogenase
GCL	Glutamate-cysteine ligase
GSH	Glutathione antioxidant system
GSK3	Glycogen synthase kinase-3
GSS	Glutathione synthetase
GSTs	Glutathione S-transferases
HLA	Human Leukocyte Antigens
HO-1	Heme oxygenase-1
HRD1	HMG-CoA reductase degradation protein 1
IDH1	Isocitrate dehydrogenase 1
IFN-γ	Interferon gamma
IL	Interleukin
IRE1α	Inositol-requiring protein 1α
IVR	Intervening region
JNK	c-Jun NH2-terminal kinase
KIR	Keap1-interacting region
KRAS	Kirsten rat sarcoma virus
Lys	Lysine
MAPK	Mitogen-Activated Protein Kinase
MAVS	Mitochondrial antiviral signaling
MDR	Multidrug resistance-associated proteins
MDSCs	Myeloid-derived suppressor cells
ME1	Malic enzyme 1

MHC	Major histocompatibility complex
miRNA	microRNA
NFE2L2	Nuclear factor erythroid 2 related factor 2 gene
NES	Nuclear export signal
Neh	Nrf2-embedded contact homology
NLS	Nuclear localization signal
NQO1	NAD(P)H quinone oxidoreductase 1
NRF-1	Nuclear respiratory factor-1
NSCLC	Non-small cell lung cancer
NTR	N-terminal region
PALB2	Partner and Localizer of BRCA2
PERK	Double-stranded RNA-activated protein kinase-like endoplasmic reticulum kinase
PGC-1a	Peroxisome proliferator activated receptor gamma co-activator 1 alpha
PIK3CA	Phosphatidylinositol-4,5-Bisphosphate 3-Kinase Catalytic Subunit Alpha
PKC	Protein kinase C
PPP	Pentose phosphate pathway
PSM	Proteasome Subunit
PTEN	Phosphatase And Tensin Homolog
ROS	Reactive oxygen species
RXRα	Retinoic X receptor α
SDS-PAGE	Sodium dodecyl-sulfate polyacrylamide gel electrophoresis
Ser	Serine
sMAF	Small musculoaponeurotic fibrosarcoma
SOD1	Superoxide dismutase 1
SQSTM1	Sequestosome 1
STING	Stimulator of Interferon genes
STK11	Serine/Threonine Kinase 11
TFBM2	Mitochondrial transcription factor B2
Thr	Threonine
TXN	Thioredoxin antioxidant system
Tyr	Tyrosine
UGT	UDP-glucuronosyltransferase
ULK1	Uncoordinated-51-like kinases 1
UPR	Unfolded protein response
UTR	untranslated region
WTX	Wilms tumour gene on X chromosome
β-TrCP	β-transducin repeat-containing protein

LIST OF FIGURES

LIST OF TABLES

CHAPTER 1

Introduction

1.1. The transcription factor Nrf2

1.1.1. Structure and role of Nrf2

All living beings are constantly exposed to environmental stresses. Organisms respond and adapt to the different types of stresses through defined regulatory mechanisms to maintain homeostasis. The transcription factor nuclear factor erythroid 2 (NF-E2)-related factor 2 (Nrf2) is a major regulator of cellular xenobiotic and oxidative stress responses. Nrf2 was first discovered in 1994 as a member of the human Cap 'N' Collar (CNC) family that contains a conserved basic leucine zipper (bZIP) structure, for the transcriptional stimulation of beta-globin genes (1). It activates the cellular antioxidant response by inducing transcription of a wide array of genes that are able to protect the cells from extrinsic and intrinsic insults, such as xenobiotics and oxidative stress. Nrf2 has been shown to protect against various diseases, e.g. neurodegenerative diseases, cardiovascular diseases, inflammation, acute pulmonary injury and cancer (2–6). Recent studies have revealed new functions of Nrf2, beyond its redox-regulating capabilities, including regulation of inflammation, autophagy, metabolism, proteostasis, and unfolded protein response (UPR), particularly in the context of carcinogenesis (7–11). Therefore, Nrf2 has become a prime target of research involving cancer prevention and treatment (12).

The main mechanism to control Nrf2 activity is by regulating its stability. Under homeostatic conditions, Nrf2 is constantly ubiquitinated by Keap1-Cul3-E3 ubiquitin ligase system and targeted for degradation. In response to oxidative stress, Nrf2 is liberated from Keap1-mediated degradation, resulting in its translocation to the nucleus and activation of the transcription of its target genes (13). Another mechanism to activate Nrf2 involves post-translational modifications, such as phosphorylation, but does not affect its stability (14–18).

Nrf2 is a 605 amino acid protein that consists of seven highly conserved functional domains, Neh1-Neh7. The major regulatory domain is the Neh2 domain, located at the N-terminus of Nrf2, and contains two sites (ETGE and DLG motifs) that interact with Keap1, a negative regulator of Nrf2 that controls its stability (19,20). Neh2 also contains seven lysine residues responsible for ubiquitin conjugation (21). The Neh1 domain allows Nrf2 to bind DNA and dimerize with other transcription factors through a CNC-type bZIP DNA-binding motif (1). Neh6 is a serine rich region that also regulates Nrf2 stability. It contains two binding sites (DSGIS

and DSAPGS motifs) for the β-transducin repeat-containing protein (β-TrCP) that can ubiquitinate Nrf2 (22–24). The Neh3-5 are included in transactivation by binding to different components of transcriptional apparatus (25,26). Interestingly, Neh7 domain is interacting with the DNA-binding domain of retinoic X receptor α, causing the repression of Nrf2 and inhibition of Nrf2 target genes expression (27) (Fig. 1).

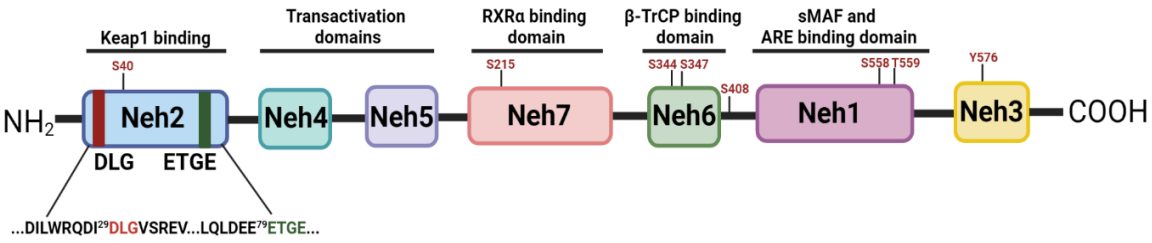

Figure 1**. Domain structure of Nrf2.** Nrf2 is a 605 amino acid protein that consists of seven highly conserved functional domains. Neh1 domain is responsible for dimerization with sMAF proteins and binding to the ARE-sequences in DNA. Neh2 domain consist of two Keap1 binding motifs (DLG ad ETGE) and seven ubiquitin residues for targeting of Nrf2 for proteosomal degradation. Neh3 is needed for transcriptional activation, while Neh4 and 5 are transactivation domains that can bind different activators or repressors. Neh6 domain regulates Nrf2 stability by binding to β-TrCP and finally, Neh7 can interact with Nrf2 repressor, RXRα. Phosphorylation of Nrf2 residues is marked in red. Created with Biorender.com.

1.2. Regulation of Nrf2

Nrf2 is primarily regulated by Keap1 (Kelch like erythroid cell-derived protein with CNC homology [ECH]-associated protein 1), a substrate adaptor for a Cullin3-containing E3 ubiquitin ligase. It belongs to the BTB-Kelch protein family and contains two common canonical domains: BTB domain (Broad Complex/Tramtrack/Bric-a-brac) and a Kelch domain (domain present in Kelch proteins). Keap1 consists of five regions: an N-terminal region (NTR), the BTB domain, an intervening region (IVR), a double-glycine repeat (DGR) domain and the C-terminal region (CTR); DGR and C-terminal domains form a Kelch domain (28) (Fig. 2). The N-terminal BTB domain, named after the *Drosophila* proteins in which it was first identified (29), is required for the homodimerization of Keap1 and interaction with Cullin 3 (Cul3) (30). The Kelch/DGR domain interacts with Neh2 domain of Nrf2. It contains several

cysteine (Cys) residues involved in ROS stress sensing (31). The IVR region is rich with highly reactive Cys residues, as a consequence of the positively charged environment of basic amino acids K131, R135, K150 and H154 near to the Cys-rich region (32). Interestingly, human Keap1 has up to 27 Cys, a twice more than the average human protein (28), which makes it highly responsive to the oxidative stress (33).

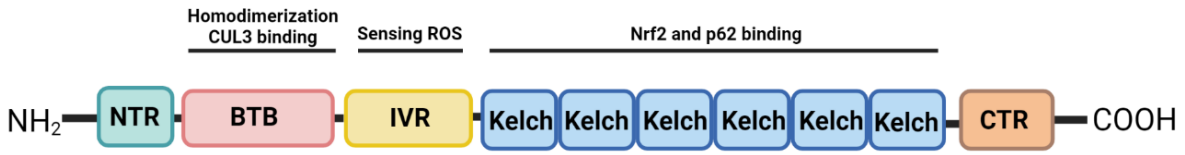

Figure 2. **Domain structure of Keap1.** Keap1 protein contains five conserved regions: N-terminal region, BTB responsible for Keap1 homodimerization and Cul3 binding, IVR region which is a cysteine rich domain and direct redox sensor, DGR/Kelch region which consists of 6 repeats of Kelch motif for binding of Nrf2 and p62, and C-terminal region. ROS, reactive oxygen species. Created with Biorender.com.

1.2.1. Keap1-dependent regulation of Nrf2

The Nrf2-Keap1 is a major cell defense and survival pathway. Detailed mechanistic studies indicate that Keap1 is the molecular switch that controls activation and inactivation of Nrf2. A two-site substrate recognition/hinge and latch model, consisting of two amino-terminal motifs, DLG and ETGE, promote efficient ubiquitination and rapid turnover. Under homeostatic conditions, the rapid turnover prevents unnecessary activation of Nrf2 target genes (34). Nrf2 degradation is mediated by the Keap1-Cul3 adaptor-substrate recognition system whereby two Neh2 recognition motifs (low affinity-DLG and high-affinity ETGE) of a Nrf2 monomer bind to Keap1 homodimer with different affinities (35). Therefore, the structural integrity of both ETGE (Hinge) and DLG (Latch) is crucial for a tightly controlled Nrf2 turnover (Fig. 3) (35).

In response to oxidative stress or chemopreventive compounds, cysteine residues on Keap1 are modified causing structural changes and the inability to bind Nrf2 via both Neh2 recognition motifs (Fig. 3). The modifications of Keap1 cysteine residues are affecting the ubiquitination activity of the Keap1-Cul3-E3 ligase complex, however they are not causing the complete dissociation between Nrf2 and Keap1 and subsequent accumulation of Nrf2 in the nucleus. The impairment of Keap1-mediated proteasomal degradation of Nrf2 allows *de novo*

synthesized Nrf2 protein to translocate to the nucleus, where it dimerizes with small musculoaponeurotic fibrosarcoma (sMAF) proteins and activates the transcription of the antioxidant/electrophile response elements (ARE/EpRE)-containing genes (34). The ARE/EpRE are cis-acting DNA enhancer sequences (the consensus sequence: 5'-RTGABnnnGCR-3' ("n", any nucleotide)) (13). The promoter region of *NFE2L2* gene also contains an ARE-sequence, providing a possible positive feedback loop.

Target genes of Nrf2 have been identified by gene expression profiling in Nrf2 knockout (Nrf2 $^{-/-}$) mice (36,37) including antioxidant enzymes, such as heme oxygenase-1 (HO-1); detoxification enzymes, including NAD(P)H quinone oxidoreductase 1 (NQO1) and glutathione S-transferases (GSTs) as well as glutamate-cysteine ligase (GCL) subunits involved in glutathione (GSH) synthesis and metabolism.

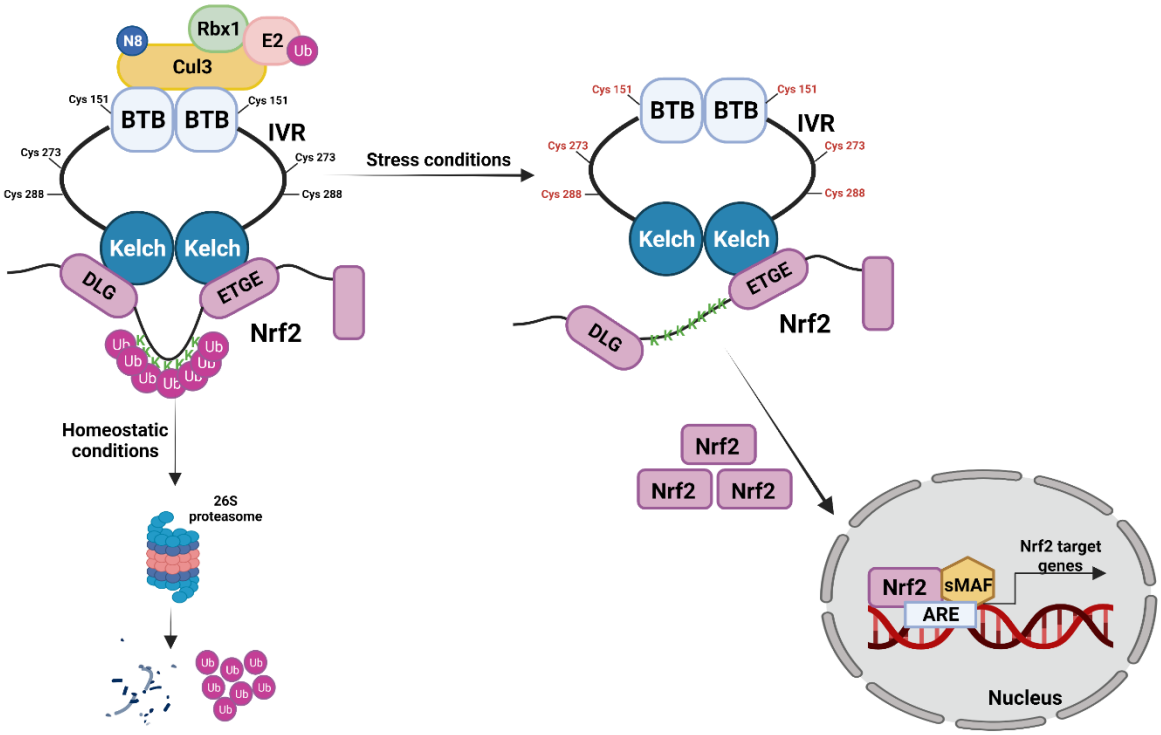

Figure 3. **The Nrf2-Keap1 signaling pathway.** Under homeostatic conditions, Nrf2 is bound to the KELCH domains of Keap1, ubiquitinated and degraded by proteasome. Upon stress, cysteine residues on Keap1 are modified, causing the liberation of Nrf2 from Keap1-mediated degradation. After the electrophilic exposure, *de novo* synthesized Nrf2 is accumulated and translocated to the nucleus, where it actives the transcription of its target genes. Created with Biorender.com.

In addition, Keap1-dependent but cysteine-independent mechanisms can interfere with formation of the Nrf2-Keap1 complex and consequently stabilize Nrf2. Autophagy cargo-adaptor p62/sequestosome 1 (SQSTM1) (38–40), dipeptidyl peptidase 3 (DPP3) (41), Wilms tumour gene on X chromosome (WTX) (42), and Partner and Localizer of BRCA2 (PALB2) (43), all contain Keap1-interacting region (KIR)-like ETGE motifs and thus compete with Nrf2 for Keap1 binding. p62 contains an STGE motif that mimics the ETGE motif upon phosphorylation of the serine residues and thus it can compete with Nrf2 for Keap1 binding (44). p62 sequesters Keap1 into the autophagosome which causes releasing of Nrf2 from Keap1-mediated degradation and its prolonged activation (40,45). p21Cip1/WAF1 (46) and Breast Cancer Type 1 Susceptibility Protein (BRCA1) (47) can also interact with ETGE motif of Nrf2 and compete with Keap1 for Nrf2 binding, while the acetyltransferase p300 interferes Nrf2-Keap1 interaction, resulting in Nrf2 stabilization and translocation to the nucleus (48).

1.2.2. Alternative degradation pathways of Nrf2

There are also alternative pathways for degradation of Nrf2 reported, including β-transducin repeat-containing protein (β-TrCP) that binds Nrf2 via Neh6 domain. In contrast to KEAP1-CUL3-RBX1 mediated degradation under basal conditions, β-TrCP-SKP1-CUL1-RBX1 mediated degradation can lead to the Nrf2 degradation under both basal and oxidative stress conditions, independent of Keap1 (24,49,50). β-TrCP can recognize two Nrf2 motifs, DSGIS and DSAPGS in the Neh6 domain. Phosphorylation of the DSGIS motif by Glycogen synthase kinase-3 (GSK3) increases the affinity of β-TrCP for Nrf2, which consequently stimulates Nrf2 ubiquitination and degradation (24,49,51). GSK3 can be inhibited by phosphorylation of an N-terminal serine residue (Ser9 in GSK-3β and Ser21 GSK-3α, respectively) by protein kinase B (PKB)/AKT, leading to the suppression of β-TrCP-mediated degradation of Nrf2 (49).

Another protein involved in Keap1-independent Nrf2 degradation is the HMG-CoA reductase degradation protein 1 (HRD1), which interacts with Neh4 and 5 domains of Nrf2 and triggers Nrf2 degradation under endoplasmic reticulum stress (52). Recently, another E3 ligase of Nrf2, the Cullin4/damaged DNA binding protein-1/WD Repeat Domain 23 (CUL4/DDB1/WDR23) was identified. WDR23 is a WD40-repeat protein that binds to the DIDLID sequence within the Neh2 domain of Nrf2 and regulates its ubiquitination and degradation (50).

1.2.3. Alterations in Nrf2-Keap1 pathway

Cancer-associated mutations in *NFE2L2* (the Nrf2 gene) and *KEAP1* cause dysfunctionality in the protection against various insults. Gain-of-function mutations in *NFE2L2* gene and loss-of-function mutations in the *KEAP1* gene are found in a subset of advanced cancers of the lung, liver, esophagus, bladder and other organs, but lung cancer has the highest frequency of *NFE2L2* or *KEAP1* alterations (31). Adenomatous and squamous lung tumors show recurrent mutations in *KEAP1*, an adaptor protein that recruits the Cul3 ubiquitin ligase to the transcription factor Nrf2, while Nrf2 is frequently mutated in squamous tumors (35,53). The systematic analysis of the *KEAP1* genomic locus in lung cancer patients and cell lines revealed deletion, insertion and missense mutations in functionally important domains of *KEAP1*. Moreover, a very high percentage of loss of heterozygosity at 19p13.2 was identified, suggesting that biallelic inactivation of *KEAP1* in lung cancer is a common event (54). Shibata et al. identified gain-of-function mutations of *NFE2L2* in approximately 11% of lung cancer, while constitutive activation of Nrf2, caused by *NFE2L2* or *KEAP1* mutations, occurs in >20% of lung cancer cases (35,54–56). *NFE2L2* point mutations surrounding the high-affinity binding site with Keap1-ETGE result in complete loss of Keap1 interaction with Nrf2, while mutations in the lower affinity binding site DLG vary in the ability to disrupt binding of Nrf2 to Keap1 (35,53,57). It is important to highlight that other mutated genes that contribute to cancer development (*EGFR, TP53, KRAS, PTEN and PIK3CA*) correlate with some *NFE2L2/KEAP1* mutations. Mutations in *NFE2L2* usually co-occur with *PI3KCA* and *TP53* mutations (58,59), while *KEAP1* mutations co-occur with *K-RAS* and *STK11* mutations (60,61).

Additionally, deletion of exon 2 and/or exon 2 and 3 in *NFE2L2* gene increases the activity of Nrf2 by removing the Keap1 interaction site, while keeping the gene functionality intact (53).

1.2.4. Keap1-independent regulation of Nrf2

Keap1 cysteine modifications, that result in Nrf2 stabilization, are the main mechanism for Nrf2-Keap1 pathway activation. However, post-translational modifications of Nrf2 play an important role in the activity and localization of Nrf2. Phosphorylation is the predominant modification at different Nrf2 residues, including Ser40, Ser215, Ser344, Ser347, Ser408, Ser558, Thr559 and Tyr576 (Fig. 1). There are different effects on Nrf2 activity depending on the phosphorylation site. Various kinases activate Nrf2-Keap1 pathway, including protein kinase C (PKC) via direct phosphorylation of Nrf2 at Ser40. Phosphorylation of Nrf2 at Ser40 and at Ser558 leads to Nrf2 nuclear translocation and activation (16–18,62). However,

phosphorylation of Tyr576, Ser344 and Ser347 leads to the Nrf2 degradation and reduces transcriptional activity (63,64). Moreover, Tyr576 is located in the nuclear export signal (NES) region and regulates nuclear export and degradation (64). Also, double-stranded RNA-activated protein kinase-like endoplasmic reticulum (ER) kinase (PERK) phosphorylates Nrf2 and causes its accumulation in the nucleus (65). Furthermore, some of the MAP kinases, like p38 MAPK, c-Jun NH2-terminal kinase (JNK), extracellular signal-regulated kinase (ERK) and phosphatidylinositol 3-kinase (PI3K) are also playing a role in Nrf2 activation (14,66,67), even though the mechanism still has to be established.

Acetylation also has a regulatory role in Nrf2 localization and mainly occurs at lysine residues in Neh1 and Neh3 domains, where NES and nuclear localization signal (NLS) are located. Furthermore, Sun et al. showed acetylation of multiple lysine residues (Lys438, Lys443, Lys445, Lys533, Lys536, Lys538) within the Neh1 domain and their role in binding of Nrf2 to the ARE promoter (68). Moreover, acetylation sites Lys596 and Lys599 were found to increase nuclear localization of Nrf2, while deacetylation of Nrf2 enhanced cytoplasmic localization (69).

1.3. The role of transcription factor Nrf2

1.3.1. Nrf2 regulates stress response and drug detoxification

Nrf2 induces the transcription of ARE-containing genes in response to oxidative/xenobiotic stress, which leads to the increased expression of phase I, II and III detoxification enzymes (Fig. 4). Phase I enzymes are catalyzing the oxidation, reduction and hydrolytic reactions of xenobiotics, including NQO1 (NAD(P)H quinone dehydrogenase 1), carbonyl reductases (CBRs), aldo-keto reductases (AKRs), and aldehyde dehydrogenase 1 (ALDH1), and certain cytochrome P450 oxidoreductases (CYPs) (70). Phase II enzymes, such as glutathione S-transferase (GST), UDP-glucuronosyltransferase (UGT), UDP-glucuronic acid synthesis enzymes and heme oxygenase 1 (HO-1) are catalyzing the conjugation reactions (70,71). Phase III enzymes are mainly drug efflux transporters, such as multidrug resistance-associated proteins (MDR), breast cancer resistant protein (BCRP), ATP-binding cassette g5 (ABCG5) and g8 (ABCG8) (70).

Nrf2 controls the expression of glutathione (GSH) and thioredoxin (TXN) antioxidant system. It regulates GSH levels by controlling the expression of the glutamate-cysteine ligase catalytic (GCLC) and modulator (GCLM) subunits as well as glutathione synthetase (GSS), which are all components involved in the GSH synthesis (11). Through the coordinated activation of GSH

production, utilization and regeneration, Nrf2 maintains the intracellular levels of reduced GSH (72). In addition, Nrf2 regulates the expression of thioredoxin, thioredoxin reductase, sulfiredoxin, peroxiredoxin, glutathione peroxidase, superoxide dismutase 1 (SOD1), catalase (CAT), and several glutathione S-transferases, which are the enzymes essential for the elimination of the reactive oxygen species (11). Therefore, Nrf2 protects the cells against different extrinsic and intrinsic insults by inducing the transcription of these cytoprotective genes. It is also important for the protection against different diseases like cardiovascular diseases, metabolic syndrome, autoimmune disorders and cancer, that have oxidative stress as a underlying pathological feature (12).

1.3.2. Nrf2 regulates protein homeostasis

A functional proteome is of crucial importance for all cells and organisms. Therefore, cells invest in an extensive network of factors that coordinate protein synthesis, folding, localization, modification and degradation, to maintain protein homeostasis (proteostasis) (73). Protein-folding stress at the endoplasmic reticulum (ER) is a feature of many human diseases, including cardiovascular disease, metabolic syndrome, cancer, and neurodegenerative disease (12). Accumulation of misfolded proteins leads to ER stress and activates the homeostatic signaling network, UPR, that orchestrates the recovery of ER function (74). Activation of the UPR is mediated by the stress sensors protein kinase RNA-like ER kinase (PERK), inositol-requiring protein 1α (IRE1α) and activating transcription factor 6 (ATF6) (74). Activation of Nrf2 during the UPR occurs via extensive production of ROS from mitochondria and ER or via PERK phosphorylation of Nrf2 (65). Nrf2 can also form a heterocomplex with ATF4, inducing the transcription of the genes responsible for the survival under proteotoxic stress (7).

The 26S proteasome degrades misfolded proteins and Nrf2 has been shown to increase proteasome activity by inducing the transcription of multiple subunits of the 20S proteasome, including PSMA1, PSMA4, PSMB3, PSMB5, and PSMB6, as well as 19S proteasome subunits PSMC1, PSMC3, and PSMD14 (9).

1.3.3. Nrf2 regulates autophagy

Autophagy is a quality control mechanism that degrades and recycles cellular components, including damaged organelles, long-lived proteins or misfolded proteins. A main role of autophagy is the maintenance of cellular homeostasis and protection against oxidative or

proteotoxic stress (75). It is also important for elimination of intracellular pathogens, in antigen presentation and in maintaining cellular longevity (76,77). Similarly to Nrf2, autophagy plays a dual role in cancer and impaired autophagic function was shown to contribute to the cancer development, while increased autophagic activity can help cancer cells to cope with proteotoxic and metabolic stress (78).

Nrf2 induces the expression of genes involved in autophagy initiation (*ULK1*), cargo recognition (*SQSTM1* and *CALCOCO2*), autophagosome formation (*ATG4D*, *ATG7* and *GABARAPL1*), elongation (*ATG2B* and *ATG5*), and autolysosome clearance (*ATG4D*), and therefore enhances autophagy (10). However, autophagy deficiency leads to the accumulation of oxidized protein and organelles, that can cause Nrf2 activation. Furthermore, the two pathways are linked by the autophagy adaptor protein p62. When autophagy is compromised, p62 sequesters Keap1 into aggregates and stabilizes Nrf2 (10).

1.3.4. Nrf2 regulates mitochondria homeostasis

The mitochondria provide the cell with the energy in the process called oxidative phosphorylation, which is closely linked to the production of ROS. In most of the cells, mitochondria and NADPH oxidase are the main sources of ROS, a common feature of many diseases, including neurodegeneration disorders, metabolic disorders, cardiovascular disease, and cancer (79).

As a part of its role as a regulator of cytoprotective genes, Nrf2 is involved in many aspects of mitochondrial physiology, including mitochondrial biogenesis, fatty acid oxidation, respiration, ATP production and redox homeostasis (12,80). Nrf2 activation increases the mitochondrial membrane potential, the availability of substrates for respiration and ATP production. It also positively regulates NADPH levels, by inducing the expression of genes encoding glucose-6-phosphate dehydrogenase (G6PD), the enzymes of the pentose phosphate pathway (PPP), malic enzyme 1 (ME1) and isocitrate dehydrogenase 1 (IDH1). Nrf2 deficiency was shown to negatively affect the mitochondrial fatty acid oxidation, respiration and ATP production, while Nrf2 activation maintains the integrity of mitochondrial DNA, which controls cell death and inflammation (81). By activating the nuclear respiratory factor-1 (NRF-1), which transcribes the key mitochondrial biogenesis factors transcription factor A, mitochondrial (TFAM) and transcription factor B2, mitochondrial (TFBM2), Nrf2 stimulates mitochondrial biogenesis program (82). Moreover, Nrf2 can affect the function of mitochondria, mostly through the regulation of the major regulator of mitochondrial function and biogenesis, peroxisome proliferator activated receptor gamma co-activator 1 alpha (PGC-1a) (83).

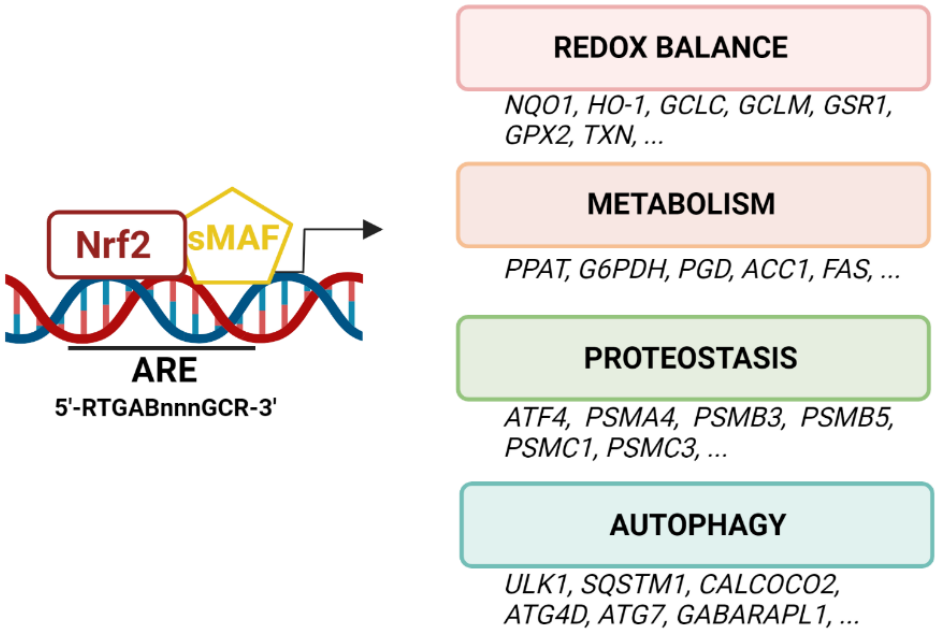

Figure 4. **Nrf2 is a master regulator of cytoprotective response.** Nrf2 heterodimerizes with sMAF proteins and binds to the genes containing ARE-sequences (5'-RTGABnnnGCR-3'). These genes participate in the maintaining of the cellular homeostasis, including redox balance; purine, pentose and lipid metabolism; proteostasis balance and autophagy regulation. ACC1, acetyl-coenzyme A carboxylase 1; ATF4, activating transcription factor 4; ATG, autophagy-related gene; CALCOCO2, calcium binding and coiled-coil domain 2; FAS, fatty acid synthase; G6PDH, glucose-6-phosphate dehydrogenase; GABARAPL1, gamma-aminobutyric acid receptor-associated protein-like 1GCLC, glutamate-cysteine ligase catalytic subunit; GCLM, glutamate-cysteine ligase modulator subunit; GPX2, glutathione peroxidase 2; GSR1, glutathione reductase 1; HO-1, heme oxygenase-1; NQO1, (NAD(P)H quinone dehydrogenase 1); PGD, phosphogluconate dehydrogenase; PPAT, phosphoribosyl pyrophosphate amidotransferase; PSMA, proteasome subunit a type; PSMB, proteasome subunit b type; PSMC, proteasome subunit c type; SQSTM1, sequestosome-1 TXN, thioredoxin; ULK1, unc-51 like autophagy activating kinase 1. Created with Biorender.com.

1.4. Dual role of Nrf2 in cancer

Nrf2 was initially regarded as a tumor inhibitor, thus providing the rationale of tumor prevention strategies using Nrf2 activators. However, this view was modified when it was recognized that deregulated Nrf2 activity can also promote cancer and favor a malignant phenotype. Accumulation of Nrf2 in cancer cells creates a protective environment against oxidative stress, chemotherapeutic agents, and radiotherapy (6,84). Although activation of Nrf2 has a protective role against various toxicants and diseases, the prolonged activation has been

shown to favor a progression of several types of cancers, such as lung, breast, head and neck, ovarian, and endometrial carcinomas (13,85–87). Cancer cells with the persistent activation of Nrf2 often develop ‘’Nrf2 addiction’’, defined as constitutive Nrf2 overexpression that maintains the malignant phenotype of cancer cells (88). There are several mechanisms by which the Nrf2 signaling pathway is constitutively activated in cancer cells: (1) somatic mutations in *KEAP1* or the *KEAP1*-binding domain, that disrupt binding of Nrf2 and Keap1; (2) epigenetic silencing of Keap1; (3) post-translational modification of Keap1 cysteines by succinylation; (4) accumulation of disruptor proteins such as p62, which leads to the dissociation of the Nrf2-Keap1 complex; (5) transcriptional induction of Nrf2 by oncogenic K-Ras, B-Raf and, c-Myc; and (6) miRNA targeting *NFE2L2* or 3’UTR of *KEAP1* mRNA (13,45,72,85–87,89,90) (Fig. 5).

High level of Nrf2 is a poor prognosis marker (91–93), partly due to Nrf2's ability to enhance cancer cell proliferation and promote chemoresistance and radioresistance. Nrf2 also supports aggressive cell proliferation through metabolic reprogramming, redirecting glucose and glutamine to synthesis pathways of purine nucleotides, glutathione and serine (87). It directly activates several genes involved in the pentose phosphate pathway by binding to their ARE-sequences. These proteins support glucose flux and generate purines, which are the building blocks of DNA and RNA, and are important for accelerating proliferation in cancer cells (13). Interestingly, Nrf2 is also a key signaling molecule that is activated in response to hypoxia and emerging evidence suggests that coordinated signaling through Nrf2 and hypoxia-inducible factor 1 (HIF-1) is critical for tumor survival and progression (94). Nrf2 is also regulating the basal expression of Mdm2, a direct inhibitor of tumor suppressor p53. Increased Nrf2 levels indirectly downregulate p53 and its apoptotic signals, leading to the cancer survival and progression (95).

Although studies with Keap1 knockout mice demonstrated that Nrf2 hyperactivity is advantageous for cancer progression, it was not sufficient for spontaneous cancer formation. Therefore, the hypothesis is that once tumor is initiated, cancer cells are using Nrf2-Keap1 pathway to acquire stress resistance (96).

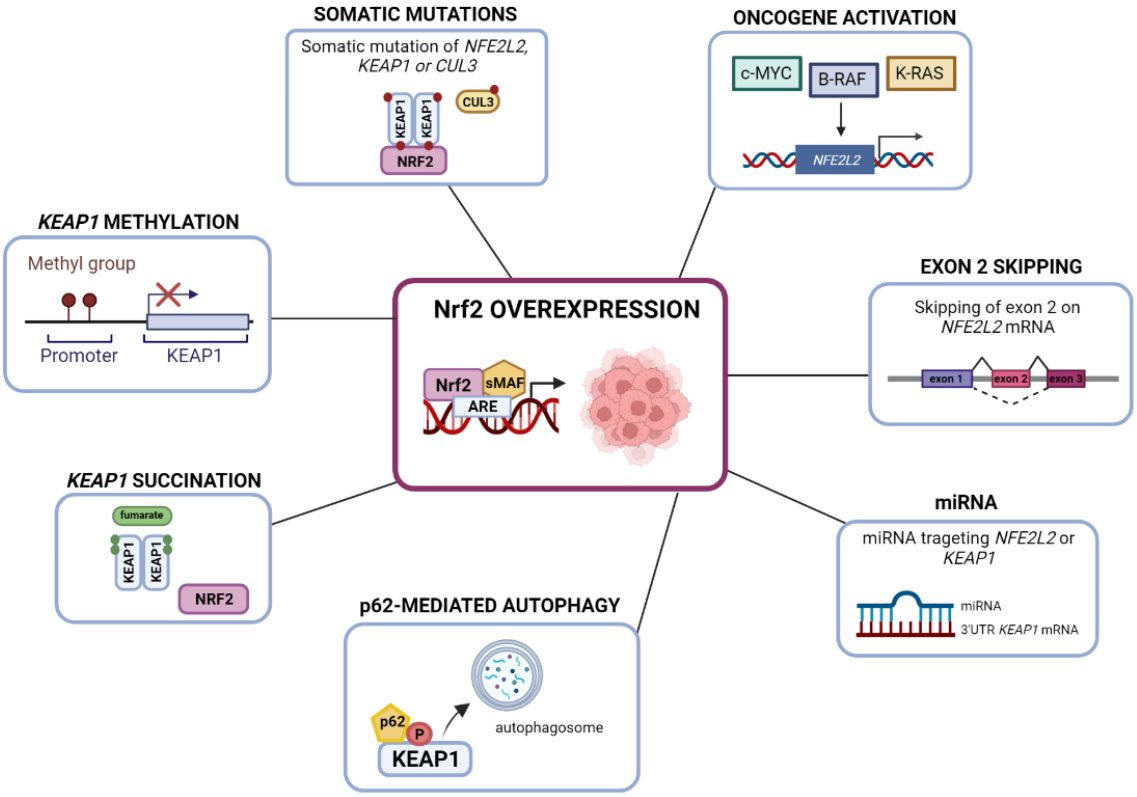

Figure 5. ''**Nrf2 addiction'' in cancer.** There are several mechanisms by which Nrf2 signaling pathway is constitutively activated in cancer cells, causing ''Nrf2 addiction''. First, somatic mutations of *NFE2L2*, *KEAP1* or *CUL3* genes - the most common are loss-of-function of *KEAP1*, mostly located in Kelch domain (13,97), and gain-of-function of *NFE2L2*, mainly seen in the DLG and ETGE motifs (98,99); second, epigenetic silencing of *KEAP1* by DNA hypermethylation; third - *KEAP1* succination, a metabolic-induced modification of Cys residues in *KEAP1* by fumarate (100); forth, accumulation of p62, which promotes Keap1 degradation by autophagy and increases Nrf2 activity (101); fifth, transcriptional activation of Nrf2 by mutations in several oncogenes, such as c-MYC, K-RAS and BRAF (31); sixth, skipping of exon 2 due to alternative splicing and small intragenic deletions (53); seventh, different miRNAs that can regulate *NFE2L2* or *KEAP1* expression levels. Increased expression of *NFE2L2* was observed by targeting the 3'UTR of *KEAP1* mRNA with miR-24-3p, miR-7, miR-200a, miR-421, miR-141, miR-626 and miR-873 (28,102). Created with Biorender.com.

1.5. Nrf2 role in immunity

1.5.1. Nrf2 role in immune surveillance

Immune surveillance is a monitoring process of the immune system to detect and destroy virally infected and neoplastically transformed cells in the body. Metabolic reprogramming mediated by Nrf2 modulates immune cell functions (12). The activation of Nrf2 in immune cells was shown to have different effects than activation of Nrf2 in cancer cells (Fig. 6). Anti-tumor immunity is mainly maintained by $CD8^+$ cytotoxic T lymphocytes (CTLs), $CD4^+$ Th1 helper cells, and natural killer (NK) cells (96), while immune-suppression is mainly mediated by regulatory T (Treg) cells and myeloid-derived suppressor cells (MDSCs).

The studies involving the lungs and the tumors of Nrf2 knockout mice and lung cancer patients suggested that Nrf2 controls tumor progression through regulation of immune cells and cytokine production. Deletion of Nrf2 significantly elevated the production of many cytokines and genes involved in the antigen processing and presentation (103). Nrf2 activation was shown to decrease IFN-γ production and increase IL-4, IL-5, and IL-13 production in $CD4^+$ T cells, which directs them towards Th2 differentiation (104,105). Activated Nrf2 in cancer cells was shown to induce IL-17D expression, leading to the increased anti-tumor immunity and NK-dependent tumor regression (106). Furthermore, higher populations of tumor-promoting macrophages and MDSCs were found in the lung and spleen, while fewer T cells, including $CD8^+$ and $CD4^+$ T cells, were found in lung in Nrf2 KO mice than in WT mice with advanced tumors (103). The reduced percentage of $CD8^+$ T cells in Nrf2 KO lungs is consistent with a higher tumor burden in the Nrf2 KO group compared with WT lungs. A series of cytokines and MHC antigen genes are expressed at higher levels in Nrf2 KO tumors and associated with more and larger tumors. Increased percentages of macrophages and MDSCs and decreased $CD8^+$ T cell populations are associated with a poor prognosis in patients and are consistent with an important beneficial regulatory role for Nrf2 in cancer immunity (103).

Nrf2 inhibition was also shown to affect the phenotype of dendritic cells, causing the lower basal GSH levels, reduced phagocytic activity, altered expression of MHC class I, enhanced co-stimulatory receptor expression (CD86 and CD80), and increased antigen-specific $CD8^+$ T cell stimulation capacity (107). On the other hand, Nrf2 activation increased the expansion of Treg cells, but inhibited the phosphorylation of Th17 transcription factor STAT3 and decreased Th17 differentiation (108).

In the context of inflammation, it was reported that activation of Nrf2 inhibits LPS-induced upregulation of pro-inflammatory cytokines including IL-6 and IL-1β, through the ROS-independent inhibition (109). It seems that Nrf2 could interact with the pro-inflammatory

transcription factors, such as p65, C/EBPβ and c-Jun, since the binding sites of Nrf2 near the IL-6 and IL-1β promoters coincide with the common binding regions of these transcription factors (109). The recruitment of Nrf2 to regulatory regions of pro-inflammatory cytokine genes might explain the inhibition of IL-6 and IL-1β after treatment with Nrf2 inducer in experimental models of multiple sclerosis and other autoimmune diseases (110–113). It would also explain a significant reduction of Th1 and Th17 cytokines, including IL-6, upon Nrf2 activation with derivatives of the triterpene oleanolic acid (114,115).

Furthermore, Nrf2 as a master regulator of antioxidant system in human cells also plays an important role in the regulation of innate immune responses during bacterial or viral infections. It seems to be involved in a wide range of different viruses and in most cases, it induces antiviral activity. Activation of Nrf2 suppresses viral replication in Severe Acute Respiratory Syndrome-Corona Virus (SARS-CoV2), Zika virus, and Herpes Simplex virus infections *in vitro* (116), however in some cases, Nrf2 activation seems pro-viral by promoting cell survival (117). Also, through the inhibition of the central signalling components of interferon-inducing pathways, including Stimulator of Interferon genes (STING) and Mitochondrial antiviral signaling (MAVS), Nrf2 is increasing susceptibility to the infection with DNA viruses (118).

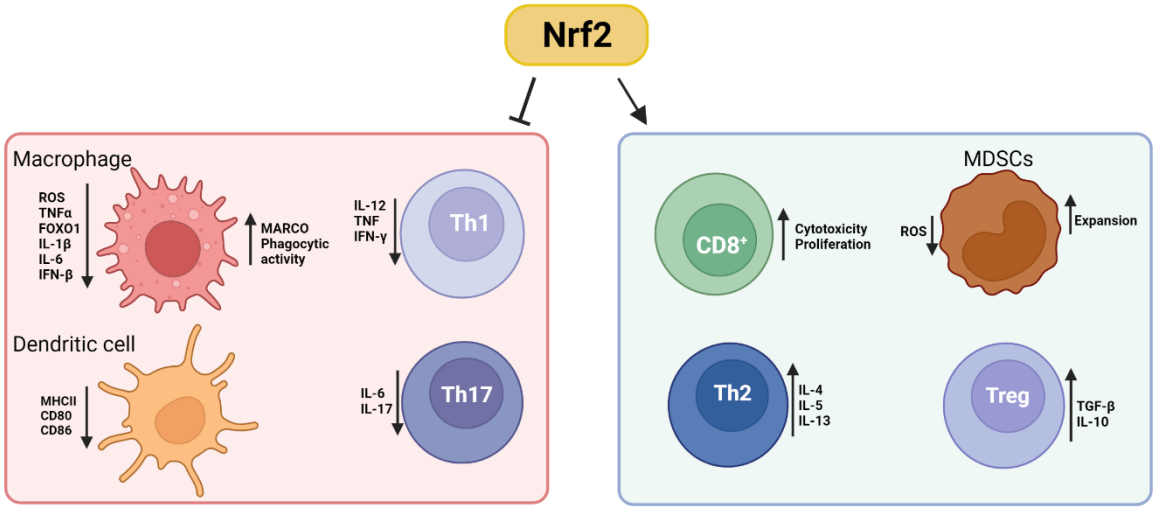

Figure 6. **Nrf2 regulates immunity and inflammation.** Activation of Nrf2 can affect differentiation, expansion and survival of the immune cells. Nrf2 suppress the expression of proinflammatory cytokines by macrophages, while it induces the expression of MARCO, scavenger receptor for bacteria, thereby enhancing bacterial clearance. Nrf2 activation also suppress inflammatory response of dendritic cells and impairs Th1-driven responses. Nrf2 deficiency decreases Th17 differentiation. On the other hand, Nrf2 activates $CD8^+$ cytotoxic T cells, induces the expansion of inhibitory MDSCs and Treg cells. Created with Biorender.com.

1.5.2. MHC class I molecules

The major histocompatibility complex I (MHC-I) is a system of genes encoding molecules (in humans called Human Leukocyte Antigens, HLAs) which, after reaching the cell surface, present antigenic peptides to the immune cells. It allows the immune system to differentiate a self cell from a non-self cell (virus-infected or tumor cell) (Fig. 7A). MHC locus is an approximately 3.6 Mb segment located on the short arm of chromosome 6 (6p21). It is one of the most dense regions in the human genome as it consists of more than 300 loci with over 160 protein-coding genes involved in the innate and adaptive immune responses, transcription regulation and signaling factors (119–121). The MHC region is divided into three sub-regions: MHC class I, class II and class III (Fig. 7B). Human MHC class I contains HLA I genes (classical: HLA-A, HLA-B, HLA-C and nonclassical: HLA-E, HLA-F and HLA-G genes) and the genes involved in antigen presentation. MHC class II contains HLA II genes (HLA-DPA1, HLA-DPB1, HLA-DQA1, HLADQB1, HLA-DRA, and HLA-DRB1) (122). Class III region contains genes implicated in inflammatory responses, leukocyte maturation and the complement cascade.

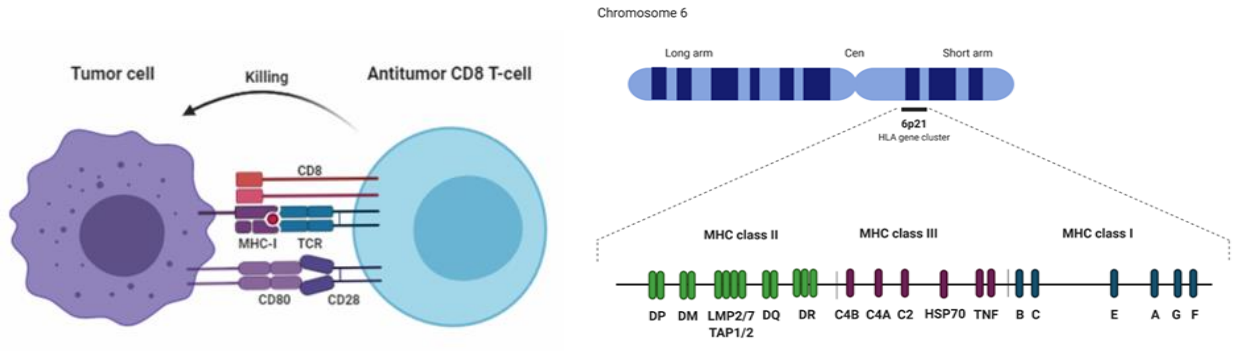

Figure 7. **MHC class I molecules**. A) MHC class I antigen presentation to $CD8^+$ cytotoxic T cells. B) MHC locus structure (121).

Two classes of HLA molecules are specialized to present antigens of different origin. HLA class I molecules present endogenously synthesized antigens (e.g. tumor associated antigens) to $CD8^+$ cytotoxic T lymphocytes, whereas HLA class II molecules present exogenously derived proteins (e.g. bacterial products) to $CD4^+$ helper cytotoxic T lymphocytes. HLA-A and -B present antigenic peptides to T cells, while HLA-C present antigens both to T cells and activate natural killer (NK) cells. The role of HLA class I molecules in the immune response is thus essential, but the functional differences between classical molecules has just

recently started to emerge. An increasing number of studies indicate that distinct classical molecules present antigens from different sources (123–125), but it is still a lot to be learnt about the function and regulation of classical HLA molecules.

Loss or downregulation of HLA-I molecules is an important immune-escape mechanisms in tumors, leading to the resistance to T cells cytotoxicity. The downregulation can occur at different levels, including transcriptional, post-transcriptional, genetic and epigenetic levels (126). There is a wide spectrum of the percentage of HLA-I loss in tumors, mostly depending on the tumor types. Cells that are highly immunogenic and express high levels of HLA-I are eliminated by cytotoxic T lymphocytes, while cancer cells with reduced HLA-I expression proliferate and result into a metastatic colonization. The defects in HLA-I expression are highly connected to the tumor progression and poor patient prognosis (121,127).

1.5.3. Crosstalk between Keap1 and MHC molecules

The interaction between cancer cells and their microenvironment is an important determinant of the pathological nature of cancers and their tumorigenic abilities. Therefore, Kitamura et al. showed that the genes down-regulated in Keap1$^{-/-}$-transformed mouse embryonic fibroblasts (TR MEFs) included those related to the immune response (128). Moreover, genes encoding MHC class I and class II and genes involved in antigen presentation were downregulated in Keap1$^{-/-}$-TR MEFs compared with WT-TR MEFs. These results support the notion that Keap1$^{-/-}$-TR MEFs tend to escape immune surveillance.

MHC class II genes are mainly expressed in immune cells, and their downregulation may lead to the decreased infiltration of immune cells to Keap1$^{-/-}$-TR tumors. In contrast, MHC class I genes are expected to be expressed in cancer cells as well as immune cells, but no clues have yet been found as to how Nrf2 could downregulate the MHC class I genes (128).

1.6. Therapeutic potential of Nrf2 in cancer prevention and therapy

Due to the broad role and interactions with various factors and signaling pathways, Nrf2 can have a protective role but can also contribute to the development of various diseases, particularly metabolism- or inflammation-associated diseases. Nrf2 can either suppress or promote host immunity in a cell type- and disease context-dependent manner.

It appears that transient activation of Nrf2 in normal cells is protective; however, in cancers, it enhances the survival and progression of cancer cells, known as the ‘’dark side of Nrf2’’. Therefore, it is important to take into consideration the dual role of Nrf2 in cancer when designing Nrf2 modulators. Furthermore, the potential effect of these modulators on non-cancer cells is important as low concentrations of Nrf2 can cause increased ROS levels and damage to the cellular molecules such as DNA, proteins and lipids, as well as apoptosis (5), while high concentration of Nrf2 can cause resistance to ROS and metabolic stress (5). Nrf2 activators can thus have a beneficial role in cancer prevention and therapy, while Nrf2 inhibitors could be useful in the response to cancer chemotherapy (129).

1.6.1. Nrf2 modulators for cancer therapy

1.6.1.1. Nrf2 activators

Many Nrf2 activators are naturally occurring, plant-derived phytochemicals. They induce the Nrf2-mediated defense response, including activation of phase II detoxification enzymes and antioxidants, to protect the cells from potential carcinogenic insults (13). One of the most extensively investigated natural product that target Nrf2-Keap1 pathway is sulforaphane (SF), an isothiocyanate present in cruciferous vegetables such as broccoli (130). SF has been shown to inhibit tobacco-induced lung carcinogenesis (131) in mouse cancer model, while the studies in humans have shown an inverse correlation between broccoli consumption and the risk of developing colon, lung, breast, liver and prostate cancer (5,132–135). Oleanolic acid and sulforaphane have been shown to stimulate the upstream regulators of Nrf2 pathway, ERK (extracellular signal-regulating kinase) and AMPK (AMP-activated protein kinase), leading to the increased Nrf2 expression (136,137). Another well-investigated chemopreventive natural compound is curcumin, extracted from *Curcuma longa* rhizomes. Curcumin has been shown to activate Nrf2 and consequently block oxidative stress and inflammation in the livers and lungs of mice treated with benzo(a)pyrene (138,139) (Fig. 8).

Synthetically developed Nrf2 activators, such as oltipraz and oleanane triterpenoids, are able to increase Nrf2 nuclear accumulation by changing intermolecular disulfide bonds between two Keap1 molecules at Cys273 and Cys288 (140). Dimethyl fumarate (DMF), another synthetic Nrf2 activator, alkylates cysteine residues on Keap1 and therefore prevents Nrf2 ubiquitination and degradation (141) (Fig. 8). An oral preparation of DMF, BG-12, has been approved by the Food and Drug Administration for the treatment of multiple sclerosis in March 2013 (http://www.fda.gov).

The classical Nrf2 activators such as curcumin, sulforaphane, and oltipraz seem to be not target specific and can cause some unwanted effects since they can interact with cysteine residues of different enzymes and proteins. Another very important issue with Nrf2 modulators is molecular instability, lower membrane permeability and poor bioavailability (129).

1.6.1.2. Nrf2 inhibitors

Based on the evidences that constitutive activation of Nrf2 promotes cancer cells proliferation and tumor survival, Nrf2 inhibition became a promising anticancer strategy, especially in cancers showing ‘’Nrf2 addiction’’ (33). Brusatol, a component of *Brucea javanica* seeds, has been shown to decrease the protein levels of Nrf2 and its target genes in cancer cells, leading to the enhanced chemosensitivity (142). Different compounds such as apigenin, omipalisib, and entinostat have been used to block Nrf2 mRNA translation (Fig. 8) and thus promoting anticancer effects in experimental models of hepatic cancer (143), gastric cancer (144), sarcoma and osteosarcoma (145).

Another strategy of Nrf2 inhibition is focused on compounds that affect Nrf2 stabilization and/or degradation. The PI3K-DNAPK inhibitor, PIK-75 was found to overcome gemcitabine resistance in pancreatic cancer by promoting Nrf2 degradation (146), while convallatoxin was shown to promote GSK-3β/β-TrCP-dependent Nrf2 degradation in the non-small cell lung cancer cells and therefore was able to restore responsiveness of cancer cells to 5-fluorouracil (147). Several other compounds suppress Nrf2 pathway, such as trigonelline, by impairing Nrf2 nuclear translocation (129) and luteolin, by inducing the degradation of Nrf2 mRNA (148).

Lastly, another promising strategy of Nrf2 inhibition is connected to disability of Nrf2 to bind to the ARE-sequences of target genes. A small molecule inhibitor, ML385, suppress Nrf2-sMAF binding and leads to increased chemosensitivity of the non-small cell lung cancer cells (149). Similarly, all-trans retinoic acid (ATRA) is promoting the association of Nrf2 with the nuclear receptor RARα and therefore prevents binding of Nrf2 to ARE-sequences of its target genes (150,151) (Fig. 8).

Taken together, these data demonstrate that Nrf2 inhibition might have a therapeutic potential in the cancer therapy. That being said, the lack of specific and selective Nrf2 inhibitors, and contradictory results regarding their effects, represent a significant limitations in their inclusion in the cancer treatment.

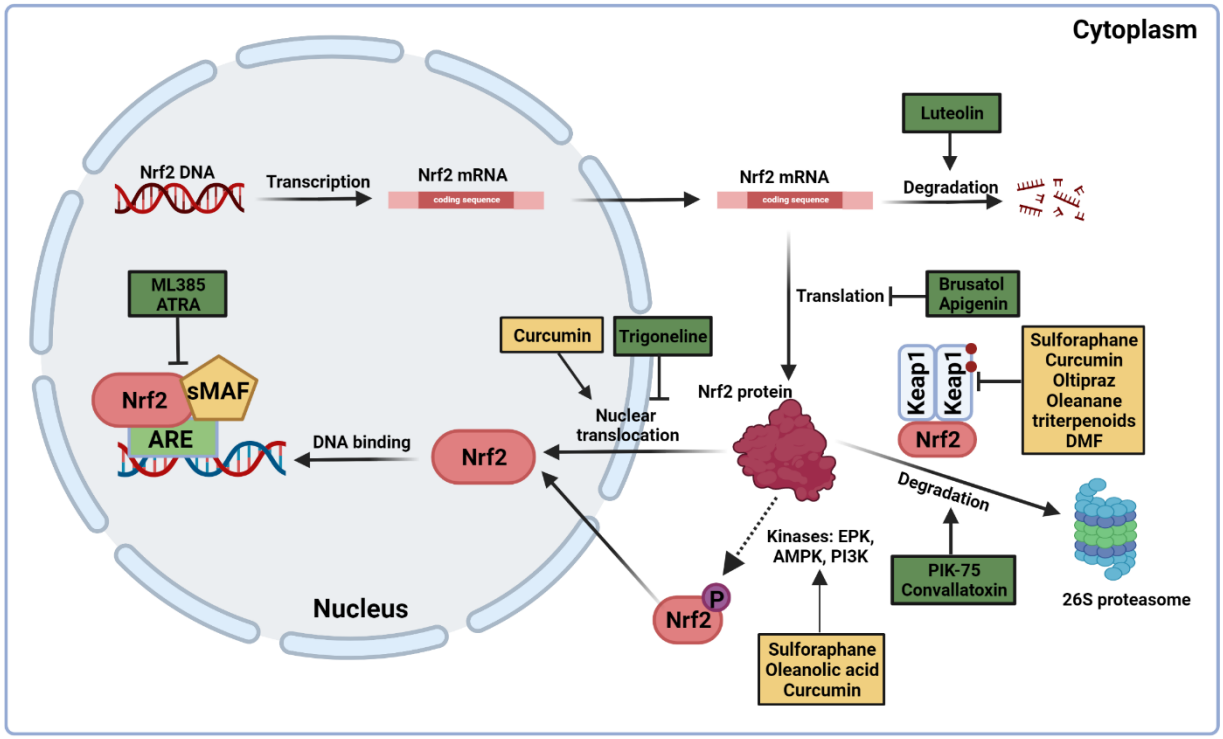

Figure 8. **Schematic overview of potential target sides and mechanisms of various Nrf2 activators and inhibitors**. Nrf2 activators are marked in yellow, while Nrf2 inhibitors are marked in green. Created with Biorender.com.

CHAPTER 2

Materials and Methods

2.1. Cell lines

Non-small cell lung cancer cell lines A549, RERF-LC-AI and H1299, as well as normal lung fibroblasts (NLF), were purchased from RIKEN BRC Cell Bank (Tsukuba, Ibaraki, Japan) and CRISPR/Cas9-induced NRF2 knockout in A549 cells (clone 2-11) was constructed and kindly provided by Prof Eric Kmiec (Gene Editing Institute, Christiana Care Health System, Newark, United States). All cancer cell lines were cultured in Dulbecco's modified Eagle's medium (Gibco, Thermo Fisher Scientific), with 8% of Fetal Bovine Serum (Gibco, Thermo Fisher Scientific) and 1% of Penicillin-Streptomycin (10 000 U/mL, Gibco, Thermo Fisher Scientific), while normal lung fibroblasts were cultured in Ham's F-12 Nutrient Mix (Gibco, Thermo Fisher Scientific), with 10% of Fetal Bovine Serum (Gibco, Thermo Fisher Scientific) and 1% of Penicillin-Streptomycin (10 000 U/mL, Gibco, Thermo Fisher Scientific). Cells were maintained at 37 °C under humidified conditions with 5% CO_2.

2.2. Isolation of non-small cell lung cancer (NSCLC) cells and depletion of $CD45^+$ cells

Cancer samples (0.25-1 g) were obtained from NSCLC patients admitted to the Clinic of Thoracic Surgery of University Clinical Centre of Medical University of Gdańsk (MUG) for surgical resection of the primary tumors. Patients were not previously treated with any anti-cancer therapy and no metastases were detected. Samples were cut into 1-2 mm fragments and washed 3 times with PBS to remove contaminating debris and erythrocytes. Subsequently digestion solution (DS) in 1:1 of DS (mL): tissue mass (g) ratio was added. The tissue was gently agitated at 37°C until single cell suspension was obtained. DS contained 5% collagenase type I (Sigma-Aldrich; 5 mg/mL), 19% of PBS and 1% of fetal bovine serum (FBS). The collagenase was inactivated with an equal volume of 10% FBS supplemented LG-DMEM medium (PAA), followed by filtration of the resulting cell suspension through a 100 µm nylon cell strainer (Falcon). Subsequently, the cells were washed with PBS. Then, erythrocyte lysis buffer was used to remove erythrocytes (10 min incubation at room temperature, RT). After subsequent centrifugation (600 x g, 10 min), the cells were washed with 4% FBS supplemented PBS and subjected for tumor infiltrating leukocyte depletion. For this purpose, positive immunomagnetic selection of $CD45^+$ cells were performed with EasySep Human CD45 Depletion Kit II (StemCell Technologies, Canada) according to the manufacturer's

instructions (post-isolation purity 96-99%). Thus, untouched NSCLC and lung-derived cells were isolated. Cells were plated into 75 cm^2 culture flasks in TumorPlus263 medium without serum. Establishment of primary cell line was confirmed with flow cytometry (FAP-$CK19^+$ phenotype; FACS Aria Fusion, BD Biosciences, USA) and when continuous proliferation of the cultured cells was observed after 2-month expansion *in vitro*. Cells that fulfilled both criteria were used for the experiments.

2.3. Lipid-mediated reverse transfection

Cells were seeded in the 6-well plates, 100 000 cells/well and transfected with control siRNA-A (ON-TARGET plus™ Control Pool, Dharmacon™, referred in text as scrRNA), as a control for transfection (25 nM), with small-interfering RNA for silencing of *NFE2L2* expression (siRNA, ON-TARGET plus™ SMART pool, Dharmacon™), small-interfering RNA for silencing of *KEAP1* expression (siRNA, Santa Cruz Biotechnology) and small-interfering RNA for silencing of *HLA-A* expression (siRNA, ON-TARGET plus™ SMART pool, Dharmacon™), in concentration of 25 nM, with 4 µL/well of Lipofectamine 3000 reagent (Invitrogen, Thermo Fisher Scientific), according to the manufacturer's instructions. Western blot was performed 48 h after transfection.

2.4. Treatment with translation inhibitor emetine dihydrochloride

Cells were seeded in 6-well plates, 300 000 cells/well. 48 hours later cells were treated with emetine dihydrochloride (20 µM), for 15 minutes, 2, 4, 8, 16 and 24 hours. Cells were collected and Nrf2 levels were analyzed by western blot with anti-NRF2 [EP1808Y] – ChIP Grade (cat. no. ab62352; Abcam). For calculation of the protein half-life, average band densities for each time point were normalized to controls, and data were fitted using nonlinear regression and a one-phase exponential decay equation using GraphPad Prism software.

2.5. Treatment with neddylation inhibitor MLN4924

Cells were seeded in 6-well plates, 500 000 cells/well. 24 hours later, cells were treated with neddylation inhibitor MLN4924 (1 µM) for 12 hours. Cells were collected and Nrf2 levels were analyzed by western blot.

2.6. Treatment with Lambda Protein Phosphatase (λPP)

800 000 cells were lysed in 250 µL of RIPA lysis buffer, sonicated for 15 min on ice and briefly centrifuged at 13,000 x g. For dephosphorylation, 40 µL of cell lysate was incubated with 400 U of λPP (New England Biolabs) in the dedicated buffer and in the presence of manganese

ions at 30°C for 30 min. Control samples underwent the same treatment, but without the enzyme. The Nrf2 phosphorylation was analyzed by western blot.

2.7. Treatment with PNGase F enzyme

500 000 cells were lysed in 40 µL of 2x Laemmli diluted in RIPA lysis buffer. Proteins were denaturated at 100°C for 10 minutes and digested with PNGase F enzyme (500 000 U/mL). Total reaction buffer of 20 µL contained 2 µL of 10x G7 Reaction Buffer, 2 µL of 10% NP40, 2 µL of PNGase F enzyme and 14 µL of lysate. Reaction was incubated overnight at 37°C and the samples were analyzed by western blot.

2.8. Treatment with Nrf2 inhibitor ML385

ML385 inhibitor (Axon Medchem) is a probe molecule that specifically binds to Neh1, the Cap 'N' Collar Basic Leucine Zipper domain of Nrf2 and interferes with the binding of sMAF-NRF2 protein complex to regulatory DNA binding sequences. It has specificity and selectivity for NSCLC cells with *KEAP1* mutation, which is associated with therapeutic resistance (149). Cells were treated with 5 µM ML385 in different time intervals, after which western blot, qPCR and flow cytometry were performed.

2.9. Cellular Fractionation

Separation of nuclei from cytoplasm was performed according to the REAP method described by Suzuki et al (152). Briefly, 4 000 0000 cells were resuspended in 400 µL of ice-cold 0.1% NP-40 in PBS by gentle pipetting and centrifuged at 500 x g for 10 seconds. Supernatant (cytosolic fraction) was collected and Laemmli buffer was added to final concentration 1x. Pellets containing nuclei were washed with 300 µL of 0.1% NP-40 in PBS, centrifuged at 500 x g for 10 seconds, resuspended in 200 µL 1x Laemmli buffer and sonicated 15 min. Samples were boiled for 10 min and analyzed by western blot.

2.10. Treatment with tert-butylhydroquinone (tBHQ)

Cells were seeded in 60 mm plates, 1 000 000 cells/plate. 24 hours later, cells were treated with tert-butylhydroquinone (tBHQ) (20 µM). Cells were collected after 6 hours and cellular fractionation was performed as previously described. Nrf2 levels were analyzed by western blot.

2.11. Co-immunoprecipitation

Cells were lysed using ice-cold lysis buffer (150 mM NaCl, 25 mM Tris-HCl, 0.5% Triton x-100; pH 7.5) and centrifuged 12,000 x g for 15 min. Lysates were pre-cleared with Protein G magnetic beads (Thermo Fisher Scientific) for 30 min at 4°C. Supernatants were incubated with the anti-HLA class I antibody (W6/32; Abcam) overnight at 4°C and HLA-antibody complexes were precipitated via 30 min incubation with beads. Beads were washed three times in PBS and proteins were eluted in 2x SDS-loading buffer, at 50°C for 10 minutes. Samples were analyzed by western blot.

2.12. Analysis of *NFE2L2* transcripts expression in A549 cells

To assess the expression of specific *NFE2L2* transcripts in A549 cell line, we have used the RNA sequencing data from the project available at NCBI Gene Expression Omnibus (GEO) public database (accession numbers GSM2308412, where A549 cell line was sequenced with paired Illumina protocol). Primary analysis of RNA-seq data included the quality control of sequenced reads with the use of FastQC (Andrews, 2010), reads trimming with the usage of Trimmomatic (153) and mapping to the reference genome based on NCBI reference human genome (assembly GRCh38.p13) and annotation (re-lease 109) (154) with the Hisat2 aligner (155). Further data preparations were performed with SAMtools software (156) and R software (157) together with Bioconductor platform. Assembly of RNA-Seq alignments into potential transcripts together with calculation of their expression levels were performed with StringTie software (158). Visualization of the alignments, identified transcripts and junctions was performed in IGV software (159).

2.13. Identification of Nrf2 transcript variants via RT-PCR

Cells were seeded at 800 000 in 60 mm plates and 24 h later RNA was isolated (Qiagen RNeasy Kit). 1 µg of RNA was reversely transcribed (Applied Biosystem), diluted 2-times and 1 µL was taken for the PCR reaction with the primers specific for different Nrf2 transcript variants. Primers were designed in a way to enable a length-based discrimination of Nrf2 transcript variants expressed in cells (Table 1). Products were separated on 2% agarose. Reaction products were cut from gel, purified and their identity was confirmed by Sanger sequencing.

Table 1. Sequences of primers for detection of Nrf2 transcript variants in RT-PCR.

Nrf2 transcript variants	Primer sequences	Product lengths
Transcript 1,6,7	For: TCATGATGGACTTGGAGCTG Rev GCAATGAAGACTGGGCTCTC	Tr 1: 475 bp Tr 6: 385 bp Tr 7: 256 bp
Transcript 6,7	For: CGACCTTCGCAAACAACTCT Rev: TGACCGGGAATATCAGGAAC	Tr 6: 817 bp Tr 7: 688 bp
Transcript 2,3,4,5,8	For: TCCTGCTTTATAGCGTGCAA Rev: GCAATGAAGACTGGGCTCTC	Tr 2: 602 bp Tr 3: 581 bp Tr 4: 476 bp Tr 5: 568 bp Tr 8: 531 bp

2.14. Evaluation of Nrf2 transcripts expression by RT-qPCR

Cells were seeded at 800 000 in 60 mm plates and 24 h later RNA was isolated (Qiagen RNeasy Kit). 1 µg of RNA was reversely transcribed (Applied Biosystems™ High-Capacity cDNA Reverse Transcription Kit), diluted 100x and 2 µL were taken for qPCR reaction. Quantification of transcript variants expression was performed according to the previously described method (160), where a product of Nrf2 gene common to all transcript variants was used as an internal reference to calculate relative expression of selected variants amplified with variants-specific primers (Table 2). Under used qPCR conditions, the reaction efficiency for each primer pair was similar (~2). First set of primers amplified product common for transcripts 1,6 and 7, second – products from transcripts 2,3 and 8 and third – product common to all Nrf2 transcript variants (Table 2). Primers used for RT-qPCR analysis in normal lung fibroblasts and A549 cell line are shown in Table 3 and Table 4. RT-qPCR analyses were performed by using the LightCycler 480 System (Roche). Actin was used as a reference gene. Relative quantitative levels of samples were determined by the $2^{-\Delta\Delta Cq}$ method.

Table 2. Primer sequences for evaluation of Nrf2 transcript variants expression via RT-qPCR.

Nrf2 transcript variant	Primer sequences	Product length
1,6,7	For: AACACACGGTCCACAGCTC Rev: TCTTGCCTCCAAAGTATGTCAA	102 bp
2,3,8	For: GACGGGATATTCTCTTCTGTGC Rev: CATACTCTTTCCGTCGCTGA	128 bp
1,2,3,4,5,6,7,8	For: GAGAGCCCAGTCTTCATTGC Rev TGCTCAATGTCCTGTTGCAT	104 bp

Table 3. Primers used for RT-qPCR analysis of normal lung fibroblasts.

Gene	Forward (5'→3')	Reverse (5'→3')
HLA-A	AAAAGGAGGGAGTTACACTCAGG	GCTGTGAGGGACACATCAGAG
NFE2L2	GAGAGCCCAGTCTTCATTGC	TGCTCAATGTCCTGTTGCAT
β-actin	TCCCTGGAGAAGAGCTACG	GTAGTTTCGTGGATGCCACA

Table 4. Primers used for RT-qPCR analysis of A549 cell line.

Gene	Forward (5'→3')	Reverse (5'→3')
HLA-A	GAGGACGGTTCTCACACCAT	GATGTAATCCTTGCCGTCGT
NFE2L2	GAGAGCCCAGTCTTCATTGC	TGCTCAATGTCCTGTTGCAT
β-actin	TCCCTGGAGAAGAGCTACG	GTAGTTTCGTGGATGCCACA

2.15. Molecular dynamics simulations and molecular modeling method

The structures for both isoforms (Isoform_1 and Isoform_2 with missing 1MMDLELPPPGLPSQQD16) of NRF2 were retrieved applying homology modeling modules implemented in the C-I-TASSER package developed in Zhang's lab (161). C-I-TASSER, uses convolutional neural-network based contact-map predictions to guide the I-TASSER fragment assembly (162). To build complete length NRF2 protein structure, the pdb id. 6gmh (163) was used as a template. These modeled NRF2 isoforms' structures were energy minimized

applying the CHARMM27 forcefield (164) implemented in the Molecular Operating Environment (MOE; Chemical Computing Group Inc., Montreal, QC, Canada) (165) package. Furthermore, the crystal structure of high affinity binding domain from NRF2 binding with Keap1 protein is available (pdb id.: 2flu (166,167), hence it was used as a template to define the conformation of full NRF2 protein structure with Keap1. The modeled NRF2-Keap1 complexes were further energy optimized in the MOE package, applying the CHARMM27 forcefield (164). Followingly, to understand the structural properties of two different systems; NRF2(isoform_1)-Keap1 and NRF2(isoform_2)-Keap1, they were further processed by molecular dynamics simulations (MDS) approach. MDS was performed using the GROMACS 4.6.5 (168) program (GROMACS; Groningen Machine for Chemical Simulations) assigning the CHARMM27 forcefield (164,169,170). Each prepared model system was solvated in simple point charge (SPC) water molecules (171) and Na^+Cl^- counter ions, and in a 10 Å thick dodecahedron simulation box. Periodic boundary conditions were applied and using steepest descent algorithm the systems were minimized for 50,000 steps. Particle Mesh Ewald (PME) method (172) and the LINCS algorithm (173) were used to treat electrostatic interactions (van der Waals and Coulomb interactions were set to 10 Å) and bond lengths, respectively. NPT (isobaric-isothermal) ensemble simulation was implemented to equilibrate all modeled systems, with temperature maintained at 300 K by V-rescale thermostat (173) and pressure at 1 bar and Parrinello-Rahman barostat (174). Leapfrog integrator (175) was used to perform 100 ns simulations of each system, and trajectories were saved every 10 ps. Results obtained from MDS were analyzed using GROMACS, VMD (Visual Molecular Dynamics) (176), and MOE (Chemical Computing Group Inc., Montreal, QC, Canada) / BIOVIA Discovery Studio (Dassault Systèmes, BIOVIA Corp., San Diego, CA, USA).

2.16. Western blot analysis

Total protein was acquired by lysing cells in RIPA buffer. Proteins were electrophoretically separated via 8% SDS-PAGE and transferred to nitrocellulose blotting membrane (Amersham Protran®). To block the membranes, 5% non-fat milk in Tris-buffered saline was applied at room temperature for half an hour. Membranes were subsequently incubated overnight with: anti-NRF2 [EP1808Y] – ChIP Grade (cat. no. ab62352; Abcam), anti-NRF2 (D1Z9C) XP antibody (cat. no. 12721; Cell Signaling Technology), anti-tubulin (DM1A, Cell Signaling Technology), anti-lamin A (C-3, sc-518013; Santa Cruz Biotechnology), anti-NQO1 (A180, NOVUS), anti-HLA class I (W6/32; ab22432, Abcam), anti-Keap1 antibody [1B4] (cat. no. ab119403; Abcam), anti-HLA-A (cat. no. ab52922; Abcam), anti-HLA-C (cat. no. ab126722; Abcam) and anti-β-actin (cat. no. A2228; Sigma-Aldrich) in blocking buffer at 4°C at 1:500 dilution. Subsequently, membranes were washed three times in TBST followed by incubation

for 1 h with HRP-conjugated goat anti-rabbit/mouse IgG (Jackson ImmunoResearch) (1:3000) dilution and washed in TBST again. Bands were visualized using chemiluminescent substrate (Clarity MaxTM Western ECL Substrate, BIO-RAD).

2.17. Immunofluorescence

Cells were seeded on 15 mm coverslips in a 12-well plate. 24 hours later, cells were fixed with 4% paraformaldehyde (PFA) for 10 minutes, rinsed 3 times with PBS and incubated 5 minutes with 0.2% Triton x100 for permeabilization. After rinsing 3 times with PBS, cells were blocked with 5% BSA in PBS, overnight at 4°C. The next day, cells were stained with primary antibodies: anti-NRF2 [EP1808Y] – ChIP Grade (cat. no. ab62352; Abcam), anti-NRF2 (D1Z9C) XP antibody (cat. no. 12721; Cell Signaling Technology), anti-Nrf2 (cat. no. ab89443; Abcam), anti-HLA-A (cat. no. ab52922; Abcam), anti-HLA-A (cat. no. TA813378; Origene) and anti-HLA-C (cat. no. ab126722; Abcam) at 1:500 dilution, at RT for 2 hours. They were washed 3 times with 1% BSA in PBS and stained with secondary antibodies (Alexa Flour 488 goat anti-rabbit and Alexa Fluor 555 goat anti-mouse; Thermo Fisher Scientific; 1:2000), in the dark at RT, for 1 hour, washed 3 times with 1% BSA in PBS and mounted using ProLong Diamond Antifade Mountant (Thermo Fisher Scientific). Specimens were imaged using a confocal laser scanning microscope (Leica SP8X, Germany) with a 63x oil immersion lens.

2.18. Flow cytometry

200 000 cells were aliquoted to flow cytometry tubes and centrifuged at 1500 rpm at room temperature. Supernatant was discarded and anti-HLA-ABC-BV711 antibody (clone G46-2.6, BD Horizon) for extracellular MHC class I protein staining was added. Samples were incubated for 30 minutes at room temperature, protected from light. Next, 1 mL of PBS was added, samples were centrifuged at 1500 rpm for 5 min and supernatant was discarded. For intracellular protein staining, 680 µL of Fix-Perm working solution was added and samples were incubated for 60 min at 4°C, protected from light. Cells were washed with Perm-Wash working solution and anti-HLA-ABC-FITC antibody (clone W6/32, Invitrogen, Thermo Fisher Scientific) for intracellular MHC class I protein staining was added. Samples were incubated for 30 min at room temperature, protected from light. Later, they were washed with Perm-Wash working solution and resuspended in 250 µL of PBS. Data acquisition and analyses were performed by fluorescence activated cell sorter ARIA FUSION (FACS Aria Fusion, BD Biosciences, USA).

2.19. Proximity ligation assay

Cells were pre-treated with respect to fixation, retrieval and permeabilization, and incubated 1 hour at 37°C in blocking solution. Primary antibodies – anti-Nrf2 (cat. no. ab89443; Abcam), anti-NRF2 [EP1808Y] – ChIP Grade (cat. no. ab62352; Abcam), anti-HLA-A (cat. no. 52922; Abcam) and anti-HLA-A (cat. no. TA813378; Origene) were diluted in antibody diluent, applied to samples and incubated at 4°C overnight, in the humidity chamber. Cells were washed in suitable buffer 2 times for 5 minutes. The two PLA probes were diluted 1:40 in probe diluent, applied to samples and incubated for 60 min at 37°C. Cells were washed in appropriate buffer 2 times for 5 minutes. Ligation and amplification were performed according to the NaveniFlex protocol (Navinci Diagnostics). Samples were stained with appropriate detection fluorophore (Atto 488) for 90 min at 37°C. Nuclei were stained with DAPI (300 nM) and samples were mounted using ProLong Diamond Antifade Mountant. Finally, specimens were imaged using a confocal laser scanning microscope (Leica SP8X, Germany) with a 63x oil immersion lens.

2.20. Click-iT labeling technology

Cells were incubated in methionine-free medium (+8% FBS) for 60 min and pulsed with L-azidohomoalanine (L-AHA) (50 μM) for 60 min. Cells were collected and co-immunoprecipitation (co-IP) was performed, as previously described. After co-IP, freshly translated proteins were detected with the use of tetramethylrhodamine (TAMRA) and samples were prepared for gel analysis, as described in Click-iT Protein Analysis Detection Kit (Thermo Fisher Scientific). For the detection of newly synthesized proteins with biotin, two types of biotin were used: 1) Acetylene-PEG4-biotin (500 μM) and 2) DADPS biotin- with cleavable DADPS linker (300 μM). After protein precipitation, streptavidin pull-down of biotin-labeled proteins was performed, proteins were eluted, stained with Flamingo stain and visualized by UV fluorescence.

CHAPTER 3

Results

PART 1. The role of Nrf2 in the MHC class I expression

3.1. Background and aim

The activation of the transcription factor Nrf2 has been shown to modulate immune cell functions and affect immune surveillance. Nrf2 plays a central role in a complex regulatory network and it interacts with variety of specific factors and signaling pathways (12). It can either suppress or promote host immunity in a cell type- and disease context-dependent manner and therefore it is important to have a better understanding of Nrf2 interaction with different components of the immune system, such as MHC class I molecules.

MHC class I molecules (in humans called Human Leukocyte Antigens, HLAs) present antigenic peptides to the immune cells allowing the immune system to differentiate self from non-self. MHC class I expression and regulation is widely investigated since their loss or downregulation are important immune-escape mechanisms in tumors, leading to the resistance to the T cells cytotoxicity (121).

Until now, the impact of Nrf2 on HLA class I molecules was not reported, however, there are indications that Nrf2-Keap1 pathway could have an influence on the expression of the genes responsible for the antigen presentation. A novel unfavorable immune signature in lung tumors from Nrf2 KO mice was reported based on 34 immune response genes significantly upregulated in tumors from Nrf2 KO mice, including genes involved in antigen processing and presentation and a series of cytokines (*Cxcl1, Csf1, Ccl9, Cxcl12*, etc.) (103). Kitamura et al. showed that genes involved in antigen presentation, including MHC class I and II, were downregulated in Keap1-deficient mouse embryonic fibroblasts (128). Based on these indications and evidences showing that oncogenic and immune pathways are interconnected (177,178), the first part of my research focused on elucidating the potential impact of Nrf2 on the antigen presentation pathway, particularly on the expression of the HLA class I molecules.

3.1.1. Methodology

In this study we have used two non-small cell lung cancer (NSCLC) cell lines: an adenocarcinoma A549, and a squamous cell carcinoma RERF-LC-AI (further referred as RERF), that differ in Nrf2 expression levels and activation status. A549 cells have a high steady-state level of constitutively active Nrf2 attributed to the homozygous *KEAP1* mutation (G333C) that disrupts binding with Nrf2 (54). Another reason for high Nrf2 levels in these cells is the trisomy of the chromosome 2 carrying the *NFE2L2* gene (while *KEAP1* is localized on the disomic chromosome 19) (179). We have used CRISPR/Cas9-induced NRF2 functional knockout (KO) in A549 cells (further referred as A549 Nrf2 KO), kindly provided by Prof. Eric Kmiec (Gene Editing Institute, Christiana Care Health System, Newark, United States). These cells have lower levels of Nrf2 as two out of three alleles have been successfully knocked out with CRISPR/Cas9 technology. The third allele has an ‘‘in frame’’ deletion within the nuclear export signal, thus the expressed Nrf2 cannot re-enter the nucleus (180). These cells were found to have a reduced proliferation phenotype and were more sensitive to chemotherapeutic agents, such as cisplatin and carboplatin. In xenograft mouse models, they proliferated at a slower rate than the wild-type cells illustrating the oncogenic role of Nrf2 in cancer cells (180). The RERF cells do not have any known *NFE2L2*/*KEAP1* mutation and therefore the Nrf2 levels are low under no stress conditions (181). We have also used primary NSCLC cell line derived from patient’s lung tumor (further referred as NSCLC 1) and normal lung fibroblasts (further referred as NLF).

To explore the effect of Nrf2 on HLA class I expression (further referred as HLA-I) in normal lung fibroblasts and lung cancer cells, analyses on the transcriptional, protein and cell surface level were performed.

3.1.2. Results

3.1.2.1. Nrf2 depletion in normal lung fibroblasts reduces HLA class I protein and cell surface levels

Firstly, to see if Nrf2 influences HLA-I expression in normal lung fibroblasts (NLF), we used siRNA to silence the expression of *NFE2L2* and looked at the RNA and protein expression of HLA-A, and cell surface expression of total HLA-I molecules as compared to a non-targeting siRNA (scrambled RNA; scrRNA) transfection control. HLA-A belongs to the HLA-I system of genes which, after reaching the cell surface, present antigenic peptides to the $CD8^+$ cytotoxic T lymphocytes. The HLA-A molecule displays specific features compared to HLA-B, that could

account for its particular role: HLA-A and HLA-B alleles carry an unpaired cysteine at different positions of the cytoplasmic tail (at positions 339 and 325), which is responsible for the formation of MHC I dimers in exosomes, targeting for degradation and influencing recognition by NK cells (182,183). Interestingly, HLA-A locus is also surrounded by HLA class Ib genes (HLA-E, HLA-H, HLA-G and HLA-F) involved in immune-modulation (183). HLA-A alleles are one of the most widely distributed class I molecules within the human population (184) and therefore, we firstly focused on analyzing their expression on the RNA and protein level. Due to the limited antibody availability and specificity for the determination of HLA-I cell surface expression, we used pan-HLA-I antibody W6/32 that detects all the HLA-I alleles together.

NFE2L2 knockdown drastically reduced HLA-A protein levels, as shown in Fig. 9A, and decreased the expression of HLA-I molecules on the cell surface (Fig. 9B). To test if the stabilization of Nrf2 would have the opposite impact on HLA-I expression, we silenced the expression of *KEAP1*, the negative regulator of Nrf2. This resulted in an accumulation of Nrf2 and its transcriptional target NAD(P)H dehydrogenase [quinone] 1 (NQO1) (Fig. 9A). Nrf2 auto-regulates its own expression and once released from Keap1, it induces its own expression (185). HLA-A protein levels were not significantly changed after *KEAP1* knockdown (Fig. 9A) and there was a subtle increase in HLA-I cell surface levels, comparable to non-targeting scrRNA transfection control (Fig. 9B). It seems that stabilization of Nrf2 caused by *KEAP1* knockdown did not show the opposite results compared to the *NFE2L2* knockdown. The reason could be the involvement of Keap1 in different pathways and therefore, its influence on HLA-I expression can be independent from Nrf2 (186).

We also made use of ML385, which is a small molecule inhibitor of Nrf2 transcriptional activity. ML385 specifically binds to the Neh1 domain of Nrf2 and interferes with the binding of Nrf2-sMAF protein complex to regulatory DNA sequences. It has specificity and selectivity for NSCLC cells with *KEAP1* mutation, which is associated with therapeutic resistance (149). ML385 decreased Nrf2 protein levels (Fig. 9A) consistent with autoregulatory capacity of Nrf2, while western blot showed that the total HLA-A protein level was not significantly changed (Fig. 9A). However, flow cytometry analysis showed that HLA-I surface expression was decreased after 48 and 72 hours of the treatment (Fig. 9B), similar to the silencing of Nrf2. These data suggest that Nrf2 controls HLA-I expression.

The *NFE2L2* RNA expression was significantly decreased after knockdown of *NFE2L2* and increased after knockdown of *KEAP1* (Fig. 9C). However, *HLA-A* RNA expression was upregulated after Nrf2 depletion (Fig. 9D), while protein and cell surface HLA-I expression was reduced after Nrf2 depletion. ML385 treatment decreased *NFE2L2* RNA expression (Fig. 9C), while *HLA-A* RNA expression was not significantly changed (Fig. 9D).

Despite not significantly increasing HLA-I expression on the cell surface, Keap1 depletion resulted in an upregulated *HLA-A* RNA expression (Fig. 9D). The reason might be that, as previously mentioned, Nrf2 is not the only client protein of Keap1 and inhibition of the Cul3 ubiquitin system can affect HLA levels independent from Nrf2. For example, it was shown that Keap1 is a novel regulator of HLA class II transcription, independently of promoter activation or mRNA stability, since Keap1 depletion decreased interferon gamma-induced MHC class II (186).

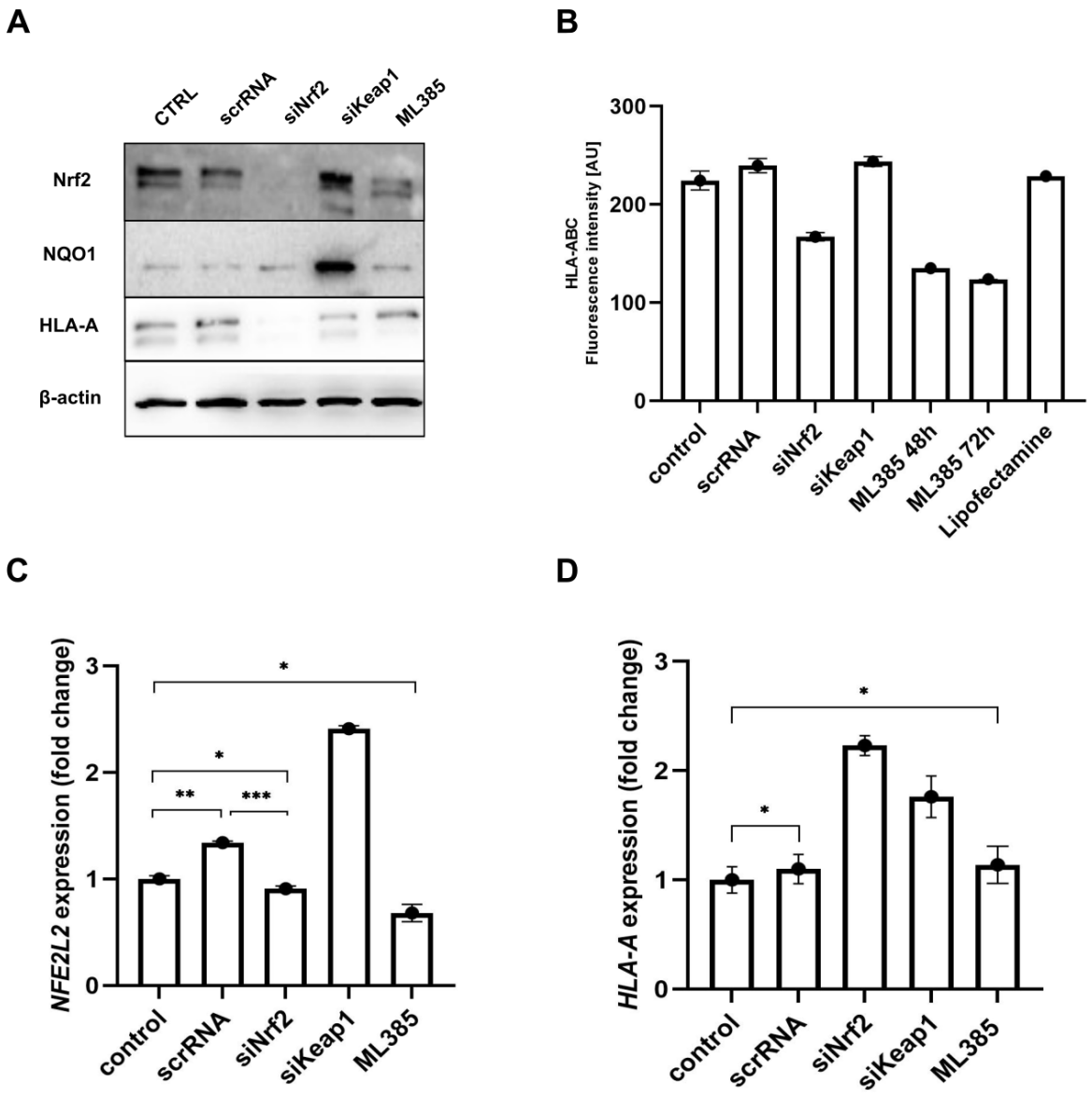

Figure 9. **Nrf2 depletion downregulated HLA-I protein and cell surface levels, but not RNA levels.** (A) Western blot analysis of NLF after silencing of Nrf2 and Keap1 expression, with the use of siNrf2 (25 nM) and siKeap1 (25 nM). Non-targeting siRNA (scrambled RNA, further referred as scrRNA) was

used as a negative control of transfection system. Cells were also treated with ML385 inhibitor (5 µM) and western blot analysis was performed 48 hours after treatment. Actin was used as a loading control. (B) Flow cytometry analysis of NLF after knockdown of *NFE2L2*, *KEAP1* and ML385 treatment for 48 and 72 hours. Cells were stained with pan-HLA-I antibodies (W6/32-FITC). Results are showing fluorescence intensity [AU] of HLA-I on the cell surface. Error bars represent SD. scrRNA and lipofectamine (reagent for transfection) were used as negative controls. (C) NLF cells were transfected with siNrf2 (25 nM) and siKeap1 (25 nM) and samples were collected after 48 hours. scrRNA was used as a negative control of transfection system. Cells were also treated with ML385 inhibitor (5 µM) for 48 hours. RT-qPCR analysis of the expression of *NFE2L2* was performed. Gene expression levels were normalized to actin. Error bars represent SD. Statistical analysis of qPCR data was performed with a t-test; *P ≤ 0.05; **P ≤ 0.01; ***P ≤ 0.001. Relative quantitative levels of samples were determined by the $2^{-\Delta\Delta Cq}$ method. (D) RT-qPCR analysis of the expression of *HLA-A.* Gene expression levels were normalized to actin. Error bars represent SD. Statistical analysis of qPCR data was performed with a t-test; *P ≤ 0.05; **P ≤ 0.01; ***P ≤ 0.001. Relative quantitative levels of samples were determined by the $2^{-\Delta\Delta Cq}$ method.

What emerges from these results is that the depletion of Nrf2 suppresses HLA-I protein, but not RNA levels. We concluded that Nrf2 might control HLA-I on the level of translation or degradation, though such function of Nrf2 has not been reported yet. The increase in the *HLA-A* RNA could represent the response of the cells to the lowered protein levels, a feedback loop aiming to increase HLA-A expression.

3.1.2.2. Functional knockout of Nrf2 reduced HLA class I protein and cell surface levels, but not RNA level

Under homeostatic conditions, A549 Nrf2 KO cells express lower levels of Nrf2 comparing to the wild-type A549 cells (A549 Nrf2 wt). The reduced expression of Nrf2 in A549 Nrf2 KO was confirmed on the protein level (Fig. 10A). Moreover, the protein expression of NQO1 was significantly lower in A549 Nrf2 KO cells compared to Nrf2 wt cells (Fig. 10A). Steady-state protein level of HLA-A was reduced in A549 Nrf2 KO (Fig. 10A) and flow cytometry showed that the expression of HLA-I on the cell surface was significantly lower in A549 Nrf2 KO cells (Fig. 10B).

The knockout of Nrf2 was also confirmed on the RNA level, since the *NFE2L2* expression was indeed very low in A549 Nrf2 KO cells comparing to the A549 Nrf2 wt cells (Fig. 10C). Interestingly, like with the NLF cells, the *HLA-A* RNA expression showed the opposite results from protein and cell surface levels. *HLA-A* RNA level was significantly higher in A549 Nrf2

KO compared to the Nrf2 wt cells (Fig. 10D). From what we observed, we can deliberate that Nrf2 affects HLA-I synthesis or degradation.

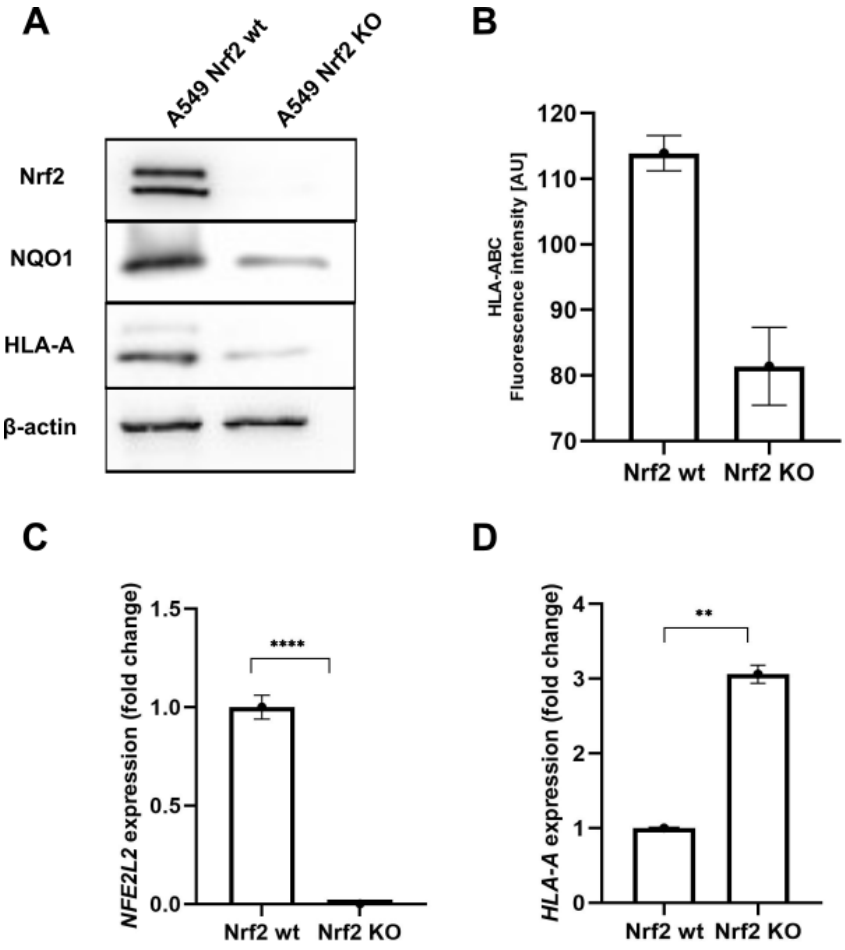

Figure 10. **Functional knockout of Nrf2 reduced HLA class I protein and cell surface levels, but not RNA level.** (A) Western blot analysis of A549 Nrf2 wt and A549 Nrf2 KO cells, 48 hours after seeding. Actin was used as a loading control. (B) Flow cytometry was performed 72 hours after cells seeding. Cells were stained with pan-HLA-I antibodies (W6/32-FITC). Results are showing fluorescence intensity [AU] of HLA-I on the cell surface. Error bars represent SD. (C) RT-qPCR analysis of *NFE2L2* expression in A549 Nrf2 wt and A549 Nrf2 KO cells, performed 48 hours after cells seeding. Gene expression levels were normalized to actin. Error bars represent SD. Statistical analysis of qPCR data was performed with a t-test; *P ≤ 0.05; **P ≤ 0.01; ***P ≤ 0.001. Relative quantitative levels of samples were determined by the $2^{-\Delta\Delta Cq}$ method. (D) RT-qPCR analysis of *HLA-A* expression in A549 Nrf2 wt and A549 Nrf2 KO cells, performed 48 hours after cells seeding. Gene expression levels were normalized to actin. Error bars represent SD. Statistical analysis of qPCR data was performed with a t-test; *P ≤ 0.05; **P ≤ 0.01; ***P ≤ 0.001. Relative quantitative levels of samples were determined by the $2^{-\Delta\Delta Cq}$ method.

3.1.2.3. Nrf2 can affect synthesis and/or degradation of HLA class I molecules?

We have observed that A549 Nrf2 KO cells have reduced HLA-I protein and cell surface levels, but not RNA level, compared to the A549 Nrf2 wt cells. In correlation with that, silencing of Nrf2 in NLF showed downregulation of HLA-I protein and cell surface expression, while RNA expression was upregulated. Based on these observations, we speculated that Nrf2 could regulate synthesis and/or degradation of HLA-I molecules.

To verify this assumption, we wanted to compare the stability of HLA-I proteins between A549 Nrf2 wt and Nrf2 KO cells. The use of protein synthesis inhibitors is the most common method to determine the stability of the protein (protein turnover rate). Emetine dihydrochloride is a translation elongation inhibitor, which binds the 40S subunit of the ribosome and inhibits ribosome movement along the mRNA (187–189). Due to the high stability of HLA-I molecules, we had to perform emetine treatment at long time points (8, 16 and 24 hours) to observe any differences in the protein amount. This long translation inhibition is not without an impact on the cells condition – it is toxic and could affect the results. Though western blot indicates that all HLA molecules are less stable in A549 Nrf2 KO cells (Fig. 11), the steady state level of HLA-I is not lower in the Nrf2 KO as it has been reported previously. Due to the high stability of HLA-A, even after 24 hours of translation elongation inhibition, at this point we also decided to look into HLA-C protein stability. That allowed us to see if there are differences in the expression of different HLA-I alleles between A549 Nrf2 wt and Nrf2 KO cells. Interestingly, unlike HLA-C levels, HLA-A levels did not change much even after 24 hours of translation inhibition, showing an extraordinary stability (Fig. 11).

Moreover, it is important to mention that we were able to detect low Nrf2 levels in the Nrf2 KO cells, due to the fact that the two out of three alleles have been successfully knocked out (Fig. 11). Thus, this knockout reduces Nrf2 protein levels and its translocation to the nucleus (180). However, Nrf2 protein is still synthesized in these cells, which could affect the results. To be able to see the straight-forward effect of Nrf2 on HLA-I stability, it would be crucial to obtain the cells with total KO of Nrf2.

Another interesting observation following the treatment with translation elongation inhibitor was the extreme stability of a second, lower band detected by Nrf2 antibodies. We had previously observed that Nrf2 antibodies mostly recognize the Nrf2 protein as two bands in the SDS-PAGE gel, however, the high stability of one of the forms was intriguing and unexpected, and is the focus of the second part of my project.

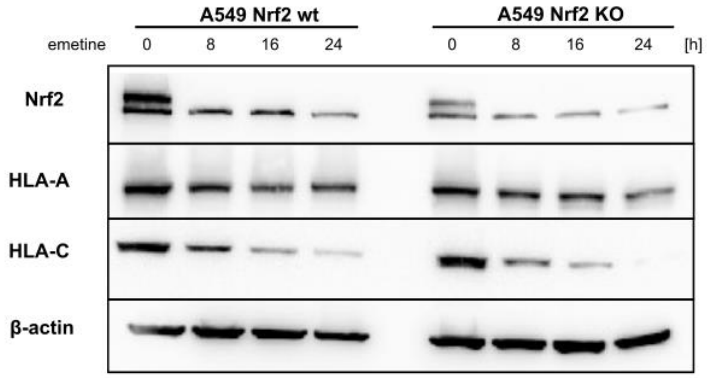

Figure 11. **High stability of HLA-I molecules upon treatment with translation elongation inhibitor.** Western blot analysis of A549 Nrf2 wt and A549 Nrf2 KO cells after treatment with translation elongation inhibitor, emetine dihydrochloride (20 μM), at different time points (8, 16 and 24 hours). Actin was used as a loading control.

The results with the translation inhibition were not conclusive and even though the use of translation elongation inhibitor can be an efficient way to determine protein stability, in this case the long treatment duration can affect the results. Therefore, we made use of Click-iT labeling technology for detection of newly synthesized HLA-I proteins after co-immunoprecipitation in A549 Nrf2 wt and Nrf2 KO cells. This method is a non-radioactive alternative to the traditional radioactive 35S-methionine pulse label technique.

Radiolabeling of nascent cellular proteins is often considered the gold standard for the pulse and chase protein analysis, due to the fact that it has minimal disturbance to the normal cellular conditions. However, the main disadvantage of this method is the use of radioisotopes, that could be potentially biohazardous, so specific equipment and facilities are necessary (190,191). Therefore, the new click-it technology approach, which involves labeling of the living cells with alkyne/azide-modified amino acids that can be fed to cultured cells and incorporated into proteins during active protein synthesis, offers an interesting alternative (192). Labeled proteins can react with alkyne/azide-containing molecule in a copper-catalyzed ‘’click’’ chemistry reaction. Finally, the modified protein is detected and analyzed using in-gel fluorescence imaging, western blot, fluorescent microscope and/or flow cytometry (Fig. 12). In our experimental set up, we used L-Azidohomoalanine (L-AHA), an amino acid analog that contains a very small modification, specifically an azido moiety that can be incorporated into proteins during active protein synthesis (192). L-AHA-labeled proteins then react with an alkyne-containing molecule and the azido modified protein is detected using the red-fluorescent tetramethylrhodamine (TAMRA) alkyne (Fig. 12). The main advantages of this

method are that L-AHA is non-toxic, non-radioactive, does not inhibit protein synthesis, and does not alter global protein ubiquitination or degradation. Moreover, the reaction between azide and alkyne is highly efficient and specific (193).

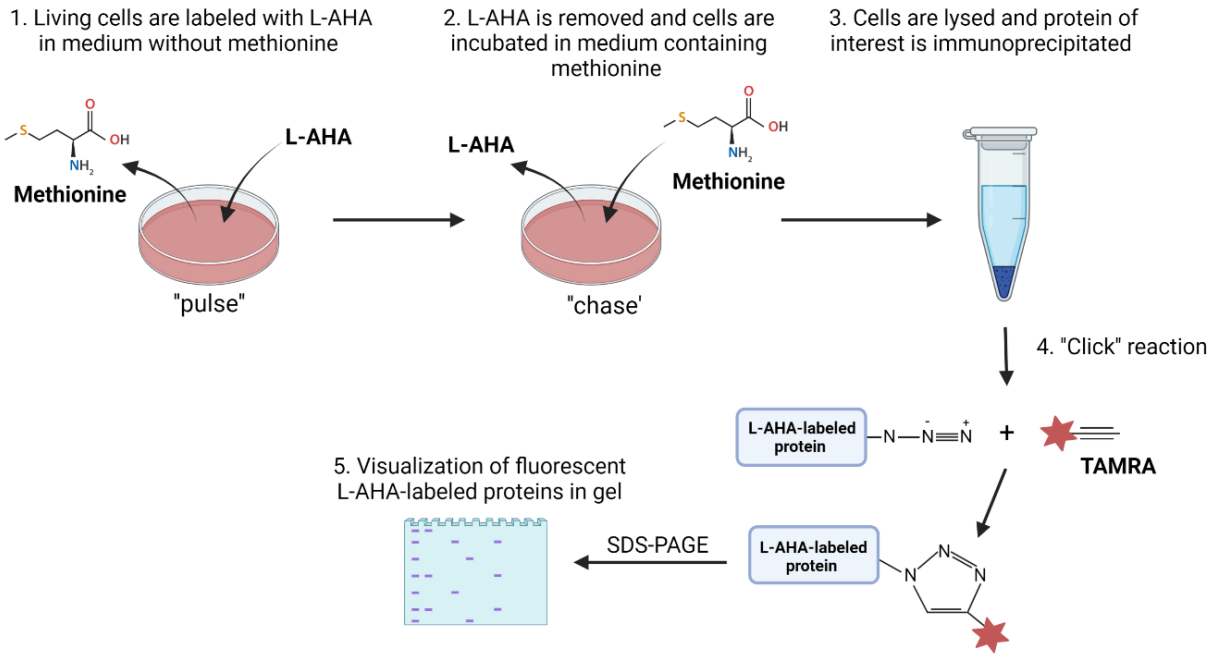

Figure 12. **Schematic overview of the click-iT labeling technology for the detection of newly synthesized proteins.** Click-iT labeling can be used for pulse analysis, to monitor protein synthesis kinetics, and for pulse and chase analysis, to monitor protein degradation kinetics. Nascent proteins in the living cells are labeled with L-AHA in the medium without methionine. For the pulse and chase assay, the medium has to be changed to the one containing methionine, at certain time points, while for the pulse assay, cells are incubated in the same medium without methionine until the lysis. After the cells are collected and lysed, protein of interest is immunoprecipitated. The next step is the ‘’click’’ reaction, in which incorporated L-AHA reacts with a fluorescent TAMRA-labeled alkyne. At the final step, TAMRA-labeled proteins are separated by SDS-PAGE and visualized by UV fluorescence.

Applying the described workflow (Fig. 12), we firstly labeled the newly synthesized proteins in A549 Nrf2 wt and Nrf2 KO cells with L-AHA for one hour. The next step was lysing the cells, perform the co-immunoprecipitation of HLA-I proteins and their detection by UV fluorescence. The results showed that A549 Nrf2 KO cells have less newly synthesized HLA-I proteins comparing to the A549 Nrf2 wt (Fig. 13).

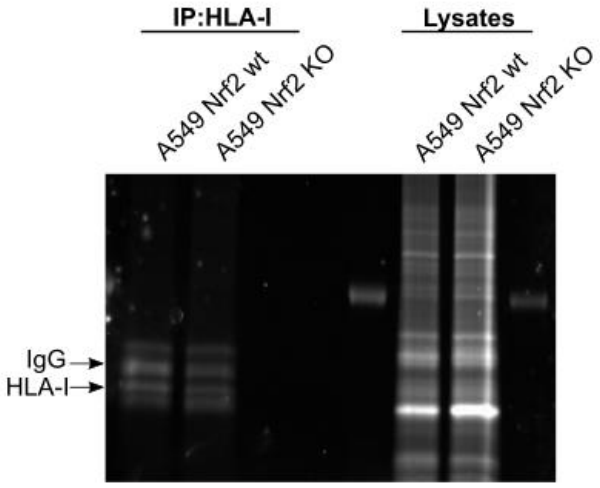

Figure 13. **A549 Nrf2 KO cells have less newly synthesized HLA-I proteins compared to A549 Nrf2 wt cells.** Click-iT labeling and gel analysis of newly synthesized HLA-I proteins after co-immunoprecipitation in A549 Nrf2 wt and Nrf2 KO cells. L-Azidohomoalanine (L-AHA; 50 μM, 1 hour) was used to label freshly synthesized proteins in living cells, while tetramethylrhodamine (TAMRA) was used for the detection. IgG; immunoglobulin G.

Furthermore, this method allowed us to use pulse-chase analysis to compare the effect of Nrf2 on the synthesis and degradation of HLA-I proteins. The results after the pulse at different time points (1, 2 and 3 hours) did not show the significant difference between the detected signals in A549 Nrf2 wt and Nrf2 KO cells (Fig. 14A). There was a slight difference after 2 hours pulse, where we could see that A549 Nrf2 wt cells have higher expression of the newly synthesized HLA-I proteins, compared to the A549 Nrf2 KO cells, which is in the correlation with our primary observation (Fig. 13). However, after 3 hours pulse, it seems that HLA-I expression in the A549 Nrf2 wt and Nrf2 KO cells is similar (Fig. 14A).

Since our assumption was that Nrf2 could affect synthesis and/or degradation of HLA-I molecules, we next performed pulse-chase analysis, that allowed us to monitor the protein degradation kinetics. Cells were pulsed for 3 hours, and then chased for 3 and 6 hours. The results again did not give a straight-forward answer, since after chase for 3 hours, we could see that the A549 Nrf2 wt cells have higher expression of the newly synthesized HLA-I proteins, comparing to the A549 Nrf2 KO cells. However, after chase for 6 hours, the result was opposite and A549 Nrf2 KO cells showed higher expression of HLA-I proteins compared to the A549 Nrf2 wt cells (Fig. 14B). One of the reasons of inconclusive results and difficulties in performing pulse-chase analysis could be the high stability of HLA-I proteins.

We have also tried a different approach to the click-iT labeling technology – labeling of freshly translated proteins with L-AHA, detection with the use of biotin and pull-down with the streptavidin beads, to omit the step with immunoprecipitation and minimize the possibility of losing the proteins during the procedure, which would give us more reproducible and therefore conclusive results. However, this approach did not give a desired outcome due to the unspecific binding to the biotin, the formation of protein aggregates and difficulties with solubilization of the precipitate (Fig. S1).

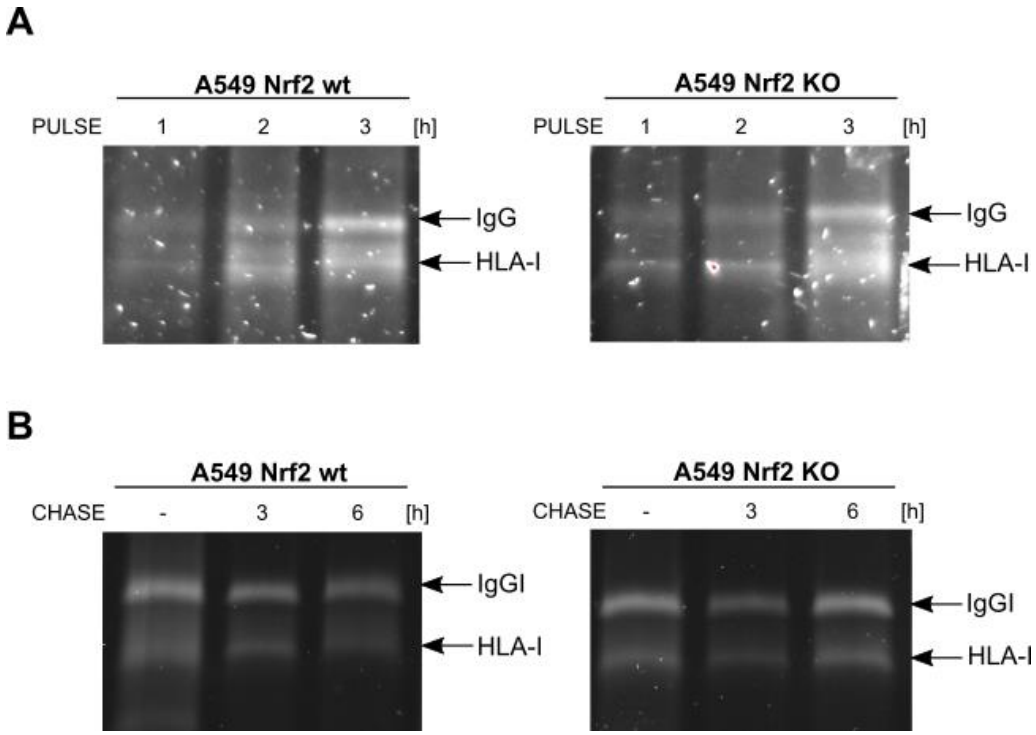

Figure 14. **Pulse and chase analysis of the newly synthesized HLA-I proteins in A549 Nrf2 wt and Nrf2 KO cells.** Click-iT labeling and gel analysis of the newly synthesized HLA-I proteins after co-immunoprecipitation in A549 Nrf2 wt and Nrf2 KO cells. (A) Pulse was performed with L-AHA (50 μM) at indicated time points, after which cells were collected and lysed. (B) For the pulse-chase analysis, cells were pulsed with L-AHA for 3 hours and chased for 3 and 6 hours. TAMRA was used for detection by UV fluorescence. IgG; immunoglobulin G.

To sum up, the click-iT labeling technique turned out to be very challenging since one of the crucial steps is co-immunoprecipitation, which makes it difficult to precisely analyze and compare the differences in the protein expression, especially when proteins are not purified, as in our case. However, the treatment with translation elongation inhibitor indicated that Nrf2 could play a role in stabilizing HLA-I molecules and preventing their degradation as well as

facilitating synthesis, since in the pulse analysis, A549 Nrf2 wt cells showed more newly synthesized HLA-I comparing to the A549 Nrf2 KO cells. To further investigate this hypothesis, we could have a look if the *NFE2L2* and *HLA-I* RNAs are translated together on the ribosome.

3.1.2.4. HLA class I stability in RERF-LC-AI cell line and in primary NSCLC cell line

To address the question about Nrf2 influence on the HLA-I expression in a lung cancer cell line without any known mutations in the *NFE2L2/KEAP1* pathway, we performed silencing of Nrf2 expression using the mixture of different Nrf2-targeting siRNAs in the RERF-LC-AI cells. Taking into consideration high stability of HLA-I molecules (especially HLA-A) and one of the detected Nrf2 forms (Fig. 15A), we combined silencing of Nrf2 with translation elongation inhibition to check the impact of Nrf2 on HLA-I stability (rate of degradation). The results have shown that Nrf2 is still expressed after siNrf2, but at the significantly lower levels. The expression of a stable Nrf2 form was significantly reduced after siNrf2 and 4 hours of emetine treatment, compared to the scrRNA control. Even though we were using a pool of anti-Nrf2 siRNAs targeting different regions of *NFE2L2* gene, a stable Nrf2 was not completely knocked-down, indicating its high stability, as previously observed. The expression of HLA-A was reduced after siNrf2 combined with translation inhibition already after 15 minutes of treatment, compared to the scrRNA. It leads to the assumption that the stable Nrf2 form can affect the stability of HLA-A proteins, although there is not much difference in HLA-A protein level between 15' and 4 hours after emetine treatment. The stability of HLA-C did not significantly change between siNrf2 and scrRNA samples (Fig. 15B).

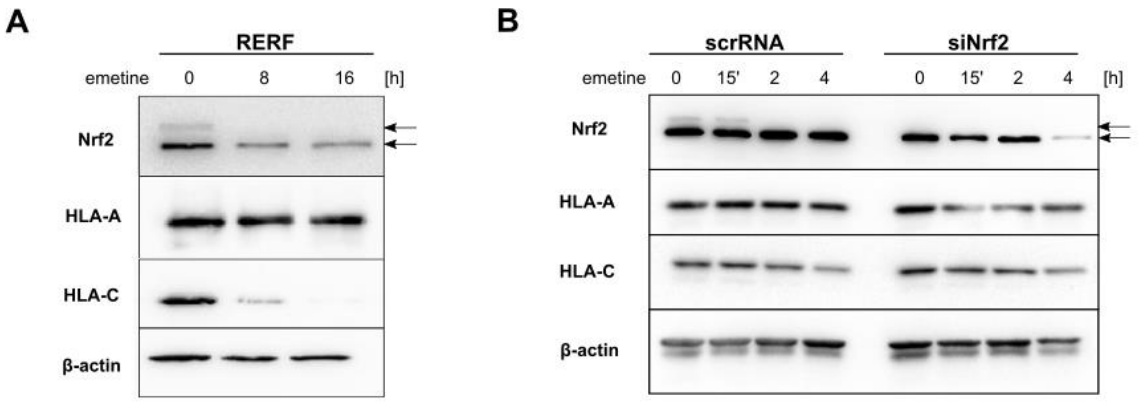

Figure 15. **HLA-I stability in lung cancer cell line RERF-LC-AI.** (A) Western blot analysis of RERF-LC-AI cells after treatment with translation elongation inhibitor emetine dihydrochloride at different time

points (8 and 16 hours). (B) Western blot analysis of RERF-LC-AI cells after transfection with scrRNA (25 nM), and siNrf2 (25 nM). 48 hours after transfection, cells were treated with translation elongation inhibitor emetine dihydrochloride at different time points (15 minutes, 2 and 4 hours). Actin was used as loading control. Arrows indicate the two detected Nrf2 forms.

Next, we performed the same experiment in the primary NSCLC cell line and compared the influence of Nrf2 on the HLA-I expression. Interestingly, in the primary NSCLC cell line, we observed a high stability of HLA-A, despite treatment with translation elongation inhibitor for 4 hours and no changes in the expression after silencing of Nrf2, comparing to the scrRNA control. However, there are significant differences in HLA-C expression after silencing of Nrf2, after 2 and 4 hours of treatment with emetine, indicating that the stable Nrf2 form could affect the stability of HLA-C in primary NSCLC cell line (Fig. 16). In the case of HLA-A, the longer time points of emetine treatment would probably allow us to see if Nrf2 affects HLA-A stability, however, longer exposure to the emetine could be harmful for the cells, which could significantly affect the results.

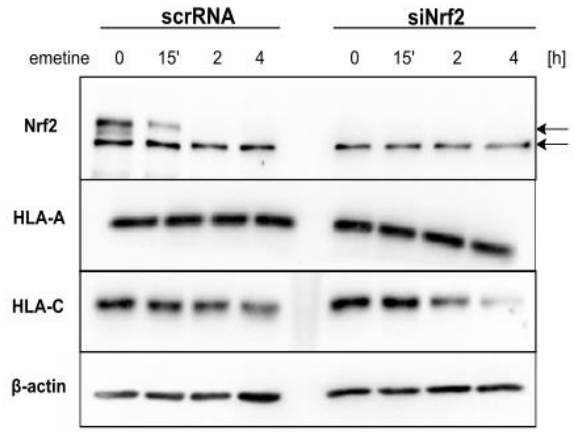

Figure 16. **HLA-I stability in primary cells derived from non-small cell lung cancer (NSCLC) patient.** Western blot analysis of NSCLC cells after transfection with scrRNA (25 nM), and siNrf2 (25 nM). 48 hours after transfection, cells were treated with translation elongation inhibitor emetine dihydrochloride at different time points (15 minutes, 2 and 4 hours). Actin was used as loading control. Arrows indicate the two detected Nrf2 forms.

3.1.2.5. Interaction between Nrf2 and HLA class I molecules

Based on the collected results, it seemed that Nrf2 can affect HLA-I expression, even though the mechanism was still uncertain. The first step in trying to determine the mechanism was to examine whether Nrf2 can directly interact with HLA-I molecules. For that purpose, we performed co-immunoprecipitation (co-IP) of Nrf2 and HLA-I proteins in the non-small cell lung cancer cell lines, A549 and RERF-LC-AI (Fig. 17A and B). The results showed that Nrf2 and HLA-I molecules co-precipitate indicating a direct interaction. Nrf2-HLA-I interaction was further validated and confirmed in primary NSCLC cell line (Fig. 17C).

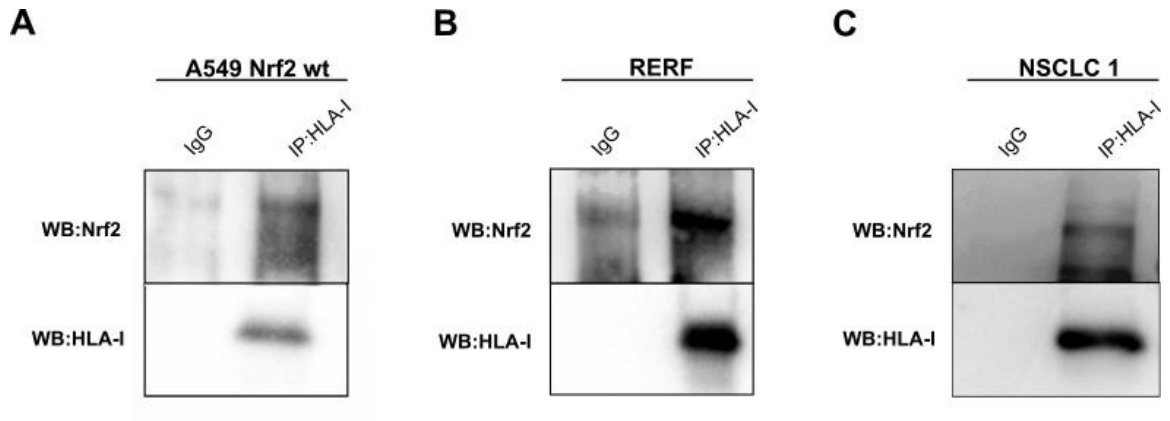

Figure 17. **Nrf2 and HLA-I molecules co-immunoprecipitate.** (A) Co-immunoprecipitation of HLA-I proteins using anti-HLA class I antibodies [W6/32] in A549 cell line. IgG mouse was used as a control. (B) Co-immunoprecipitation of HLA-I proteins using anti-HLA class I antibodies [W6/32] in RERF-LC-AI cell line. IgG mouse was used as a control. (C) Co-immunoprecipitation of HLA-I proteins using anti-HLA class I antibodies [W6/32] in primary NSCLC cell line. IgG mouse was used as a control.

The next step was to see where this interaction between Nrf2 and HLA-I molecules could take place. For this purpose, we made use of the immunofluorescent staining and confocal microscopy. In A549 cells, Nrf2 was localized in the nucleus and in the cytoplasm, however nuclear localization was prevalent and was expected since these cells have a constitutive activation of Nrf2 which means constant nuclear translocation of Nrf2 (Fig. 18A). HLA-I molecules were observed in the ER and the Golgi apparatus, as expected, since they fold and bind the cytosolically derived peptides within the ER lumen. After peptide loading, HLA-I molecules traffic through the Golgi apparatus to the plasma membrane (124). We observed the co-localization of Nrf2 and HLA-A, however it is hard to precisely say if the co-localization is mainly in the cytoplasm, but it seems that it could be also in the endoplasmic reticulum (ER)

and/or Golgi (Fig. 18A). The known localization of Nrf2 under no stress conditions is in the cytoplasm, therefore the co-localization with HLA-I molecules is probably happening there. Nrf2 signaling was shown to be critical for the cell survival following ER stress (15), however Nrf2 localization was not previously reported in the ER.

Interestingly, the co-localization was also observed in the nucleus, which was quite peculiar, taking into consideration that to the best of our knowledge, HLA-I molecules have not been reported in the nucleus. However, our observation was the same while using different anti-HLA-A antibodies (anti-HLA-A antibody from Origene and KO validated anti-HLA-A antibody from Abcam) indicating that it is not the case of the unspecific antibody signal (Fig. 18A and 19A). Similarly, we observed the co-localization of HLA-C and Nrf2 in cytoplasmic cellular compartments, indicating the possibility of their interaction (Fig. 18B).

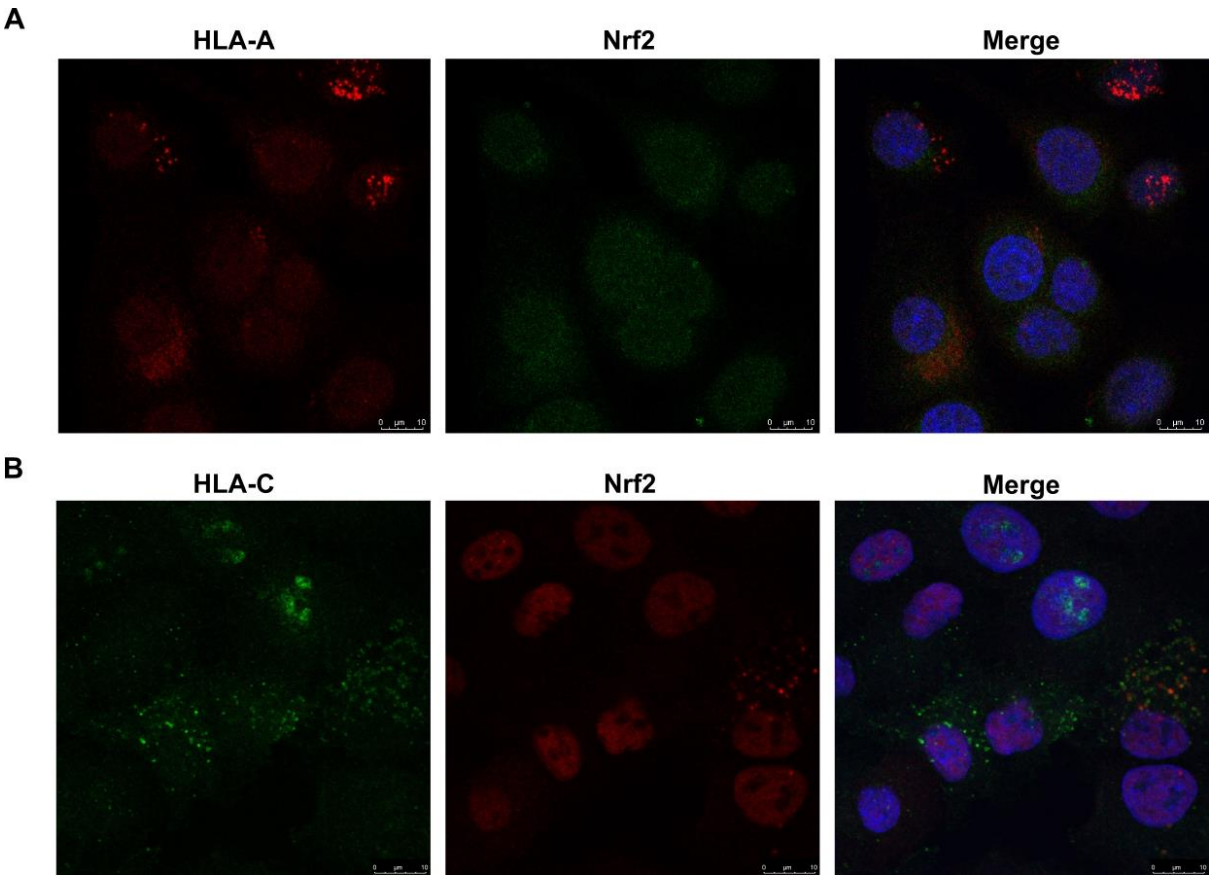

Figure 18. **Nrf2 is co-localizing with HLA-A and HLA-C in A549 cell line**. (A) For immunofluorescence, A549 cells were stained with primary anti-Nrf2 (1:500) and anti-HLA-A (1:500; Origene) antibodies, overnight. After washing, cells were stained with secondary antibodies, Alexa Flour 488 goat anti-rabbit and Alexa Fluor 555 goat anti-mouse, and visualized using confocal microscope. (B) A549 cells were stained with primary anti-Nrf2 (1:500) and anti-HLA-C (1:500) antibodies, overnight.

After washing, cells were stained with secondary antibodies, Alexa Flour 488 goat anti-rabbit and Alexa Fluor 555 goat anti-mouse and visualized using confocal microscope. Nuclei were stained with DAPI.

The immunofluorescence staining of another lung cancer cell line, RERF-LC-AI, showed similar co-localization of HLA-A and Nrf2 mostly in the cytoplasmic cellular compartment. Interestingly, Nrf2 was mostly localized in the cytoplasm in these cells, comparing to the A549 cells, confirming that indeed in the cells without any known mutation in the pathway and under no stress conditions, Nrf2 is mostly localized in the cytoplasm and could be translocated in the nucleus upon activation. Also, as mentioned before, the localization of HLA-A was again observed in the nucleus even though different anti-HLA-A antibody was used (Fig. 19A). Regarding staining with HLA-C antibodies, the signal was quite weak, but mostly localized in the ER, where it is co-localized with Nrf2 (Fig. 19B).

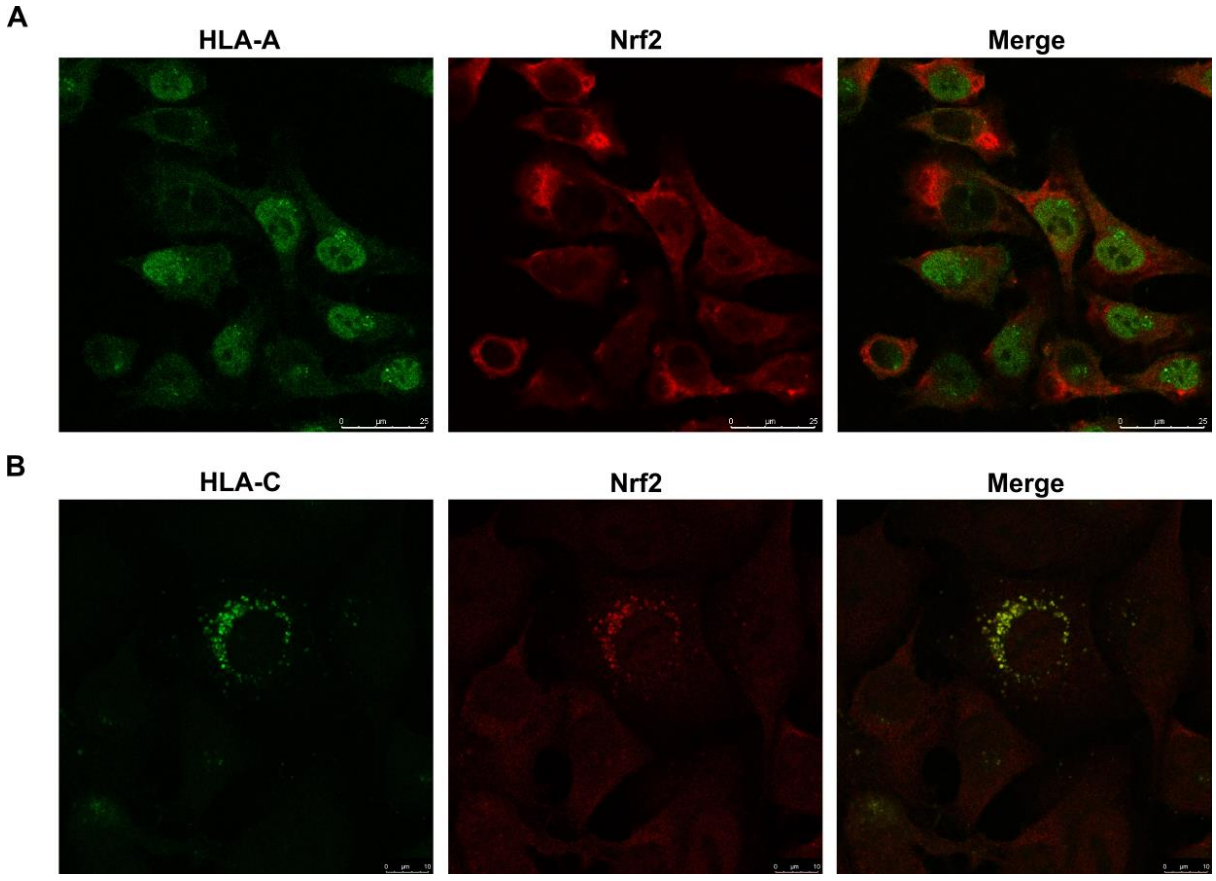

Figure 19. **Nrf2 is co-localizing with HLA-A and HLA-C in RERF-LC-AI cell line**. (A) For immunofluorescence, RERF cells were stained with primary anti-Nrf2 (1:500) and anti-HLA-A (1:500; Abcam) antibodies, overnight. After washing, cells were stained with secondary antibodies, Alexa Flour 488 goat anti-rabbit and Alexa Fluor 555 goat anti-mouse, and visualized using confocal microscope.

(B) RERF cells were stained with primary anti-Nrf2 (1:500) and anti-HLA-C (1:500) antibodies, overnight. After washing, cells were stained with secondary antibodies, Alexa Flour 488 goat anti-rabbit and Alexa Fluor 555 goat anti-mouse, and visualized using confocal microscope.

To sum up, although the co-localization does not have to mean that the proteins are in the direct interaction, it can give an insight if the proteins are localized in the same cellular compartment, which increases the chances of their direct interaction. In the case of A549 and RERF lung cancer cell lines, Nrf2 is co-localizing with HLA-A and HLA-C in the different cellular compartments. HLA-I molecules were observed in the ER and the Golgi apparatus, as expected, however, HLA-A was also observed in the nucleus, in both cell lines and using two different types of anti-HLA-A antibodies. This was further confirmed with the silencing of the HLA-A expression using siRNA and immunofluorescent staining (Fig. S2). Additionally, we managed to co-immunoprecipitate HLA-A with the nuclear marker histone H2B, indicating that indeed HLA-A can be localized in the nucleus (Fig. S3).

Following the co-localization studies, we performed proximity ligation assay (PLA). It is a unique method for the detection of protein-protein interactions *in situ* at endogenous protein levels. The method utilizes specific antibodies for the proteins of the interest, covalently linked with specific single-stranded oligonucleotides (PLA probes). A hybridization step is followed by DNA amplification with fluorescent probes that permit visualization of the spots of proximity by confocal microscopy (194,195).

To be able to perform PLA, it is crucial to have specific antibodies for the proteins of interest coming from different species. We obtained mouse and rabbit antibodies for both, Nrf2 and HLA-A proteins, to be able to check different combinations. In A549 lung cancer cells, we detected positive proximity signals of Nrf2 and HLA-A, comparing to the appropriate negative controls (Fig. 20). These results confirmed that Nrf2 and HLA-A proteins are in close proximity and that they are interacting. We also detected an unspecific positive signal in the samples stained only with HLA-A (R; rabbit) antibodies, however when we quantified the green foci detected in the control samples and in the PLA samples, there was a significantly more spots detected in the PLA samples, indicating the reliability of the results (Fig. 20A). We also performed the PLA with the opposite combination of antibodies; HLA-A (M; mouse) and Nrf2 (R; rabbit) and observed the weaker signal of the proximity. However, the difference between control samples and PLA samples was significant, indicating that also with the opposite combination of the antibodies, the interaction between HLA-A and Nrf2 was detected (Fig. 20B). The interaction was observed in the different cellular compartments, including nucleus, which is in the correlation with the co-localization results.

Similarly, in RERF lung cancer cells, HLA-A (R) antibodies have shown a false positive signal in the control samples, while Nrf2 (M) antibodies were a proper negative control. In the PLA sample, we detected a significantly higher number of green foci per cell, comparing to the controls, confirming the interaction of HLA-A and Nrf2 also in RERF cells (Fig. 21A). In the case of HLA-A (M) and Nrf2 (R) antibodies, the detected signal was weak, showing no significant difference between the negative controls and PLA samples (Fig. 21B).

To sum up, HLA-A and Nrf2 were shown to be in the close proximity indicating their direct interaction in A549 and RERF lung cancer cells. HLA (R) antibody was shown to give unspecific positive signals, however, in the samples stained with both HLA-A (R) and Nrf2 (M), the detected signal was much stronger and the number of the detected green foci was significantly higher. In the opposite case, when the samples were stained with HLA-A (M) and Nrf2 (R) antibodies, the signal in the both tested cell lines was quite weak and the number of detected foci was lower, probably due to the weaker antibodies specificity.

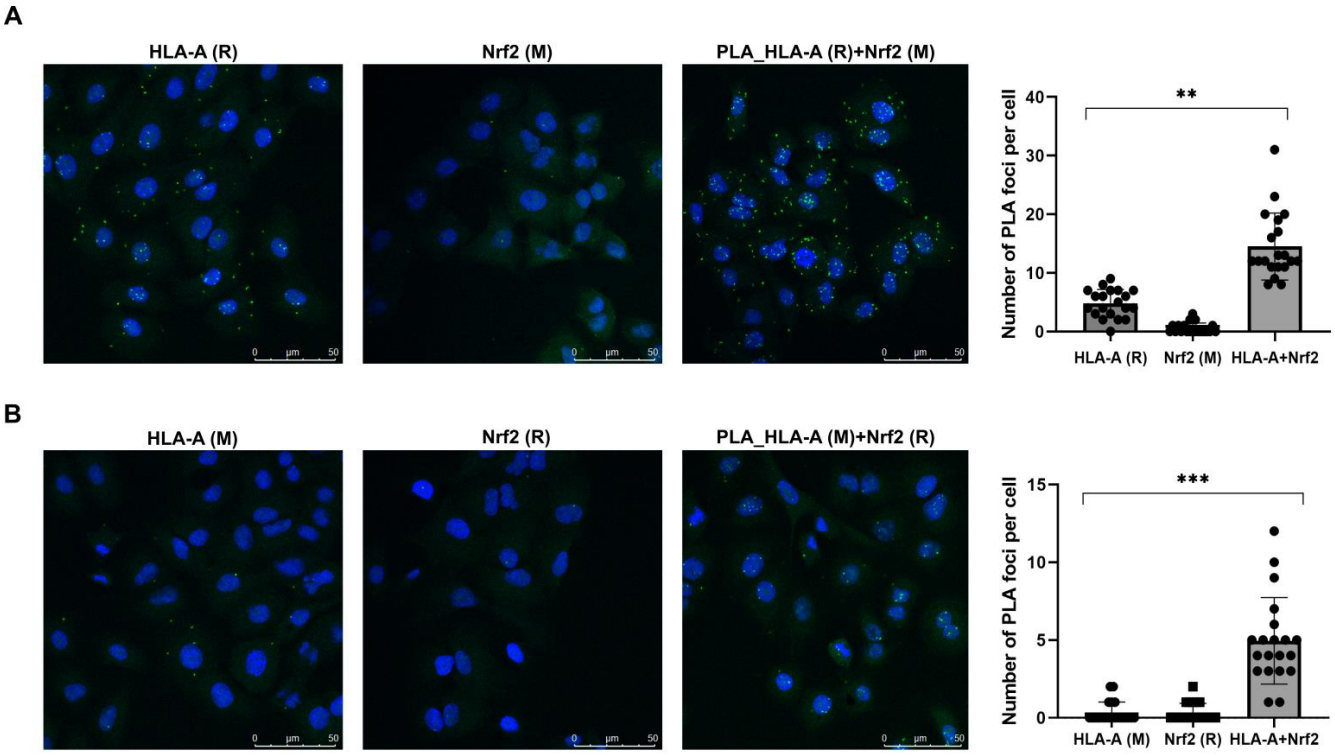

Figure 20. **HLA-A and Nrf2 are in close proximity in A549 cells.** A549 cells were stained with (A) anti-HLA-A (R) and anti-Nrf2 primary antibodies and (B) anti-HLA-A (M) and anti-Nrf2 (R) primary antibodies overnight, washed in suitable buffer and incubated with PLA probes for 60 minutes. The next steps were hybridization and amplification. Finally, the samples were incubated with Atto488 fluorophore, while nuclei were stained with DAPI. Cells were mounted with mounting medium and analyzed with confocal microscope. Representative images of PLA (green) and quantification of PLA

are shown. Statistics were performed with a one-way ANOVA with post hoc test (Bonferroni correction) and Brown-Forsythe test in GraphPad Prism, where n = 20, **p < 0.0026, ***p = 0.0001.

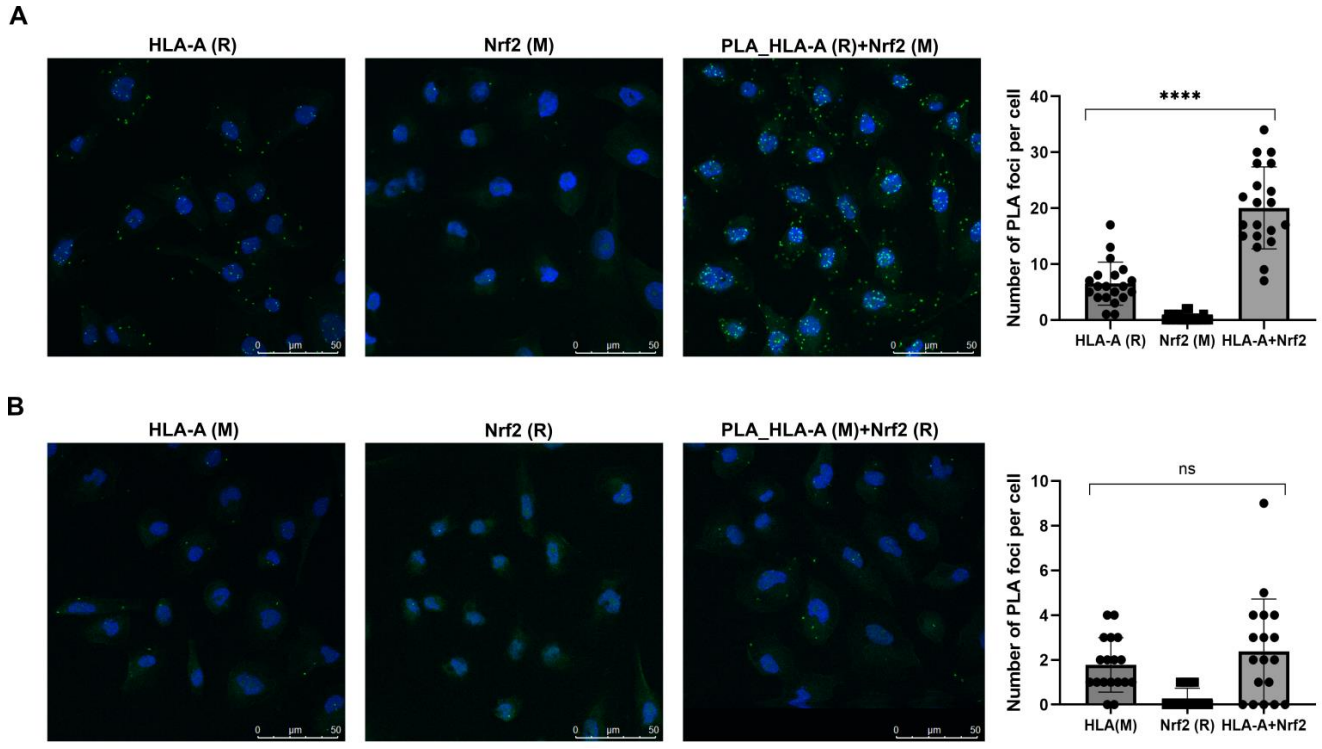

Figure 21. **HLA-A and Nrf2 are in close proximity in RERF cells.** RERF cells were stained with (A) anti-HLA-A (R) and anti-Nrf2 primary antibodies and (B) anti-HLA-A (M) and anti-Nrf2 (R) primary antibodies overnight, washed in suitable buffer and incubated with PLA probes for 60 minutes. The next steps were hybridization and amplification. Finally, the samples were incubated with Atto488 fluorophore, while nuclei were stained with DAPI. Cells were mounted with mounting medium and analyzed with confocal microscope. Representative images of PLA (green) and quantification of PLA are shown. Statistics were performed with a one-way ANOVA with post hoc test (Bonferroni correction) and Brown-Forsythe test in GraphPad Prism, where n = 20, ****p < 0.0001, ns=not-significant.

Next, in the collaboration with Dr Monikaben Padariya and Dr Umesh Kalathiya, we obtained the data from molecular modeling and molecular dynamics simulations, predicting the interaction between Nrf2 and HLA-I molecules. Since A549 cell line is fully sequenced, they performed the modeling of HLA-A, B, and C and Nrf2 based on the A549 cell line specific sequence (https://web.expasy.org/cellosaurus/CVCL_0023) (Fig. 22).

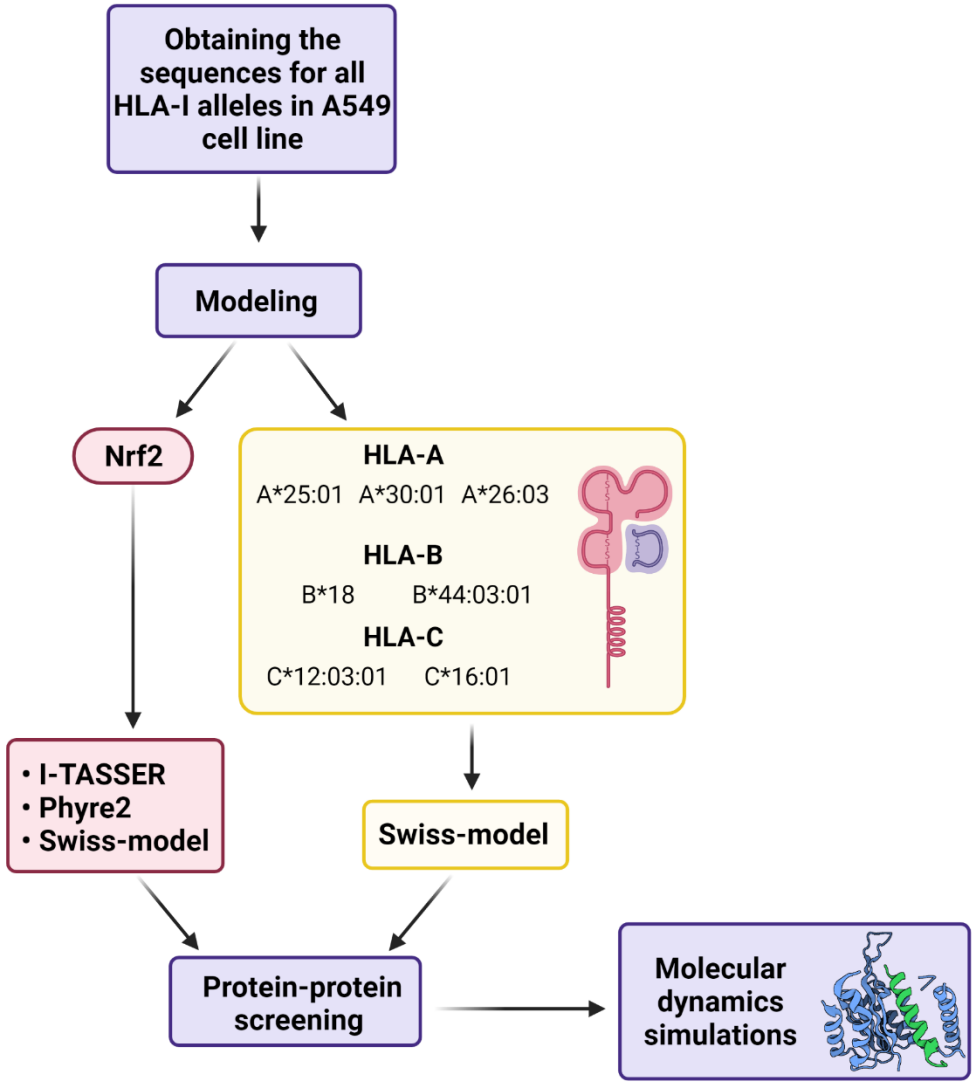

Figure 22. **Schematic overview of molecular modeling and molecular dynamics simulations workflow.** The sequences for all HLA-I alleles in A549 cells were retrieved from publicly available data (http://www.iedb.org). The structures of the Nrf2 and different HLA class I molecules were modeled and protein-protein screening was performed choosing the best Nrf2/HLA-A, B and C allele. Finally, molecular dynamics simulations allowed to see the changes in the confirmations in time and influence of Nrf2 on HLA-I stability.

The screening of Nrf2 against different HLA-A molecules showed that all three haplotypes of HLA-A are forming high number of interactions with Nrf2 (Fig. 23). The binding energies of different HLA-A alleles with Nrf2 have shown that the interactions between HLA-A and Nrf2 are strong. The values of binding energies for each HLA-A allele are similar, with the highest binding affinity for HLA-A*25:01 allele (Fig. 23D). Moreover, in the case of HLA-A, Nrf2 is bound to the place in the structure that could include the stability of HLA-A. Regarding the HLA-B alleles, the Nrf2 binding pattern is different. It binds to the peptide cavity of both HLA-B alleles, therefore the number of interactions is lower and the binding affinity is weaker (Fig. 24). Binding pattern of Nrf2 and HLA-C alleles is similar to the binding with HLA-B alleles. Nrf2 binds to the peptide cavity of HLA-C alleles and forms a lower number of interactions comparing to the binding with HLA-A alleles (Fig. 25).

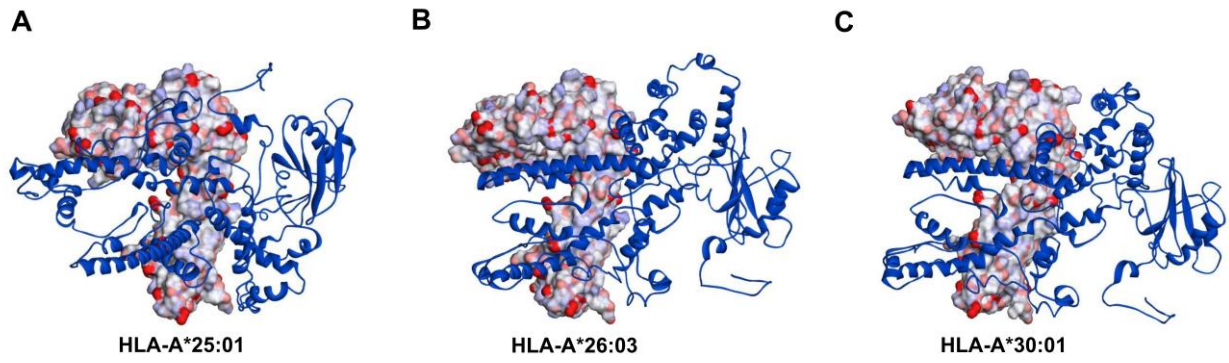

D

HLA-A allele	Binding energy with Nrf2 (kcal/mol)
A*25:01	-65.75
A*26:03	-72.71
A*30:01	-73.24

Figure 23. **HLA-A alleles are forming high number of interactions with Nrf2.** Molecular modeling predictions of binding between Nrf2 and different HLA-A alleles, based on the binding energies. (A) Binding of HLA-A*25:01 allele with Nrf2. (B) Binding of HLA-A*26:03 allele with Nrf2. (C) Binding of HLA-A*30:01 allele with Nrf2. (D) Binding energies (kcal/mol) of the each HLA-A allele with Nrf2. Nrf2 structure is marked in blue.

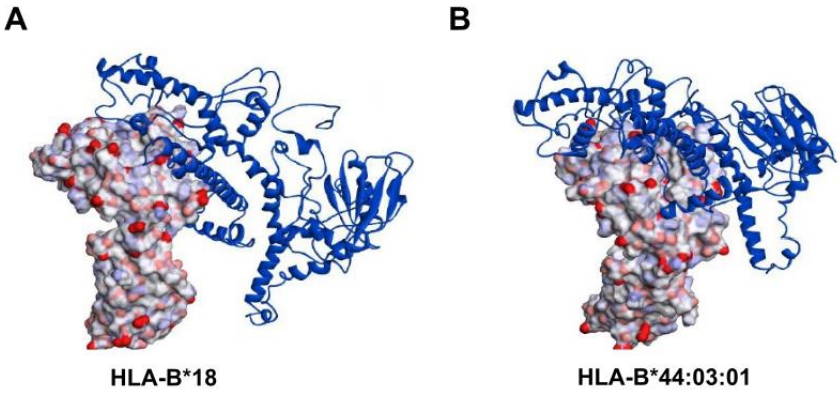

C

HLA-B allele	Binding energy with Nrf2 (kcal/mol)
B*18	-72.95
B*44:03:01	-76.45

Figure 24. **HLA-B alleles are forming low number of interactions with Nrf2.** Molecular modeling predictions of binding between Nrf2 and different HLA-B alleles, based on the binding energies. (A) Binding of HLA-B*18 allele with Nrf2. (B) Binding of HLA-B*44:03:01 allele with Nrf2. (C) Binding energies (kcal/mol) of the each HLA-B allele with Nrf2. Nrf2 structure is marked in blue.

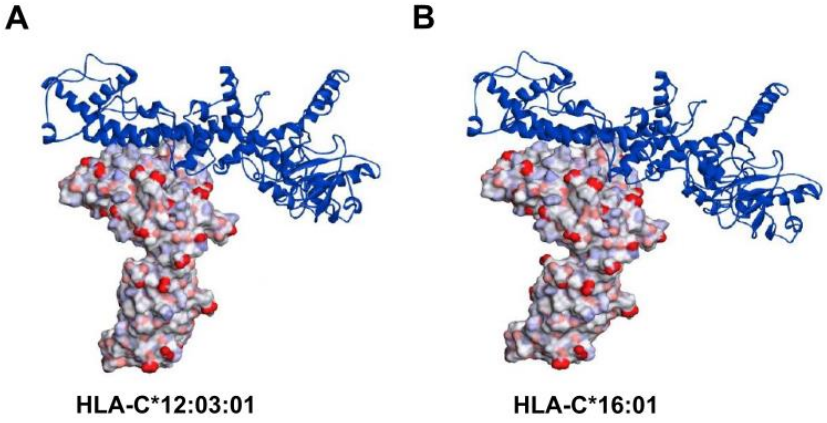

C

HLA-C allele	Binding energy with Nrf2 (kcal/mol)
C*12:03:01	-72.99
C*16:01	-75.53

Figure 25. **HLA-C alleles are forming low number of interactions with Nrf2.** Molecular modeling predictions of binding between Nrf2 and different HLA-C alleles, based on the binding energies. (A) Binding of HLA-C*12:03:01 allele with Nrf2. (B) Binding of HLA-C*16:01 allele with Nrf2. (C) Binding energies (kcal/mol) of the each HLA-C allele with Nrf2. Nrf2 structure is marked in blue.

The predictions have shown the two possible conformations that Nrf2 can form with HLA molecules: binding to the peptide cavity and binding to the place that could induce HLA stability. In the case of HLA-A molecules, Nrf2 binds to the place that could induce the HLA-A stability, while in the case of HLA-B and HLA-C, the binding pattern is different and Nrf2 binds to the peptide cavity.

To check the stability of the HLAs with/without Nrf2, the RMSDs (root-mean-square deviations) were computed (Fig. 26). RMSD calculations are usually used for measuring the difference between the backbones of a protein from its initial structural conformation to its final position. The stability of the protein relative to its conformation can be determined by the deviations produced during the course of its simulation (196). The RMSDs suggests that the presence of Nrf2 protein in the complex stabilizes HLA-A molecules (Fig. 26A). In the case of HLA-B and HLA-C, such a significant difference was not observed, however only for HLA-C*12:03:01 allele, we observed higher stability when Nrf2 protein was present in the complex (Fig. 26C). The HLA-B showed the highest stability in general and was not affected much by the presence or absence of the Nrf2 protein in the complex (Fig. 26B). Furthermore, it was confirmed that all three haplotypes of HLA-A molecules are forming high number of interactions with Nrf2, while in the case of HLA-B and HLA-C, the binding pattern is different (Fig. 27).

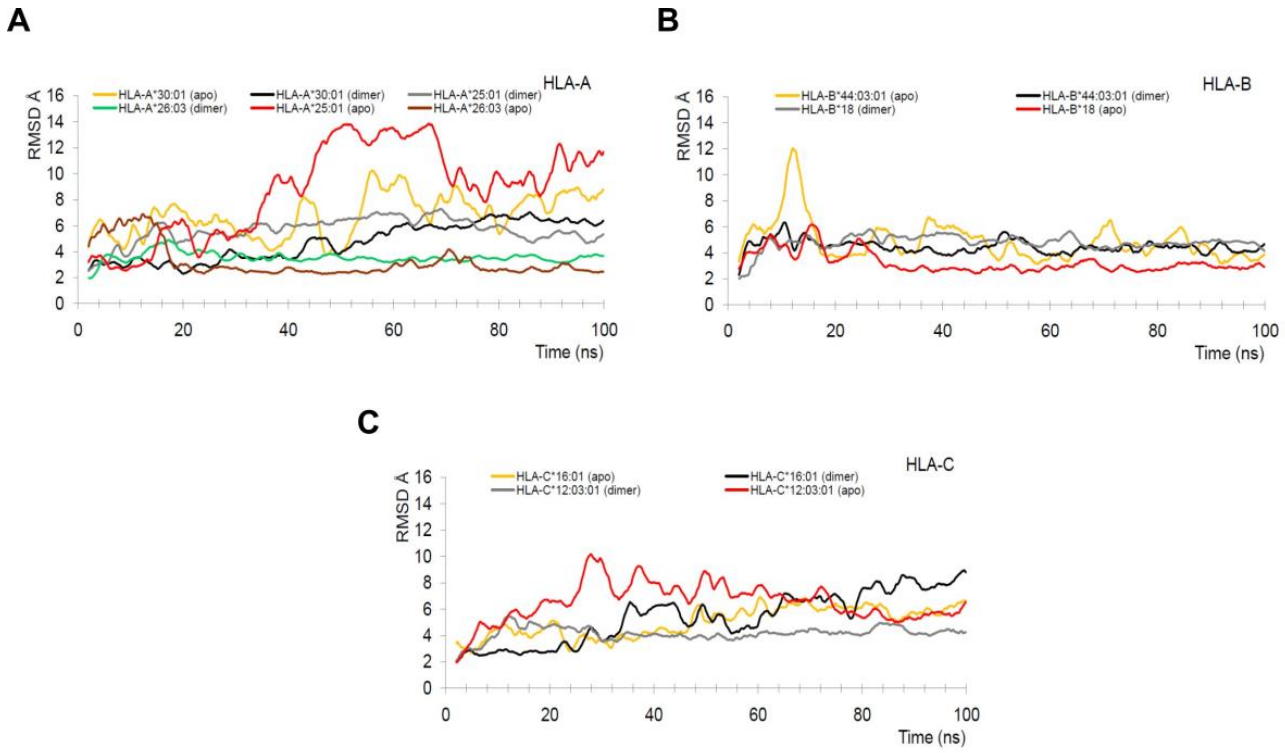

Figure 26. **Stability check for HLA molecules with/without Nrf2.** In order to check the stability of HLAs with/without Nrf2, the RMSDs (root-mean-square deviations) were computed. A RMSD value is expressed in Ångström (Å) which is equal to 10^{-10} m. (A) RMSD calculations for HLA-A molecules showed large destabilizing structures for the apo-HLA system, while the presence of Nrf2 protein in the complex stabilizes HLA-A molecules. (B) RMSD calculations for HLA-B molecules showed stabilized system, not affected much by presence or absence of Nrf2 protein in the complex. (C) RMSD calculations for HLA-C molecules showed also quite stable system. The significant difference was only observed in the case of HLA-C*12:03:01, that was stabilized upon the presence of Nrf2 in the complex. Apo, HLA-I only; Dimer, HLA-I in the presence of Nrf2.

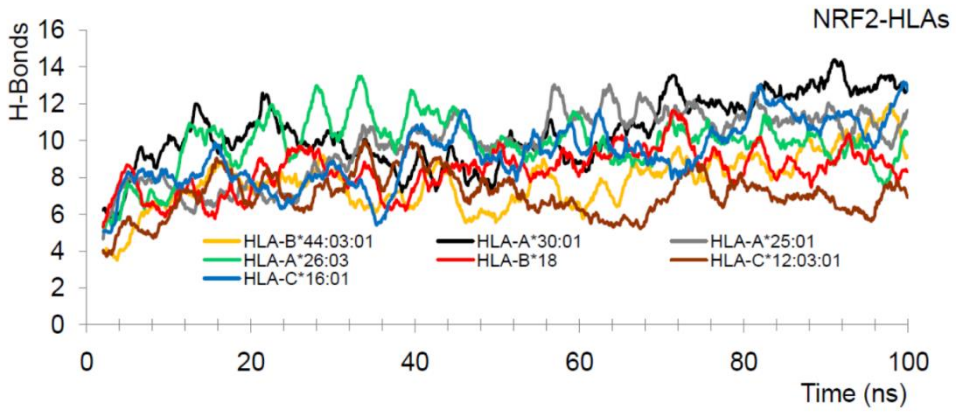

Figure 27. **Nrf2 forms a high number of interactions with HLA-A molecules.** The graph presents the calculations from molecular dynamics simulations and number of hydrogen bonds created in time, between the Nrf2 protein and different alleles of HLA-A, HLA-B and HLA-C molecules. All three haplotypes of HLA-A form a high number of interactions with Nrf2, while the binding pattern with HLA-B and HLA-C is different.

3.1.2.6. Extracellular and intracellular HLA class I expression in A549 Nrf2 wt and Nrf2 KO cells

Taking into consideration all the collected results, it seems that Nrf2 can affect the stability of HLA-I molecules, particularly HLA-A, and that Nrf2 and HLA-I molecules are in the direct interaction. To see if there are any differences between the expression of HLA-I molecules on the cell surface and intracellularly in A549 Nrf2 wt and Nrf2 KO cells, we performed extracellular and intracellular staining of the cells and analyzed them with flow cytometry.

The flow cytometry data have shown an interesting differences between extracellular and intracellular HLA-I expression in A549 Nrf2 wt and A549 Nrf2 KO. On the cell surface, A549 Nrf2 wt cells have shown higher expression of HLA-I molecules comparing to the Nrf2 KO cells, while intracellularly Nrf2 KO cells showed slightly higher expression of HLA-I molecules (Fig. 28). These results indicate that Nrf2 could be responsible for sequestration/stabilization of HLA-I molecules on their way to the cell surface, where they present antigenic peptides to the cytotoxic T cells.

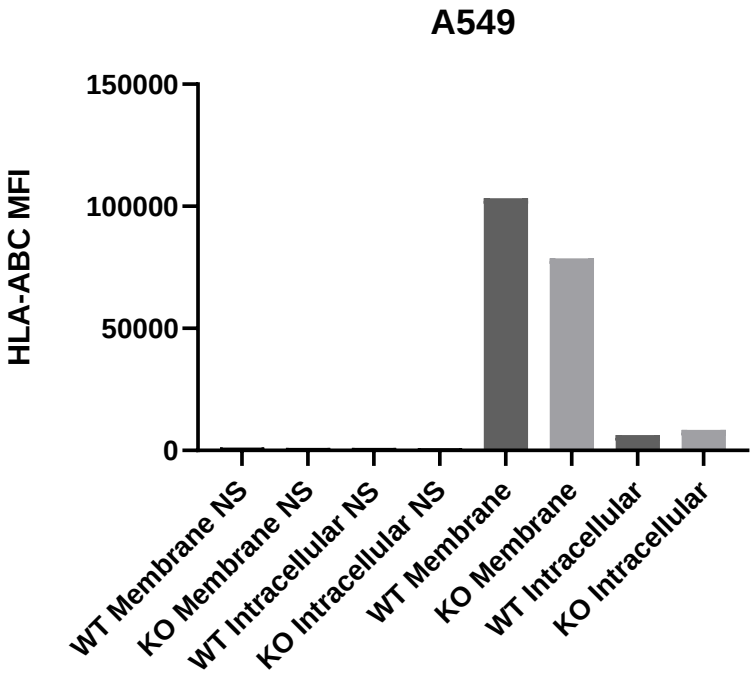

Figure 28. **A549 Nrf2 wt cells have lower expression of intracellular, but higher expression of extracellular HLA-I compared to the A549 Nrf2 KO cells.** Flow cytometry analysis of A549 Nrf2 wt and Nrf2 KO cells under no stress conditions. Extracellular (membrane) HLA-I were stained with anti-HLA-ABC-BV711 antibody, while intracellular HLA-I were stained with anti-HLA-ABC-FITC antibody. Data acquisition and analyses were performed by fluorescence activated cell sorter ARIA FUSION. NS, not stained.

3.1.3. Discussion

Nrf2 has a role in immune surveillance through the modulation of the immune cells functions. Its role was mostly described on the transcriptional level and as a crosstalk with different factors and pathways. However, our results have shown for the first time that the role of Nrf2 could be beyond the transcriptional regulation of its target genes. Until now, the effect of Nrf2 on the antigen presentation pathway has not been reported, however, there were indications that Nrf2 could affect the expression of HLA-I molecules and genes involved in the antigen presentation (103,128).

Our results have shown that the depletion of Nrf2 in normal lung fibroblasts and in lung adenocarcinoma A549 with functional knockout of Nrf2 decreased HLA-I protein and cell surface expression. However, this effect was not observed on the RNA level, it was rather opposite, implying an existence of a positive feedback loop. These results indicated that Nrf2 could affect the synthesis of HLA-I proteins or alternatively, their degradation. This observation was quite unexpected, since Nrf2 was mostly described as a transcription factor which influences the transcription of its target genes and in that way regulates their protein expression. However, in this case, the effect on the *HLA-I* RNA level after silencing of *NFE2L2* expression was opposite, compared to the HLA-I protein and cell surface expression.

To be able to investigate the possible impact of Nrf2 on HLA-I stability (rate of degradation), we had to combine the *NFE2L2* knockdown with the translation elongation inhibition. Taking into consideration the general differences between HLA-I alleles and the extraordinary stability of HLA-A, we also looked at the HLA-C protein expression in these stability experiments. In the squamous lung cancer cell line RERF-LC-AI, the expression of HLA-A protein levels was significantly reduced after siNrf2 combined with translation inhibition already after 15 minutes of treatment, leading to the assumption that Nrf2 can affect the stability of HLA-A proteins. In the primary cell line from NSCLC patient, silencing of Nrf2 and inhibition of translation reduced the expression of HLA-C proteins, while HLA-A expression remained stable, even after 4 hours of emetine treatment. These results indicated that there are differences in the expression and stability between different HLA-I alleles and that it could be important to investigate each of them separately. However, sometimes that is not possible due to the antibody availability and specificity, e.g. while determining HLA-I cell surface expression, where the commonly used antibody (pan-HLA-I antibody W6/32) detects all the HLA-I alleles together.

When we compared the stability of HLA-I molecules in A549 wild-type and Nrf2 KO cells, we observed that HLA-I molecules are less stable in the Nrf2 KO cells. In addition, the click-it labeling technology allowed us to compared the rate of the newly synthesized HLA-I molecules

and the results have shown that A549 Nrf2 KO cells have less newly synthesized HLA-I molecules, compared to the A549 wild-type cells. These results indicated that Nrf2 could play a role in stabilizing HLA-I molecules and preventing their degradation as well as facilitating synthesis. To further investigate this hypothesis, we could have a look if the *NFE2L2* and *HLA-I* RNAs are translated together on the ribosome.

The collected data up to this point indicated that Nrf2 has an influence on the HLA-I expression, however the mechanism was unclear. Therefore, it was important to examine if the direct interaction between Nrf2 and HLA-I is possible. The co-immunoprecipitation results suggested direct protein-protein interaction between Nrf2 and HLA-I, in both tested cell lines and in primary cell line from NSCLC patient, under homeostatic conditions. Immunofluorescence gave us an insight where this interaction could be happening. Nrf2 was localized in the cytoplasm in both A549 and RERF cells, however since A549 cells have a constitutively active Nrf2, there was a high amount of Nrf2 observed also in the nucleus under homeostatic conditions. We were surprised to see that HLA-A was not only localized in the cytoplasmic compartment, but also in the nucleus, which was not reported before. HLA-C was mostly localized in the ER. In addition to the immunofluorescence results, proximity ligation assay showed that Nrf2 and HLA-A are in the close proximity, therefore indicating a direct interaction.

Based on the experimental data, Dr Monikaben Padariya and Dr Umesh Kalathiya performed molecular modeling and molecular dynamics simulations for predicting the interactions between Nrf2 and HLA-I molecules. The results have shown that all three haplotypes of HLA-A are forming high number of interactions with Nrf2 and Nrf2 in the complex stabilizes HLA-A molecules. Nrf2 binding pattern with HLA-B and HLA-C is different, comparing to the HLA-A, and only one HLA-C allele is stabilized by Nrf2 binding. The predictions confirmed the differences between the HLA-I alleles and their interaction with Nrf2, and have shown that the interaction with HLA-A is the strongest. It would be interesting to further investigate the possible interaction and proximity of HLA-C and Nrf2 and compare it to the Nrf2 interaction with HLA-A.

The flow cytometry data have shown that A549 Nrf2 KO have higher expression of intracellular HLA-I compared to the A549 Nrf2 wt cells, however the situation is opposite on the cell surface, where HLA-I are presenting antigenic peptides to the cytotoxic T cells. This was an additional proof that Nrf2 affects the stability of HLA-I expressed on the cell surface, confirming the molecular modeling and molecular dynamics predictions.

Up until now, Nrf2 was described as transcription factor which can affect protein expression through transcriptional regulation. However, our results have shown that Nrf2 stabilizes HLA-I expression in the direct protein-protein interaction, suggesting a novel, transcription-independent role of Nrf2.

PART 2. Identification of a stable, non-canonically regulated Nrf2 form in lung cells

3.2. Background and aim

Most often studies on Nrf2 include antibodies, but there are concerns regarding Nrf2 migration in the sodium dodecyl sulfate–polyacrylamide gel electrophoresis (SDS-PAGE) and the specificity of some anti-Nrf2 antibodies. Although in the first part of my project we were using commercially available Nrf2 antibodies, we have observed the multiple Nrf2 band detection. Specifically, the detected band showing high stability upon translation elongation inhibition caught our attention. Therefore, the second part of my project was focused on the precise validation of the commercially available Nrf2 antibodies, to be able to identify the protein bands in SDS-PAGE that correspond to Nrf2.

One significant obstacle in the proper detection of Nrf2 is ‘’unusual’’ migration from its predicted size. Predicted molecular weight for migration of Nrf2 is ~55-65 kDa, according to Nrf2’s open reading frame size of ~2.2-kb, but Lau et al. have provided evidence that the biologically relevant species of Nrf2 migrate between ~95 and 110 kDa. The pattern of unexpected Nrf2 migration is still uncertain but the abundance of acidic residues in Nrf2 could be the main reason (45). In addition, Kemmerer et al. have compared different human Nrf2 antibodies in order to validate their specificity. They have reported that the Nrf2 monoclonal antibody EP1808Y from Abcam, detects another protein that co-migrates with the verified Nrf2. By using siRNA and immune-depletion experiments, they excluded the possibility that the detected band ~95 kDa corresponds to any form of Nrf2 (90).

Additionally, Nrf2 is phosphorylated by various kinases, but even after phosphatase treatment, two Nrf2 forms were detected (17,197,198). The origin of these forms is not clear. Latest studies indicate that the existence of multiple Nrf2 forms of increased stability, that lack exon 2 or exon 2 and 3, is due to an alternative splicing in lung and head and neck cancers (53).

3.2.1. Methodology

In this study, we have used three NSCLC cell lines: an adenocarcinoma A549, a squamous cell carcinoma RERF-LC-AI (further referred as RERF) and H1299, that differ in the Nrf2 level and activation status. A549 cells have a homozygous *KEAP1* mutation (G333C) that disrupts

binding of Keap1 and Nrf2, leading to accumulation and constitutive activation of Nrf2 (54). The RERF and H1299 cells do not have any known *NFE2L2/KEAP1* mutation (181,199) and therefore, low levels of Nrf2 under homeostatic conditions. We have also made use of A549 Nrf2 functional KO cells (180), two primary NSCLC cell lines derived from lung tumors of two patients (further referred as NSCLC 1 and NSCLC 2) and normal lung fibroblasts (further referred as NLF).

3.2.2. Results

3.2.2.1. Different Nrf2 forms are expressed in lung cells

Firstly, we analyzed the Nrf2 migratory pattern using 8% SDS-PAGE with Abcam EP1808Y and Cell Signaling D1Z9C antibodies that recognize different Nrf2 epitopes. The epitope of the EP1808Y antibody is located in the C-terminus, surrounding 550 aa, while the epitope of D1Z9C is located in the middle of Nrf2 protein – in the proximity of 275 Ala (200).

Both antibodies detected two bands in A549 Nrf2 wt cells, the lower one of ~105 kDa and the upper, below 130 kDa, while in RERF cells only the lower 105 kDa was detected under steady-state conditions. Interestingly, in the functional Nrf2 KO cells, both the 105 kDa and 130 kDa signals were significantly weaker or disappeared, indicating that both bands are Nrf2-specific (Fig. 29). It is important to highlight again that the reason we were able to detect Nrf2 protein in A549 Nrf2 KO cells, is that even though this is the Nrf2 KO cell line, Nrf2 protein can still be produced in this cells, but its functionality is significantly reduced. Since these two antibodies were mostly recognizing the same Nrf2 pattern, we decided to further use Abcam EP1808Y antibody because of its higher specificity and better signal.

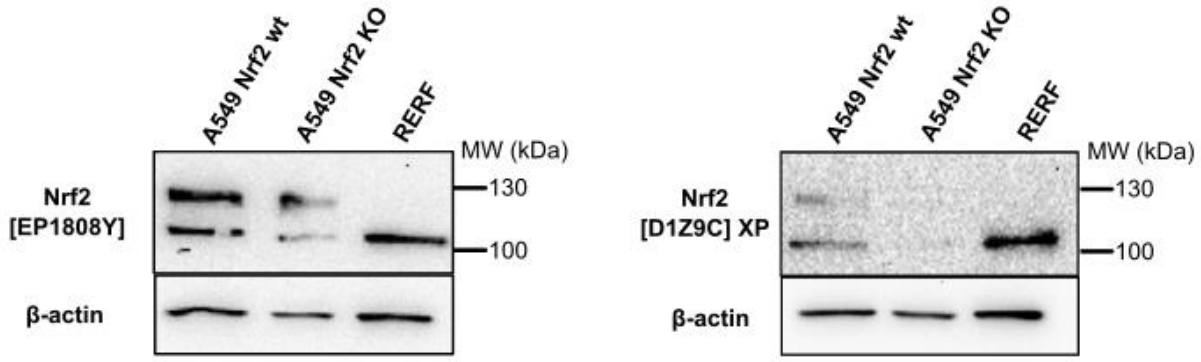

Figure 29. **Nrf2 migratory pattern in lung cancer cells.** Nrf2 migratory pattern in 8% SDS-PAGE gel, in A549 Nrf2 wt, A549 Nrf2 KO, and RERF cells with two monoclonal anti-Nrf2 antibodies—Abcam [EP1808Y] and Cell Signaling (CS) (D1Z9C). Actin was used as a loading control.

Further results have shown that endogenous Nrf2 actually migrates in 8% SDS-PAGE not as two, but as three bands in all lung cancer cell lines, primary cell lines and normal lung fibroblasts (Fig. 30). The middle band is not always visible, probably due to the close proximity to the upper ~130 kDa band and inability to separate them in every gel. The lowest Nrf2 migrating form of ~105 kDa is differently expressed between cells with the highest expression in RERF, followed by A549, NLF, H1299 and primary NSCLC cells, which have the lowest expression of all three Nrf2 forms.

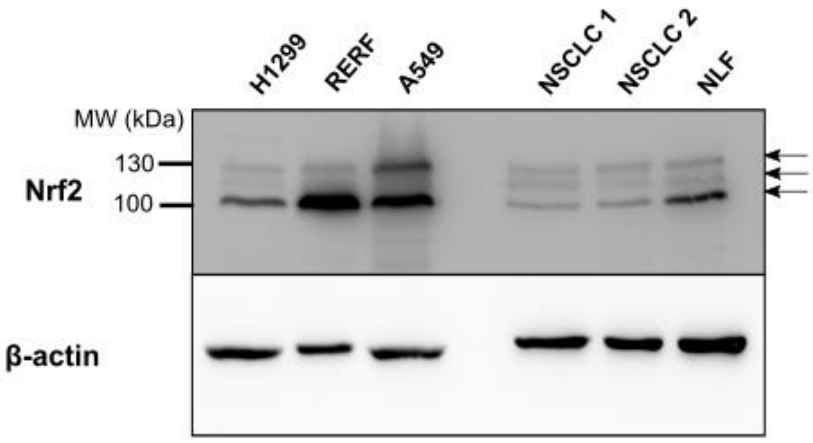

Figure 30**. Nrf2 is migrating as three protein forms in 8% SDS-PAGE.** Western blot analysis of the most abundant Nrf2 forms in lung cancer cell lines H1299, RERF and A549, in primary cell lines from NSCLC patients (NSCLC 1 and 2) and in normal lung fibroblasts (NLF). Arrows are indicating three different Nrf2 forms. Nrf2 was detected with Abcam EP1808Y antibodies. Actin was used as a loading control.

In the next step, we had to make sure that all three detected bands correspond to the Nrf2 protein. For that purpose, we made use of a pool of anti-Nrf2 siRNAs, targeting different regions of *NFE2L2* gene, and confirmed that all three bands are Nrf2 forms, since their expression was significantly reduced after Nrf2 knockdown. However, the 105 kDa Nrf2 was not completely knocked-down in the case of A549 and NSCLC 1, indicating its high stability, that was previously observed (Fig. 31A and B).

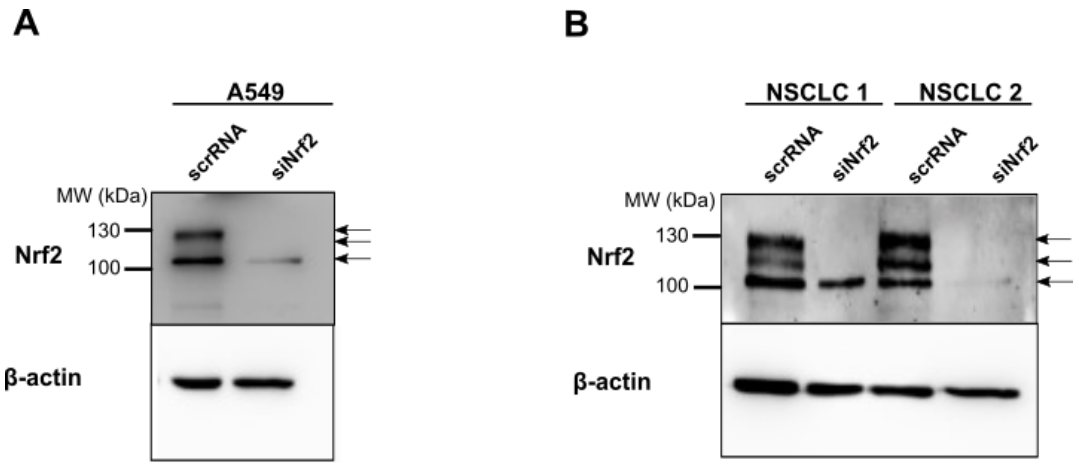

Figure 31. **Silencing of *NFE2L2* gene proved that the three detected bands are corresponding to the Nrf2 protein forms.** Western blot analysis after Nrf2 knockdown with the pool of Nrf2-targeting siRNA (25 nM) for 48 hours in (A) A549 and in (B) NSCLC 1 and NSCLC 2. Arrows are indicating three different Nrf2 forms. Nrf2 was detected with Abcam EP1808Y antibodies. Actin was used as a loading control.

3.2.2.2. Newly identified Nrf2 form is stable and does not translocate to the nucleus

To test the stability of the 105 kDa form of Nrf2, we made use of emetine dihydrochloride to look at the protein stability (201). Treatment with the translation elongation inhibitor revealed the high stability of the 105 kDa form (marked as Nrf2*), with the half-life ranging up to 2.1 hours in H1299 (Fig. 32). The middle Nrf2 form had the lowest stability, while the half-life of the top one (~130 kDa) corresponded to the values found in literature, defining Nrf2 as a labile protein of a half-life ranging from less than 30 min~2 h depending on the cell type (13,202–204). The low stability and low expression of the upper ~130 kDa Nrf2 form under no stress conditions, indicates that this is the full-length Nrf2 form, which is well-characterized and well-described. The high stability of the 105 kDa form indicates a different mechanism of regulation compared to the full-length Nrf2, which is constantly degraded by Keap1 under homeostatic conditions.

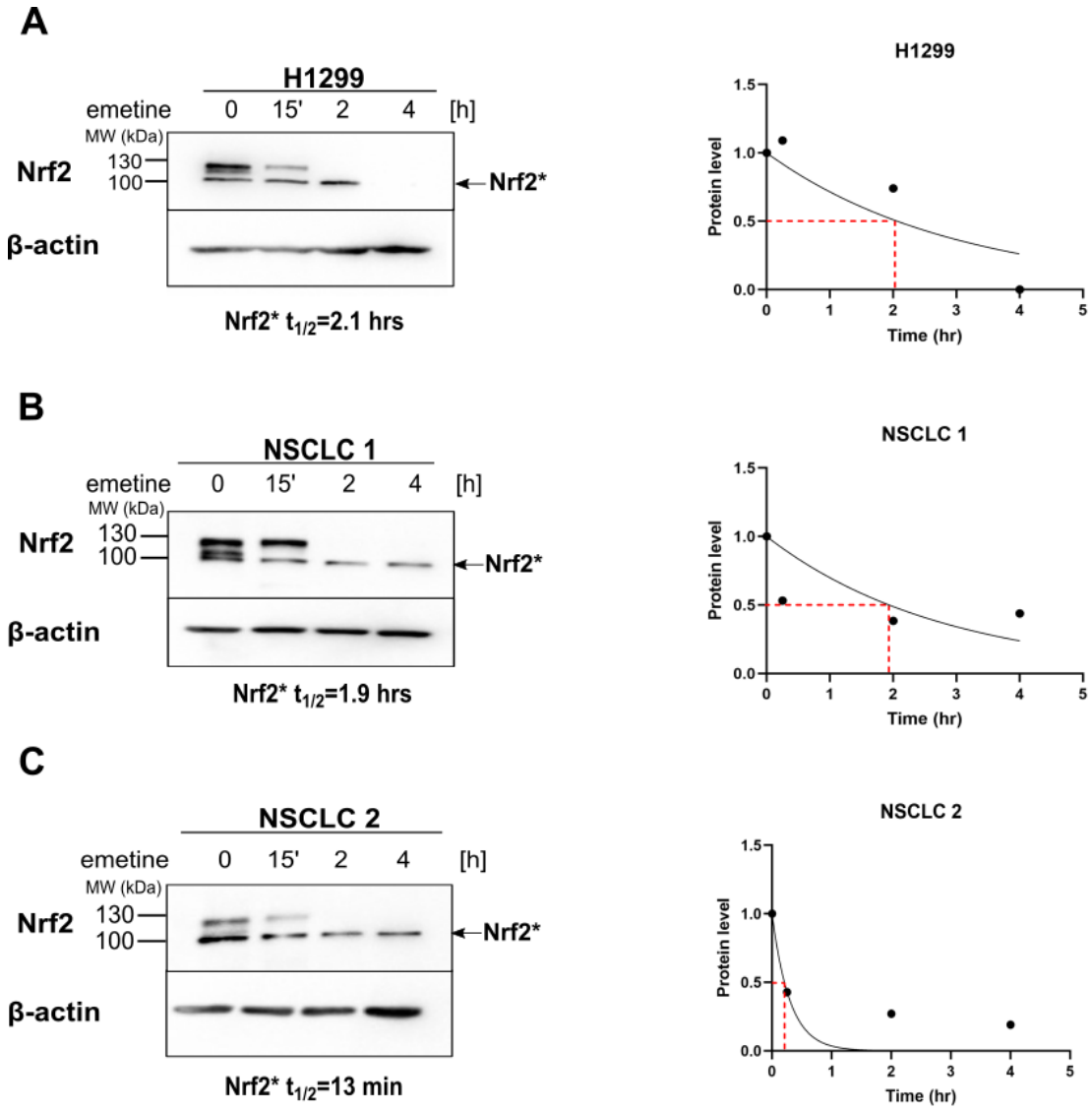

Figure 32. **Nrf2 stability after translation elongation inhibition.** Western blot analysis of (A) H1299, (B) NSCLC 1 and (C) NSCLC 2 after treatment with translation elongation inhibitor emetine dihydrochloride (20 µM) at indicated time points. Nrf2 was detected with Abcam EP1808Y antibodies. Actin was used as a loading control. Average band densities for each time point were normalized to time point zero. Curves show data fitted using nonlinear regression and a one-phase exponential decay equation (*Table S1-S3*) used for calculating the half-life of protein. Nrf2*, stable 105 kDa Nrf2 form.

3.2.2.3. A stable Nrf2 form is not phosphorylated

The question that arises next is what is the source of these distinct Nrf2 forms. One option is the post-translational modification of Nrf2 that could account for differences in mass and stability. Phosphorylation is the predominant Nrf2 modification and various Nrf2 residues are

phosphorylated, including Ser40, Ser215, Ser344, Ser347, Ser408, Ser558, Thr559, and Tyr576 (Fig. 1) (14,18,62,65,66). Their impact on Nrf2 stability and activity can be different and is thought to depend on the phosphorylation site. Thus we have asked if the Nrf2 forms detected with Abcam EP1808Y antibodies are the phosphorylated and dephosphorylated Nrf2 forms. We made use of lambda protein phosphatase (λPP), which removes phosphate groups from phosphorylated serine, threonine and tyrosine residues and observed that in RERF and H1299 cells, as well as NSCLC 1 cells, the heavier upper band is affected by λPP treatment, but the lower 105 kDa band is not (Fig. 33A and B). Interestingly, after λ phosphatase, the molecular weight of the upper Nrf2 form was reduced to ~110 kDa, which is visible as a band migrating just above the abundant 105 kDa Nrf2. It indicates that the 105 kDa Nrf2 is not simply a dephosphorylated Nrf2, but rather a shorter Nrf2 form, and that the middle form corresponds to the dephosphorylated 130 kDa full-length Nrf2 form. This is consistent with the observed stability – phosphorylated Nrf2 form is more stable than dephosphorylated Nrf2 (Fig. 32).

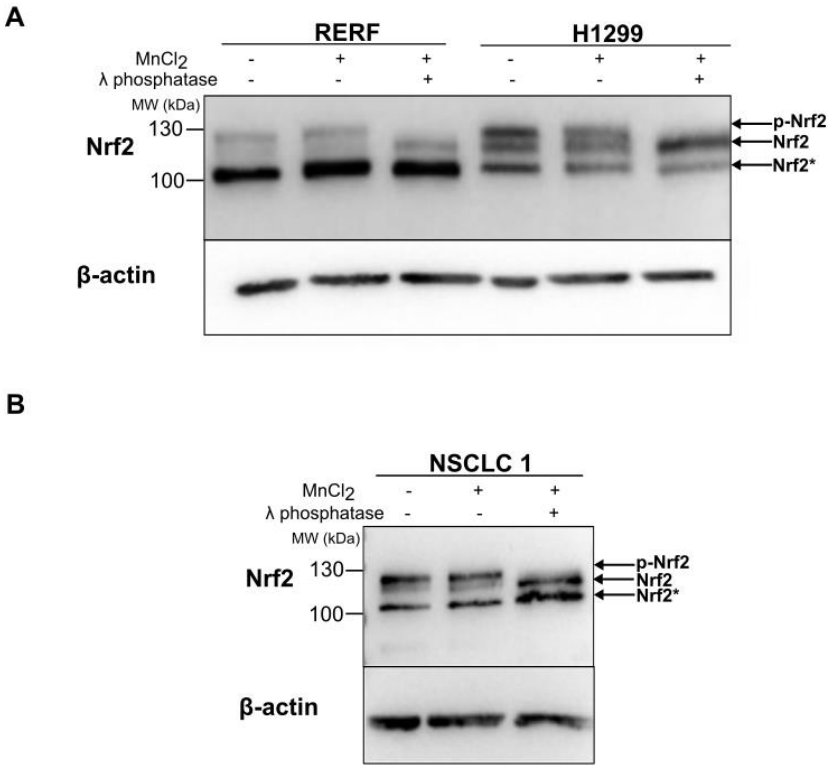

Figure 33. **Stable 105 kDa Nrf2 form is not phosphorylated.** (A) Lambda protein phosphatase (λPP) treatment of (A) RERF and H1299 lysates and (B) NSCLC 1 lysate. Cell lysates were incubated with or without λ phosphatase for 30 min in 30°C in the presence of $MnCl_2$. Arrows indicate different Nrf2 forms: ←p-Nrf2 for phosphorylated Nrf2; ←Nrf2 for dephosphorylated Nrf2; ←Nrf2* for stable Nrf2. Nrf2 was detected with Abcam EP1808Y antibodies. Actin was used as a loading control.

In addition, Nrf2 stability and oncogenic activity was shown to be dependent on Fructosamine-3-kinase (FN3K)—a kinase that triggers protein de-glycation. In its absence, Nrf2 is extensively glycated, unstable, and defective at binding to sMAF proteins (205). Thus we asked if a presence of sugar moieties might differentiate between the two detected Nrf2 forms and used the endoglycosidase PNGase F that specifically removes N-linked glycans from glycoproteins. This treatment did not diminish the 130 kDa Nrf2, thus it is not the presence of N-linked sugars that produces these Nrf2 forms of different stability (Fig. 34).

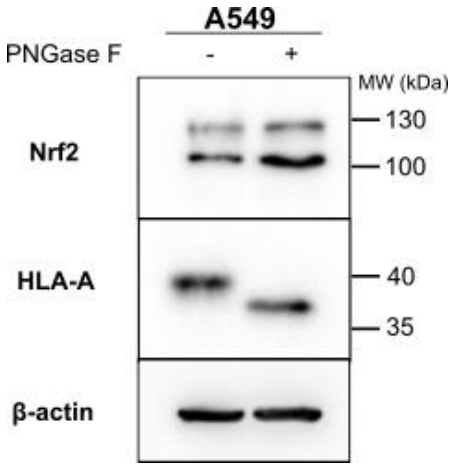

Figure 34. **Stable 105 kDa Nrf2 is not de-glycated form of full-length Nrf2.** A549 cell line was treated with PNGase F enzyme (500 000 U/mL) for 24 hours. HLA-A, known to carry N-linked glycans, was used as a control for PNGase activity. Nrf2 was detected by western blot analysis using Abcam EP1808Y antibodies. Actin was used as a loading control.

3.2.2.4. P2 transcript variants encoding Nrf2 isoform 2 are the source of a stable Nrf2 form

Since post-translational modifications did not seem to be the source of a stable Nrf2 form, we assumed that it might represent a product of an alternative transcription or/and translation, especially that Nrf2 isoforms resistant to Keap1-Cul3-mediated degradation have been described before (53). The skipping of exon 2, that encodes the Keap1-binding motifs, or exons 2+3 in *NFE2L2* gene was observed in lung and head and neck cancers, resulting in Nrf2 forms resistant to Keap1-mediated degradation (53).

It is already well-known that the efficient production of functional proteins from stress-responsive cytoprotective genes is regulated over transcript isoform usage. Upon exposure to

the stress, the expression of Nrf2 target genes increases substantially, indicating that there may be an alternative use of exons or transcript isoforms, which would produce diverse proteins in various stress-mediated context (206). The use of alternative transcription start and/or termination site and alternative splicing enable the production of multiple transcript variants and protein isoforms in the cells. Usually, the promoters that have different regulatory elements which are specific for a tissue and/or developmental stage, allow diverse regulations of gene expressions in various environment (207–209). Also, structural changes on mRNA level are causing the modifications of the reading frame and affect the efficiently of mRNA translation, resulting in multiple protein isoforms. It has been reported that the sequences of over 80 000 protein-coding transcripts expressed from approximately 20 000 protein-coding genes have been available in public databases (210). More than 90% of multiexon genes undergo alternative splicing, while 60% of genes in humans have at least one alternative transcription start site (211–213).

In the collaboration with Dr Alicja Szabelska-Beresewicz, we analyzed the *NFE2L2* transcripts expressed in fully sequenced A549 cell line, using the RNA sequencing data, from the project available at *NCBI Gene Expression Omnibus* (GEO) public database. We identified six different transcripts expressed under homeostatic conditions in A549 cells (Fig. 35). One of those transcripts, NM_001313904.1, has an extremely short exon 2, translated to three amino acids, due to an alternative translation initiation site and a truncated 3' terminus of this exon (in-frame splice site in the 3' region of exon 2) (Fig. 35A). Since two motifs required for Nrf2 binding to Keap1 are located within the exon 2, Nrf2 expressed from this transcript most probably escapes Keap1-Cul3-mediated degradation. On the other hand, transcript NM_001313902.1 has a full sequence of exon 2, but lacks exon 3, due to alternative splicing (Fig. 35B). The protein expressed from this transcript might fold in a way that DLG and ETGE motifs are not accessible to the Keap1 (200).

Our initial hypothesis was based on the fact that the newly identified Nrf2 form is not regulated through Keap1, thus these two transcripts were our primary candidates for the source of this Nrf2 form. It was difficult to hypothesize which transcript it could be, basing on the calculated molecular weight (MW) of the Nrf2 form it encodes, as Nrf2 migrates in SDS-PAGE much slower than the calculations suggest. The transcript NM_001313904.1 with alternative translation initiation site encodes for a protein of a calculated MW of 56 kDa (protein isoform 6, NCBI Reference Sequence: NP_001300833.1), while the Nrf2 form encoded by transcript NM_001313902.1 (protein isoform 4, NP_001300831.1) calculates at 64.5 kDa. Since the predicted MW of the full-length *NFE2L2* transcript (NM_006164.5 encoding isoform 1, NP_006155.2) is 68 kDa and all the isoforms migrate in 8% SDS-PAGE above 100 kDa, further studies were needed to reliably assess the origin of the 105 kDa Nrf2 form.

Interestingly, Goldstein et al. have shown that the Nrf2 protein expressed from the transcript that lacks exon 2 in *NFE2L2* gene, migrates around 75 kDa (53), indicating that the origin of our newly identified Nrf2 form is not that same transcript. If we look at the molecular weights, the difference between the phosphorylated full-length Nrf2 (migrating around 130 kDa in 8% SDS-PAGE) and the newly identified form (migrating around 105 kDa in 8%SDS-PAGE), is rather smaller comparing to the lack of the whole exon 2, which switched our further focus on the other transcripts with smaller alterations, while compared to the full length Nrf2 isoform 1.

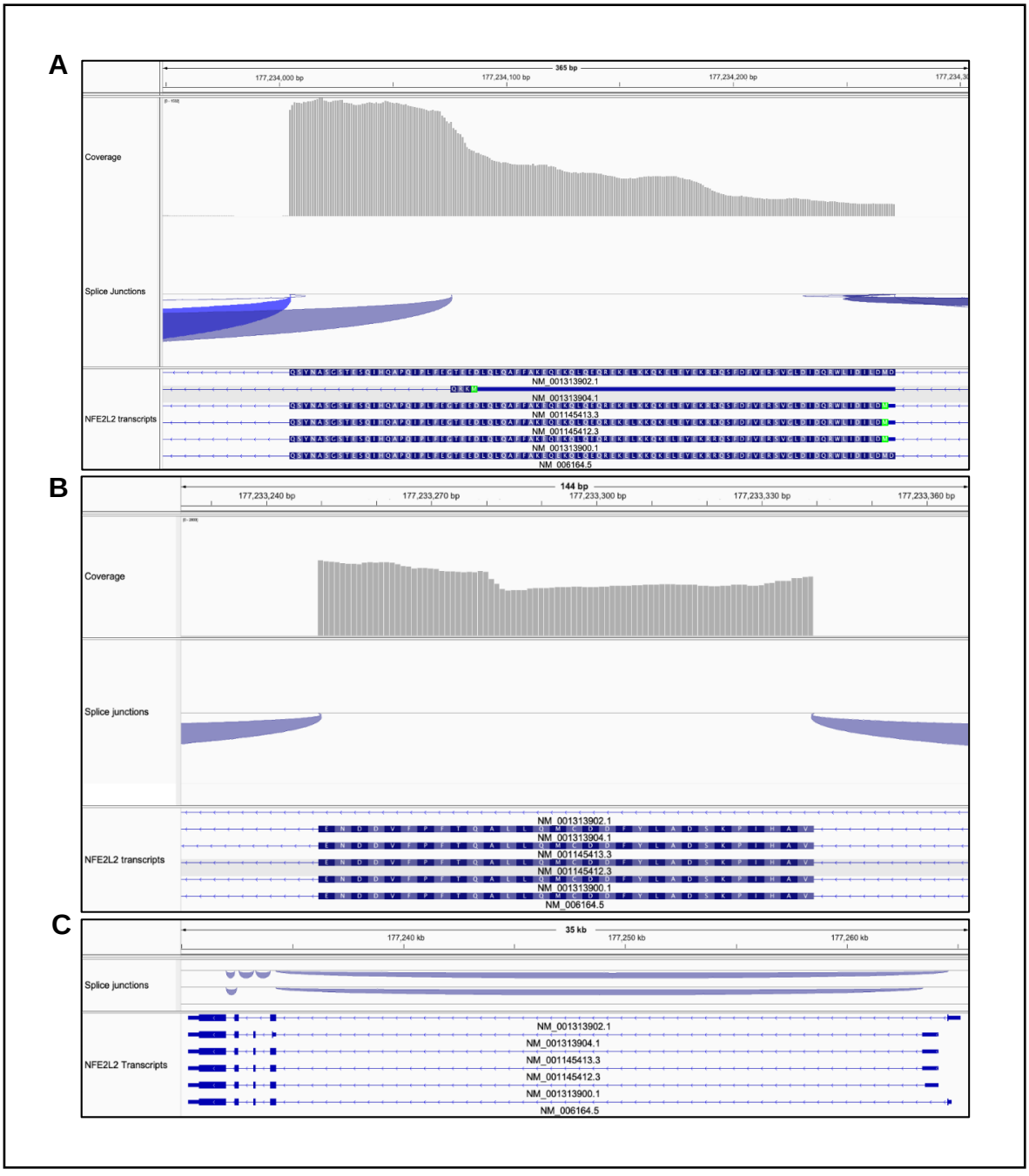

Figure 35. **Expression of different *NFE2L2* transcripts in A549 cells based on RNA sequencing data** (200)**.** (A) Visualization of sequence reads alignments within exon 2. Beginning of the exon 2 is on the right-hand and the end on the left-hand side. Splice junctions are represented by arches. Apart from classical junctions at the beginning and the end of the exon, in a portion of reads the 3' end of exon 2 was spliced out. These reads have been aligned to the transcript NM_001313904.1 (transcripts references are below each transcript). Transcripts sequence within the exon was translated to the encoded amino acids. (B) Visualization of sequence reads alignments within exon 3. In the transcript NM_001313902.1 exon 3 is spliced out. (C) Visualization of all the transcripts (6) identified in A549 cells. Exon 1 is on the right-hand and exon 5 on the left-hand side. Assembly of RNA-Seq alignments into potential transcripts together with calculation of expression levels for those transcripts were performed with StringTie software (157). Visualization of the alignments identified transcripts and junctions was performed in IGV software (158).

To further investigate the origin of a stable and shorter Nrf2 form, we studied which Nrf2 transcripts are expressed in lung cells (Fig. 36). Based on the publicly available NCBI data, *NFE2L2* gene is expressed from two promoters which produce eight Nrf2 transcripts (Fig. 36A). Promoter 1 (P1) gives rise to transcript one, six and seven and promoter two (P2) produces transcript two, three, four, five and eight. Transcripts coming from P2 utilize different AUG to initiate translation than transcripts coming from P1. It is localized 5' downstream to the first AUG, thus protein products of P2 transcripts are N-terminally truncated. To the best of our knowledge, only transcripts coming from P1 promoter were shown to be translated (53), while protein products produced from P2 transcripts have not been reported so far. Eight Nrf2 transcript variants give rise to the six different protein isoforms. Isoform 1 is encoded by transcript variant 1 and represents the full-length Nrf2 protein (605 aa). Isoform 2 represents a shorter Nrf2 form (589 aa) which results from an alternative promoter usage and an alternative translation initiation site and is encoded by three transcript variants: 2, 4 and 5, differing in a 5' untranslated region length. Isoform 3 is encoded by a transcript variant 3 and in comparison with isoform 2, it has an additional splicing within exon 4, making it a 7 aa shorter than isoform 2 (582 aa). Isoform 4 (575 aa) encoded by transcript variant 6 has the same promoter and translation initiation site as the full-length isoform 1, but exon 3 is spliced out. Isoform 5 (532 aa) is encoded by transcript variant 7 that utilizes the same promoter and translation initiation site as isoform 1 and 4, but due to alternative splicing, majority of exon 2 is spliced out. Finally, the shortest isoform 6 (505 aa) encoded by transcript variant 8 uses the same promoter as transcripts 2,3,4 and 5 but yet another translation initiation site.

With two sets of primers used in RT-PCR (indicated as black arrows in Fig. 36A), we could discriminate between Nrf2 transcripts by length in agarose gel (Fig. 36B). Table 1 in Material and Methods presents primer sequences and expected amplicon length. In all tested lung

cells: cancer cell lines, primary NSCLC cells and normal lung fibroblasts, transcript 1 and 2 were dominantly expressed. Transcript 4 and 6 were also detected (Fig. 36B). Transcript 1 produces a full-length Nrf2 isoform 1 (605 aa) that is regulated via Keap1-Cul3-E3 ubiquitin ligase. Both transcript 2 and 4 give rise to the same protein – Nrf2 isoform 2, which lacks first 16 amino acids (aa) at the N-terminus due to the utilization of an alternative AUG for translation initiation. This analysis indicates that both Nrf2 isoform 1 and 2 are highly expressed in all tested cell types.

Indeed, when we quantified the ratio of expression of these two forms with quantitative RT-PCR (Real-time qPCR), we observed that on the RNA level, the expression of P1 and P2 transcripts is similar, only RERF and NLF produced slightly more P1 transcripts (Fig. 36C).

From this analysis, we concluded that the fastest migrating 105 kDa Nrf2 form, detected in Western blot, is produced from transcript 2 and 4 and represents Nrf2 isoform 2. We have named it ΔN-Nrf2 due to the N-terminal truncation. The full-length Nrf2 originates from transcript 1 and it is 16 amino acids longer compared to the ΔN-Nrf2. It was detected in Western blot migrating just above ΔN-Nrf2, as the middle band, while the slowest migrating 130 kDa band belongs to the phosphorylated full-length Nrf2.

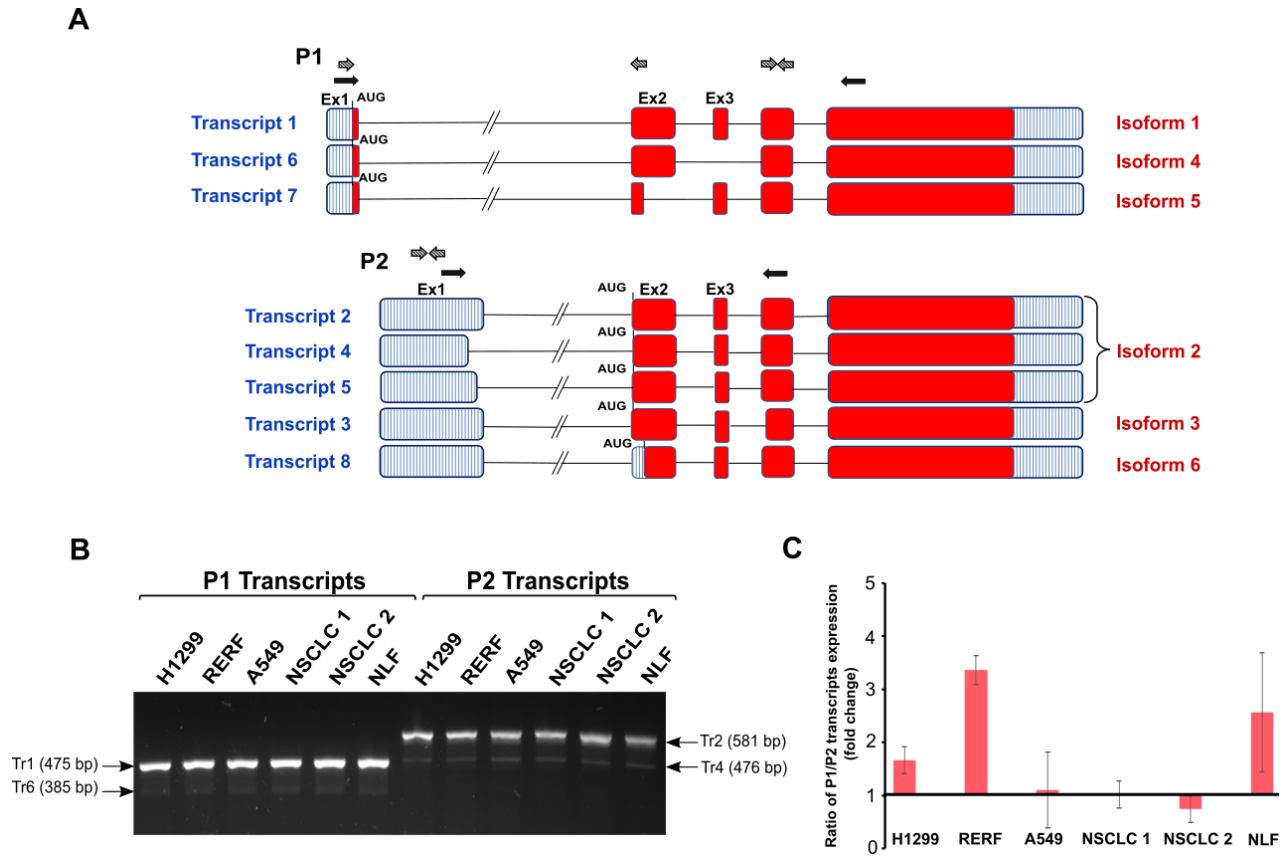

Figure 36. **Expression of Nrf2 transcripts in lung cells.** (A) A scheme of all possible transcript variants of Nrf2 gene (*NFE2L2*) and corresponding proteins according to NCBI. mRNA is presented in vertical blue lines and protein encoding regions are in red. Black arrows represent primers used in RT-PCR to identify expressed transcripts. Dashed arrows show primers for Real Time qPCR to evaluate level of expression of identified transcripts. P1, promoter 1; P2, promoter 2. (B) Agarose gel (2 %) after polymerase chain reaction (PCR) in lung cancer cell lines and NSCLC cells. Arrows indicate identified transcripts with two sets of primers. (C) Ratio of P1 transcripts vs. P2 transcripts expression in lung cancer cell lines, NLF and NSCLC cells analyzed by qPCR (mean ± SD, n = 3 independent experiments).

3.2.2.5. The deletion of 16 amino acids in ΔN-Nrf2 causes impaired binding to Keap1

To be able to understand the structural differences between Nrf2 isoform 1 and isoform 2 and their impact on the dynamics of Keap1 binding, we made use of molecular modeling and molecular dynamics simulations, in the collaboration with Dr Monikaben Padariya and Dr Umesh Kalathiya. From the model of the full-length Nrf2-Keap1 complex, designed based on the available crystal structure of their binding domains (166,167), we could see that deletion of the first 16 amino acids in isoform 2 is causing the alternations in the protein structure and differences in the binding to the Keap1, comparing to the full-length isoform 1 (Fig. 37A and B). The deletion of the first 16 amino acids in isoform 2 is causing the impairment of Keap1 binding to Nrf2 via a low affinity binding Nrf2 motif LWRQDIDLG (23–31 aa) which possesses a helix structure and binds weakly with Keap1 (57) (Fig. 38).

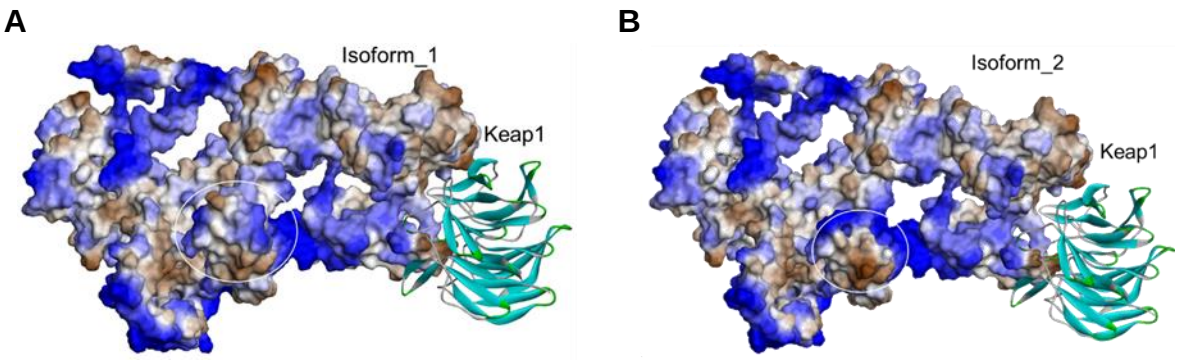

Figure 37**. Structural differences between full-length Nrf2 isoform 1 and ΔN-Nrf2 isoform 2.** (A) Structure of Nrf2 isoform 1 protein bound to the Keap1. (B) Structure of ΔN-Nrf2 isoform 2 protein bound to the Keap1. White circles represent the difference in the structure of isoform 1 and isoform 2, due to the deletion of the first 16 amino acids.

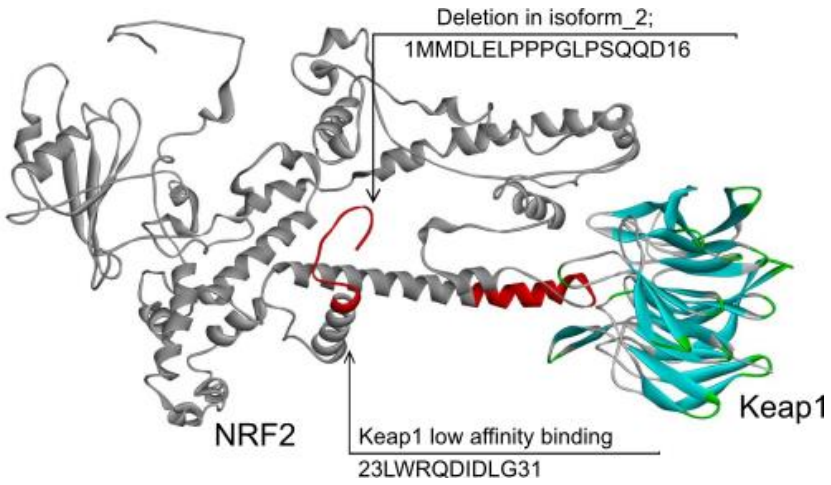

Figure 38. **The deletion of the first 16 amino acids in ΔN-Nrf2 is causing the impairment of the Keap1 binding.** Structure is showing the position of the deletion in Nrf2 isoform 2 (LWRQDIDLG), which affects the binding of Nrf2 and Keap1 via low affinity binding motif DLG.

Molecular dynamics simulations have shown that the deletion of the amino acids in the ΔN-Nrf2 isoform 2 is not only causing the impairment in the Keap1 binding, but it consequently causes the changes in ubiquitination and degradation of Nrf2. The ubiquitination site in Nrf2, consisting of seven lysine residues, is located between two binding sites with Keap1 (low-affinity DLG and high-affinity ETGE), thus when the low affinity is impaired, as in ΔN-Nrf2 isoform 2, the lysins are not exposed to ubiquitination anymore and Nrf2 gets stabilized (Fig. 39).

It is important to highlight that the binding between ΔN-Nrf2 isoform 2 and Keap1 is possible regardless the alterations in the structure, however, the binding is weaker and Keap1 bound to the ΔN-Nrf2 is more loose, compared to the Keap1 bound to the full-length isoform 1 (Fig. 39). Molecular dynamics simulations have revealed that the first 16 amino acids in Nrf2 are stabilizing a closed conformation of Nrf2 and sustain binding with Keap1. Deletion of these amino acids causes the conformational change of Nrf2 and destabilization of binding with Keap1 (Fig. 39). Calculations of the number of hydrogen bonds created in time between Nrf2 isoform 1 and Keap1, and ΔN-Nrf2 isoform 2 and Keap1 confirmed that even though in the beginning, ΔN-Nrf2 creates more hydrogen bonds with Keap1, this amount is rapidly decreased in time, while isoform 1 is creating more hydrogen bonds in time, thus making the binding with Keap1 stronger and more efficient (Fig. 40).

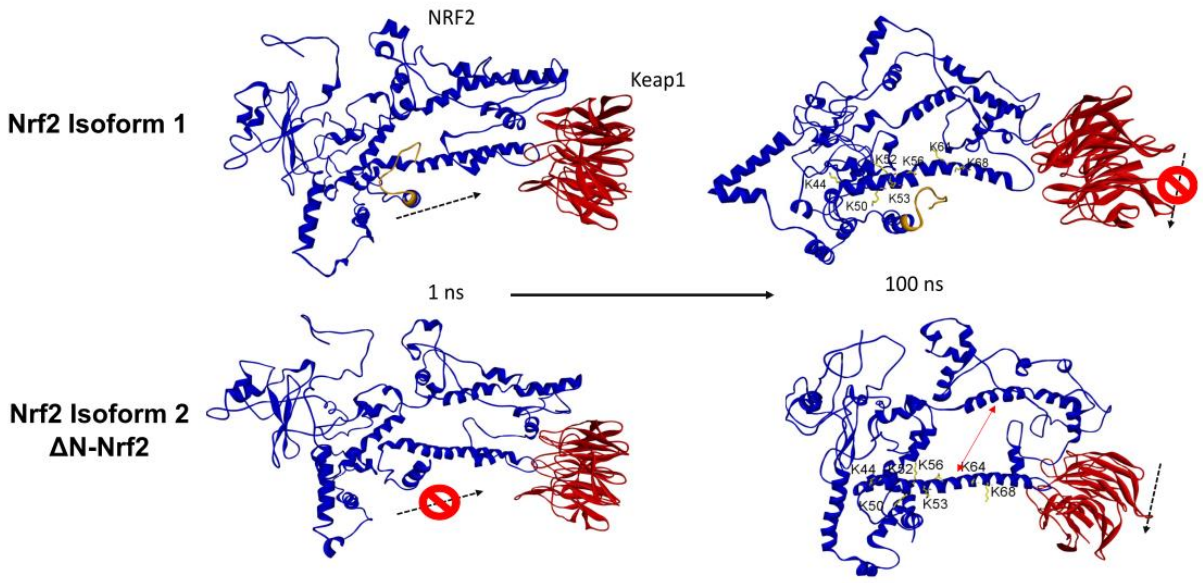

Figure 39. **The ubiquitination site in ΔN-Nrf2 isoform 2 is not exposed due to deletion of the first 16 amino acids.** Molecular dynamics simulations revealed that the binding of Nrf2 isoform 2 (ΔN-Nrf2) to the Keap1 is weaker comparing to the Nrf2 isoform 1. Due to the changes in the structure, the lysine residues of ΔN-Nrf2 isoform 2 (marked with K in the structures) are not exposed for ubiquitination.

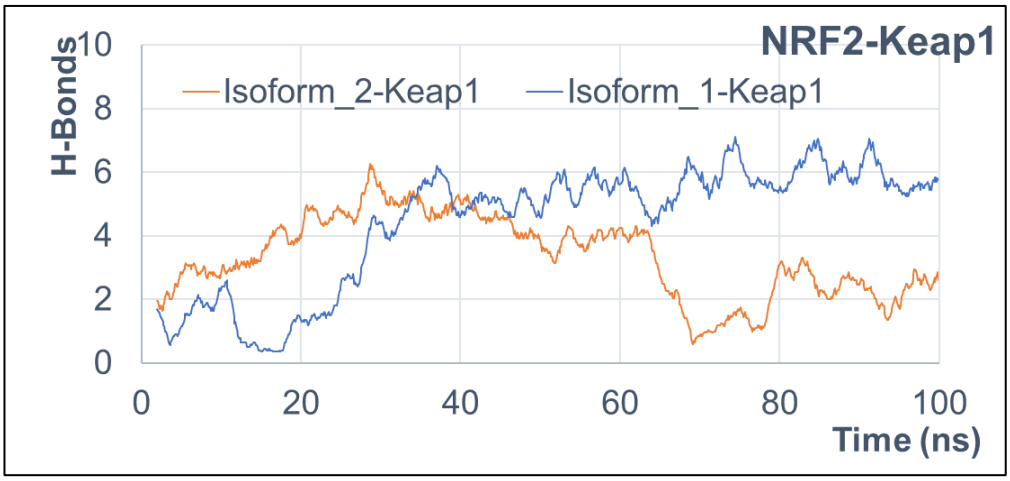

Figure 40. **Nrf2 isoform 1 creates more hydrogen bonds, thus the binding with Keap1 is stronger, comparing to the ΔN-Nrf2 isoform 2.** The graph presents the calculations from molecular dynamics simulations and number of hydrogen bonds created in time, between the Nrf2 isoform 1-Keap1 and Nrf2 isoform 2-Keap1.

To prove the different binding affinity of Nrf2 isoforms with Keap1, we made use of neddylation inhibitor MLN4924. MLN4924 is a specific small molecule inhibitor of NEDD8-activating enzyme E1 (NAE), that catalyzes the reversible modification by adding ubiquitin-like protein NEDD8 (Neural precursor cell expressed developmentally down-regulated 8) to cullins. This modification is called neddylation and it is necessary for the full activation of the Cullin-Ring ligases (CRLs). MLN4924 binds to the NAE, blocks its enzymatic activity which subsequently causes an inhibition of the neddylation of all cullins, leading to the accumulation of their substrates (214,215). Since the Keap1-dependent regulation of Nrf2 requires active Keap1-Cul3-E3 ligase complex, introduction of MLN4924 inhibitor leads to the inhibition of neddylation and disability of Cul3-containing E3 ubiquitin ligase to target Nrf2 for ubiquitination and degradation by proteasome (Fig. 41).

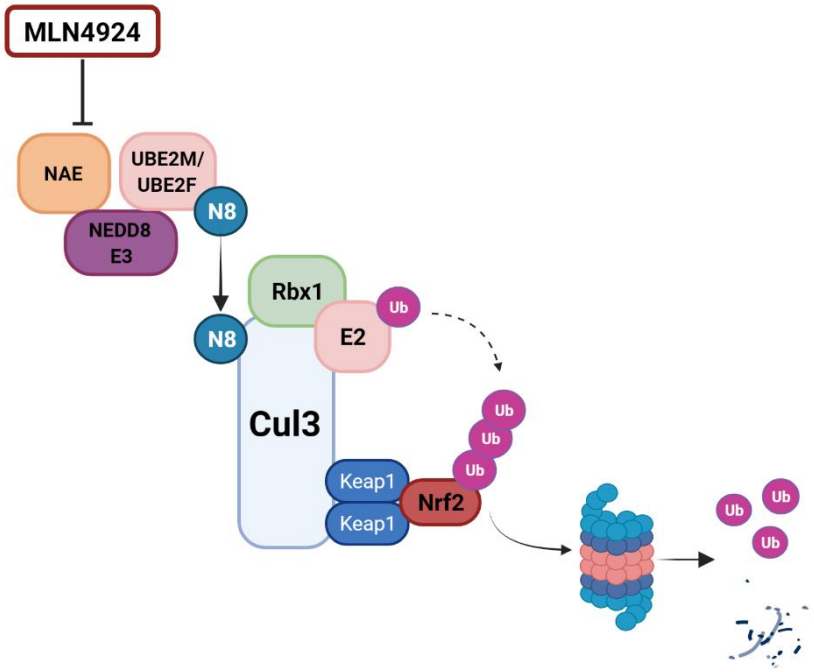

Figure 41. **Regulation of the Keap1-Cul3-E3 ligase complex**. The Keap1-Cul3-E3 ligase complex is active when it is in the neddylated state, resulting in Nrf2 ubiquitination and degradation. The complex is inactivated by neddylation inhibitor MLN4924, which binds to the NAE, blocks its enzymatic activity which subsequently causes an inhibition of the neddylation and accumulation of the substrate. CUL3, cullin 3; E2, ubiquitin-conjugating enzyme; N8, NEDD8; NAE, NEDD8-activating enzyme; NEDD8, NEDD8 ubiquitin-like modifier; RBX1, RING-box 1; UBE2M, ubiquitin-conjugating enzyme E2M; UBE2F, ubiquitin-conjugating enzyme E2F; Ub, ubiquitin. Created with Biorender.com.

Indeed, after the treatment with neddylation inhibitor, the full-length Nrf2 is accumulated and the amount of Keap1 bound to Nrf2 increases dramatically in RERF cells (Fig. 42). Since the amount of ΔN-Nrf2 isoform 2 has not changed, this increase is due to the Keap1 binding to Nrf2 isoform 1. These results are in line with the molecular modeling and molecular dynamics simulations showing that ΔN-Nrf2 can bind Keap1 but with a low affinity compared to the full length Nrf2.

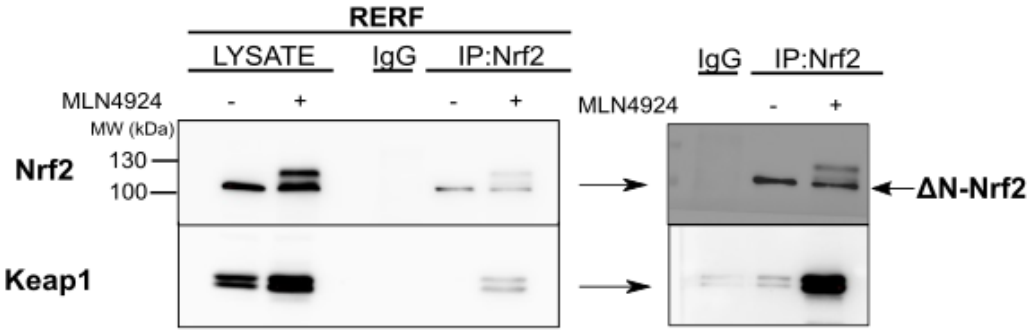

Figure 42. **Keap1 weakly binds to the ΔN-Nrf2 under homeostatic conditions.** Western blot analysis of RERF cells after co-immunoprecipitation of Nrf2, under homeostatic conditions and after treatment with neddylation inhibitor MLN4924 for 12 hours. Precipitates were probed with anti-Keap1 antibodies to analyze levels of Nrf2-bound Keap1. Right side panel presents western blot results in co-immunoprecipitation of Nrf2 and IgG samples after longer exposure. Nrf2 was detected with anti-Nrf2 Abcam [EP1808Y] antibodies. ΔN-Nrf2, the N-terminally truncated Nrf2 isoform 2.

3.2.2.6. ΔN-Nrf2 is not canonically regulated through Keap1-Cul3-E3 ubiquitin ligase pathway

The full-length, canonically regulated Nrf2 is constantly degraded through Keap1-Cul3-E3 ligase system under homeostatic conditions. Since results collected up to this point indicated that Keap1 binds weakly to the stable ΔN-Nrf2 and ΔN-Nrf2 has significantly higher stability compared to the full-length Nrf2, we assumed that the ΔN-Nrf2 could be regulated differently. To be able to test this hypothesis, firstly we silenced the expression of *KEAP1*, negative regulator of Nrf2 in the canonical pathway. The results showed that after knockdown of Keap1, only the upper 130 kDa Nrf2 form was accumulated, indicating that only this form is canonically regulated through Keap1 (Fig. 43).

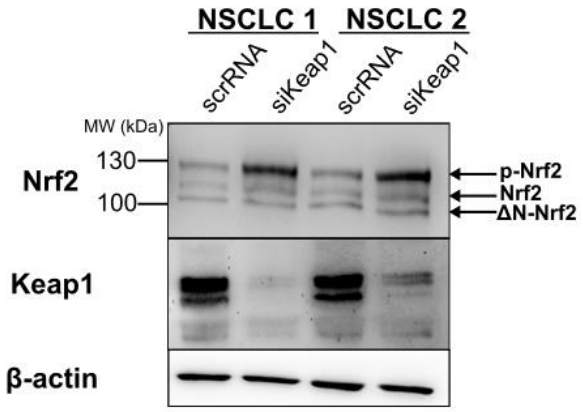

Figure 43. **Stable ΔN-Nrf2 is not accumulated after silencing of *KEAP1* expression.** *KEAP1* knockdown with the siRNA (Santa Cruz Biotechnology) (25 nM) in NSCLC primary cell lines for 48 hours. Nrf2 was detected using Abcam EP1808Y antibodies. Keap1 was detected using anti-Keap1 antibody [1B4] (Abcam). Actin was used as a loading control. Arrows indicate different Nrf2 forms: ←p-Nrf2 for phosphorylated Nrf2; ←Nrf2 for dephosphorylated Nrf2; ←ΔN-Nrf2 for the N-terminally truncated Nrf2 isoform 2.

Furthermore, to confirm that non-canonically regulated Nrf2 cannot be degraded via Keap1-Cul3-E3 ubiquitin system, we made use of neddylation inhibitor, MLN4924. Indeed, when we introduced MLN4924 to the cells, we observed the accumulation only of the upper, canonically regulated Nrf2 form, while the expression of ΔN-Nrf2 remained the same, indicating that the inhibition of the neddylation and disability of Cul3-containing E3 ubiquitin ligase to ubiquitinate Nrf2 did not cause its accumulation. This results suggest that the newly identified ΔN-Nrf2 is not ubiquitinated and degraded through the canonical Keap1-Cul3-E3 ubiquitin ligase pathway. We combined the MLN4924 treatment with λPP treatment, and confirmed that the middle band is dephosphorylated full-length Nrf2, since after the treatment with λPP, the molecular weight of the upper form was reduced to the ~110 kDa, while the ΔN-Nrf2 remained unchanged (Fig. 44).

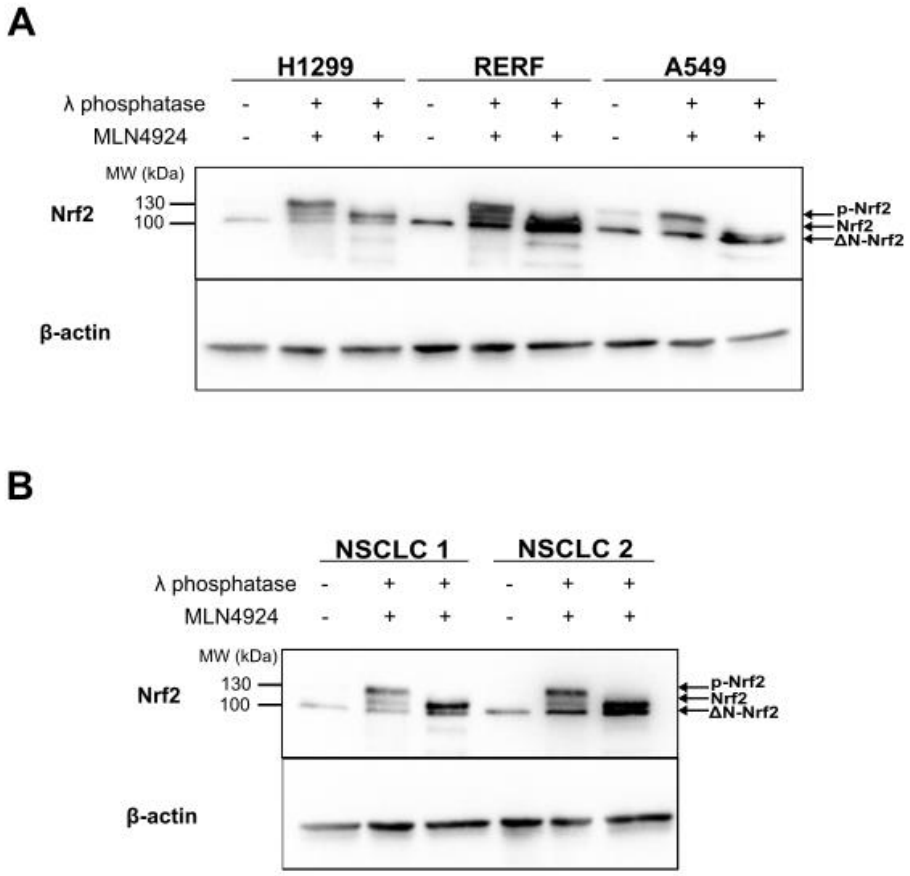

Figure 44. **ΔN-Nrf2 is not regulated through Keap1-Cul3-E3 ubiquitin ligase system.** Cells were treated with neddylation inhibitor MLN4924 (1 μM) for 12 h and incubated with or without λ phosphatase for 30 min in 30°C. (A) Western blot analysis of lung cancer cell lines H1299, RERF and A549 cells. (B) Western blot analysis of primary cell lines NSCLC 1 and NSCLC 2. Arrows indicate different Nrf2 forms: ←p-Nrf2 for phosphorylated, canonical Nrf2; ←Nrf2 for dephosphorylated, canonical Nrf2; ←ΔN-Nrf2 for the N-terminally truncated, non-canonically regulated Nrf2 isoform 2. Nrf2 was detected using Abcam EP1808Y antibodies. Actin was used as a loading control.

3.2.2.7. ΔN-Nrf2 does not respond to the tBHQ-induced oxidative stress and remains in the cytoplasm

Based on the collected results suggesting non-canonical regulation of ΔN-Nrf2, the next step was to determine its localization. Therefore, in the next step, we studied the cellular distribution of different Nrf2 forms. We performed nuclear and cytoplasmic fractionation of H1299, RERF and A549 cell lines, primary NSCLC cell lines and NLF, and analyzed the distribution of Nrf2.

Under no-stress conditions, the stable ΔN-Nrf2 and phosphorylated, full-length Nrf2 were both detected in the cytoplasm, while only the phosphorylated Nrf2 form was translocated to the nucleus. It seems that there is always a low level of full-length Nrf2 localized in the nucleus under homeostatic conditions, which could explain the basal regulation of the Nrf2 target genes. In the case of A549 cells, we observed the accumulation of the phosphorylated full-length Nrf2 in the nucleus, which was expected, since this cells have a constitutive active Nrf2 due to the *KEAP1* mutation (54). Also, in A549 cells, low level of a stable ΔN-Nrf2 was detected in the nucleus (Fig. 45).

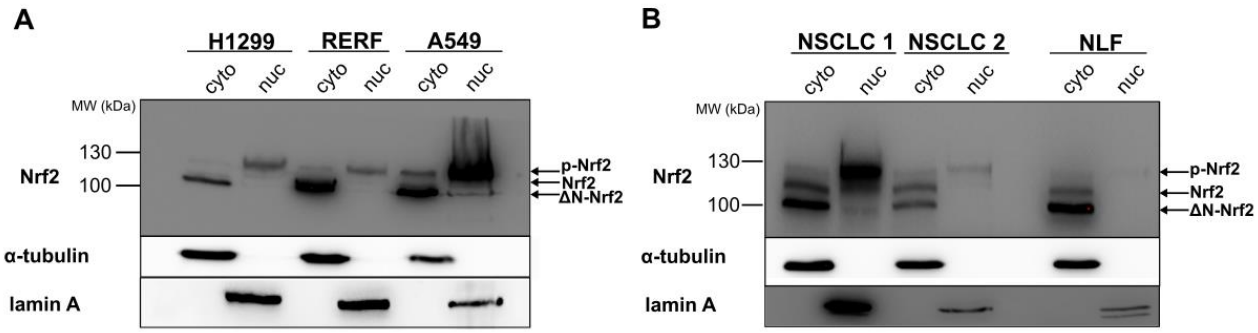

Figure 45. **Cellular distribution of Nrf2 under homeostatic conditions.** (A) Western blot analysis after cellular fractionation under homeostatic conditions in H1299, RERF and A549 cell lines. Lamin A was used as nuclear marker, while α-tubulin was used as a cytoplasmic marker. Nrf2 was detected with Abcam EP1808Y antibodies. (B) Western blot analysis after cellular fractionation under homeostatic conditions in primary NSCLC cell lines and normal lung fibroblasts. Lamin A was used as nuclear marker, while α-tubulin was used as a cytoplasmic marker. Nrf2 was detected with Abcam EP1808Y antibodies. Arrows indicate different Nrf2 forms: ←p-Nrf2 for phosphorylated, canonical Nrf2; ←Nrf2 for dephosphorylated, canonical Nrf2; ←ΔN-Nrf2 for the N-terminally truncated Nrf2 isoform 2.

In the next step, we checked *in situ* Nrf2 localization in A549 and RERF cells with the use of immunofluorescent staining. Under no-stress conditions, Nrf2 was localized in both, nuclear and cytoplasmic compartment, which is in the correlation with the cellular fractionation results. We've tested both Nrf2 antibodies and could detect some differences. EP1808Y antibodies gave better signal and were able to detect nuclear and cytoplasmic Nrf2 in both cell lines, while D1Z9C recognized primarily nuclear Nrf2 (Fig. 46).

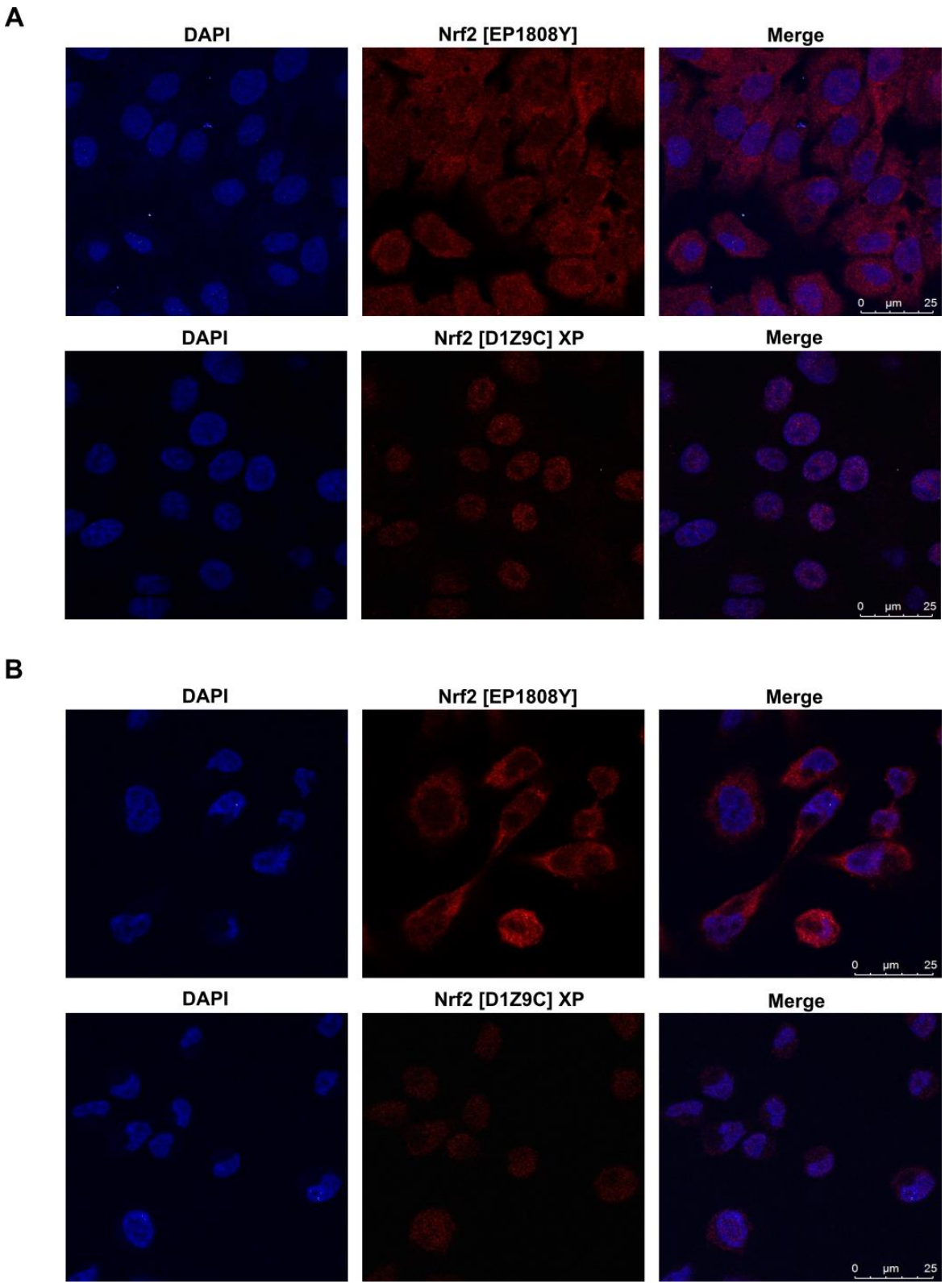

Figure 46. **Cellular Nrf2 localization under homeostatic conditions.** Cellular Nrf2 localization detected with Nrf2-specific monoclonal antibodies EP1808Y and D1Z9C in A549 (A) and RERF (B) cells. After fixation, cells were stained with Abcam (EP1808Y) and Cell Signaling (D1Z9C) antibodies followed by Alexa Fluor 488 goat anti-rabbit secondary antibodies. Nuclei were stained with DAPI. Specimens were visualized by confocal microscope.

To be able to understand if ΔN-Nrf2 is responsive to the stress in the same way as full-length Nrf2, we treated cells with the widely used Nrf2 activator, tert-butylhydroquinone (tBHQ). tBHQ is a metabolite of the chemical compound butylated hydroxyanisole (216). It can interact with reactive cysteine residues on Keap1, such as Cys151 (217), which would lead to the dissociation of Nrf2 from Keap1 and translocation to the nucleus (Fig. 47). In addition to modifying cysteine residues on Keap1, tBHQ has been shown to stimulate Nrf2 activity by inducing mitochondrial oxidative stress, regulated by mitochondria-specific antioxidant, thioredoxin-2 (Trx2) (216). Moreover, tBHQ can transcriptionally activate antioxidant response elements/electrophile response elements, leading to the increased expression of the cytoprotective genes (218).

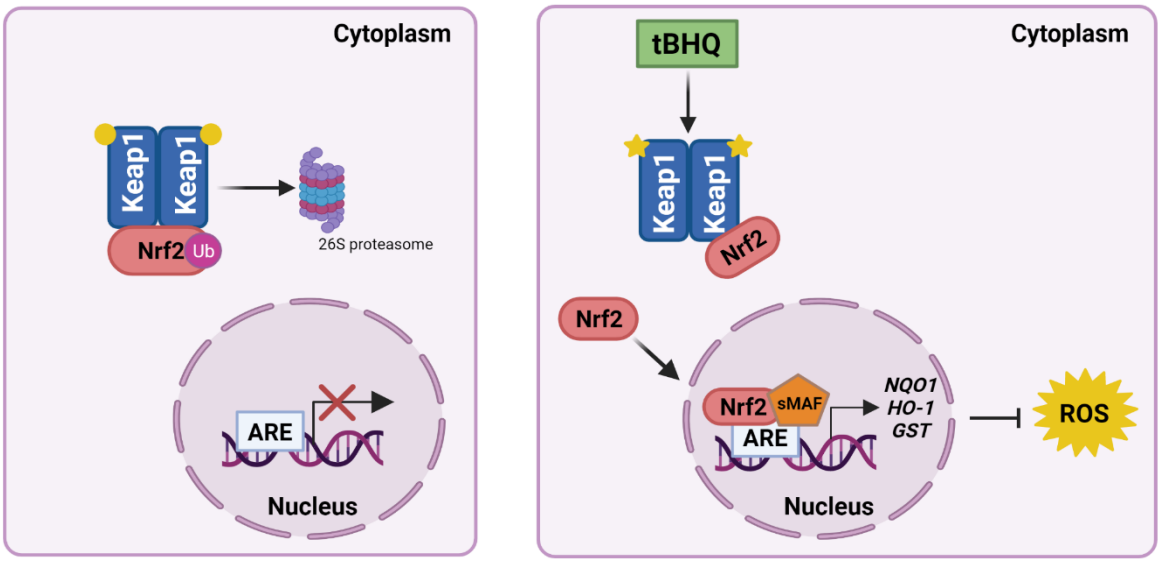

Figure 47. **Schematic overview of the mechanism of Nrf2 activator tert-butylhydroquinone (tBHQ).** Under normal conditions, Nrf2 is bound to Keap1 dimer, ubiquitinated and degraded by proteasome. Upon tBHQ activation, cysteine residues on Keap1 dimer are modified, Nrf2 is liberated from Keap1-mediated degradation, resulting in its translocation to the nucleus and activation of the transcription of its target genes. ARE, antioxidant-response elements; Ub, ubiquitination; NQO1, NAD(P)H Quinone Dehydrogenase 1; HO-1, Heme oxygenase 1; GST, Glutathione S-transferase; ROS, reactive oxygen species. Created with Biorender.com.

Upon treatment with tBHQ and Nrf2 activation, we observed the accumulation of the two Nrf2 forms, phosphorylated and dephosphorylated full-length Nrf2, while ΔN-Nrf2 did not show significant accumulation comparing to the control (Fig. 48A and B). When we performed cellular fractionation after tBHQ activation, the phosphorylated full-length Nrf2 responded to

the Nrf2 activation and it was translocated to the nucleus, however ΔN-Nrf2 remained mostly in the cytoplasm (Fig. 48C and D). In the case of A549 cells, there was a low level of ΔN-Nrf2 detected in the nucleus upon activation with tBHQ, similarly as in the cellular fractionation under no-stress conditions (Fig. 45). It was previously shown that, as a response of Nrf2 to the oxidative stress, protein kinase Cδ (PKCδ) induces activation of Nrf2 phosphorylation at Ser40 residue, which results in releasing of the phosphorylated Nrf2 from Keap1. Nrf2 is then stabilized and can bind to the ARE-sequences in DNA, to activate the transcription of the target genes. Furthermore, PKCδ phosphorylation is likely to involve specifically the nuclear cytoplasmic shuttling step and it does not appear to play a role in Nrf2 accumulation and stabilization (18). Nrf2 does not require phosphorylation to accumulate in the nucleus and to activate the target genes expression (16), which explains the nuclear translocation of phosphorylated, but also, in some cases, dephosphorylated Nrf2 form upon tBHQ treatment (Fig. 48C and D).

Based on our previous observations regarding the high stability of ΔN-Nrf2 and its different regulation compared to the full-length Nrf2, its inability to translocate to the nucleus upon tBHQ treatment was not a surprise. Mechanism of tBHQ-activation of Nrf2 is based on the modification of the cysteine residues in Keap1, therefore, if ΔN-Nrf2 is not regulated through Keap1-Cul3-E3 ubiquitin ligase system, the modification of Keap1 cysteine residues would not have such an impact on its expression. We could speculate that another Nrf2 activator might cause the translocation of ΔN-Nrf2 to the nucleus, however, most of them are activating Nrf2 through Keap1, thus would probably have the similar effect.

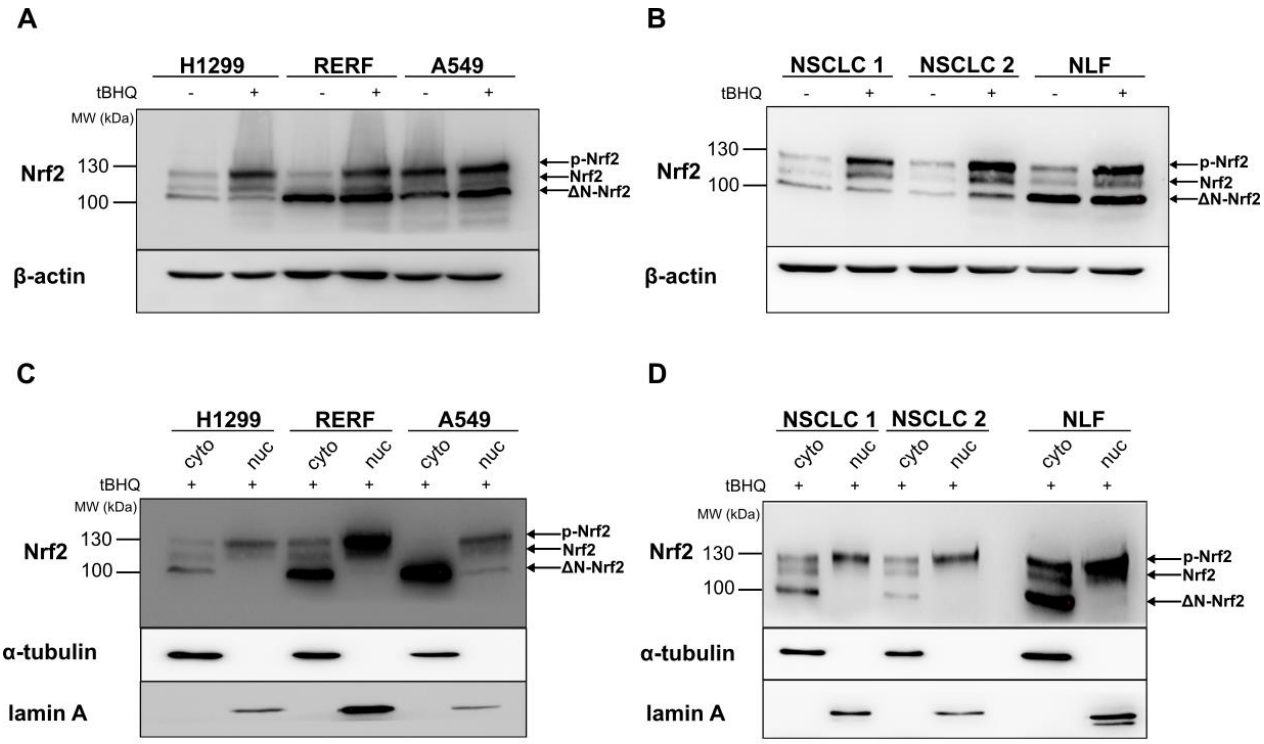

Figure 48. **ΔN-Nrf2 does not translocate to the nucleus in response to electrophilic stress.** (A) Western blot analysis of H1299, RERF and A549 cells, after activation of Nrf2 with tBHQ (20 uM) for 6 hours. Actin was used as a loading control. (B) Western blot analysis of NSCLC 1, NSCLC 2 and NLF cells, after activation of Nrf2 with tBHQ (20 uM) for 6 hours. Actin was used as a loading control. (C) Western blot analysis of H1299, RERF and A549 cells, after activation of Nrf2 with tBHQ (20 uM) for 6 hours and cellular fractionation. Lamin A was used as nuclear marker, while α-tubulin was used as a cytoplasmic marker. (D) Western blot analysis of NSCLC 1, NSCLC 2 and NLF cells, after activation of Nrf2 with tBHQ (20 uM) for 6 hours and cellular fractionation. Lamin A was used as nuclear marker, while α-tubulin was used as a cytoplasmic marker. Nrf2 was detected with Abcam EP1808Y antibodies. Arrows indicate different Nrf2 forms: ←p-Nrf2 for phosphorylated, canonical Nrf2; ←Nrf2 for dephosphorylated, canonical Nrf2; ←ΔN-Nrf2 for the N-terminally truncated Nrf2 isoform 2.

3.2.3. Discussion

The canonical regulation of Nrf2 assumes its constant degradation via Keap1-Cul3-E3 ubiquitin ligase complex and therefore low level of the protein expressed in cells under homeostatic conditions. Nrf2 controls the expression of genes that represent the most important cytoprotective defense system in a cell, and the full-length Nrf2 protein is already widely described and characterized. However, the expression of the different Nrf2 isoforms under various conditions is not well-investigated yet, even though it was shown that not one, but two transcript variants of *NFE2L2* gene are the most abundantly expressed in the cells under homeostatic and stress conditions (206). The use of an alternative transcription start and/or termination site or alternative splicing enables a cell to produce multiple transcripts. Transcript diversity and structural changes on the mRNA level, which can affect the efficiency of the translation, are resulting in the production of multiple protein isoforms with different expression in the stress-mediated context (206). Therefore, it is important to investigate the expression of different transcript variants and Nrf2 protein isoforms that they are encoding.

Here we found that the stable and shorter form of Nrf2 (named ΔN-Nrf2) is abundantly expressed in lung cancer cell lines, in primary cell lines derived from non-small cell lung cancer patients and in normal lung fibroblasts under homeostatic conditions. We identified the stable form as Nrf2 isoform 2, which is the product of Nrf2 transcript variants 2 and 4 that give rise to the same protein. ΔN-Nrf2 isoform 2 lacks the first 16 amino acids at the N-terminus due to the utilization of an alternative AUG for translation initiation, in comparison to the full-length Nrf2 isoform 1. Interestingly, using isoform sequencing (Iso-seq) analysis, Otsuki et al. have found that the two transcripts of *NFE2L2* gene, that are the most abundantly expressed in cells, are encoding full-length Nrf2 protein - isoform 1 and N-terminally truncated isoform 2 (206). They highlighted the limitations of the short-read RNA-sequencing and an importance of the different transcript variants expression under exposure to stress. This long-read transcriptome data supports our experimental findings, since we have also detected transcripts that are encoding isoform 1 and isoform 2 as the most abundantly expressed in all tested cell lines.

The newly identified ΔN-Nrf2 form was shown to be more abundant and more stable under homeostatic conditions, compared to the full-length Nrf2, indicating that it might not be regulated through the same Keap-Cul3 pathway. Comparing the stability of the two isoforms, isoform 1 has a high turnover rate, while isoform 2 has shown higher stability. The reason could be different localization of the protein isoforms and due to that, different interacting proteins affecting the stability. Interestingly, under homeostatic conditions, but also upon activation of full-length Nrf2, ΔN-Nrf2 remains in the cytoplasm. It is important to mention that,

upon oxidative stress, dissociation between Nrf2 and Keap1 is not the only trigger for accumulation of Nrf2 in the nucleus. It seems that additional activation of Nrf2 is needed, which can be caused by either post-translational modifications (e.g. phosphorylation) or through some alternative signal transduction pathways (34). Phosphorylation was shown to play a role in the localization of Nrf2, however as previously mentioned, it is not necessary for nuclear translocation of Nrf2 (16). We have also observed that in our cellular fractionation results, where the phosphorylated but also dephosphorylated full-length Nrf2 were localized in the nucleus. Based on that, it is most probable that lack of phosphorylation is not the only factor responsible for cytoplasmic localization of ΔN-Nrf2.

The studies on the localization of Nrf2 suggest that the balance between nuclear export and import determines nuclear and cytosolic distribution of Nrf2. Li et al. have identified a functional NES in the transactivation domain of Nrf2, which seem to be crucial in the regulation of nuclear translocation of Nrf2 (219). These results implicated that Keap1 may not be the only factor responsible for the sequestration of Nrf2 in the cytoplasm. In addition to NES, there are few functional NLS sequences identified in Nrf2, including two NLS motifs identified in murine Nrf2 – one located near N-terminal region (amino acid residues 42-53) and the other located near the C-terminal region (amino acid residues 587-593) (220). Both sequences were also found to be present in human Nrf2. It was shown that the functionality of all the identified NLS sequences is crucial for nuclear translocation of Nrf2 (202,220). We could speculate that the NLS motif located near N-terminal region, in the Neh2 domain of Nrf2, could be disrupted in the ΔN-Nrf2 due to the deletion of the first 16 amino acids, which could explain the inability of ΔN-Nrf2 to translocate to the nucleus.

Molecular modeling and molecular dynamics simulations revealed that the depletion of the first 16 amino acids in ΔN-Nrf2 isoform 2 is causing the impairment of Keap1 binding to Nrf2 through the low-affinity DLG motif. This small change in the Nrf2 structure is the reason why lysine residues are not exposed to the ubiquitination, which explains the higher stability of ΔN-Nrf2 and resistance to the Keap1-mediated degradation. Even though the ΔN-Nrf2 has an altered protein structure, Keap1 can still be bound, but the binding is much weaker compared to the full-length Nrf2. Based on these predictions, but also on the fact that ΔN-Nrf2 did not accumulate after inhibition of the canonical Keap1-Cul3-E3 ubiquitin ligase degradation pathway with MLN4924, we assumed that the regulation of the ΔN-Nrf2 is different compared to the full-length Nrf2. However, when we think about the known alternative degradation pathways, e.g. β-TrCP-SKP1-CUL1-RBX1 and CUL4/DDB1/WDR23, we have to take into consideration that MLN4924 inhibits all the cullins, therefore, these alternative pathways should have been inhibited too. There is another alternative degradation pathway with HRD1 protein, that was shown to trigger Nrf2 degradation under endoplasmic reticulum stress. HRD1

protein is an E3 ubiquitin ligase that directly binds to the Neh4 and Neh5 domains of Nrf2 and was shown to suppress Nrf2 expression in liver cirrhosis (52). Interestingly, HRD1 was firstly identified as a ER membrane protein that is responsible for ER-associated degradation (ERAD), however it was shown to cause the degradation of non-ERAD substrates in the cytoplasm such as p53, IRE1 and Nrf1 (221–223). Therefore, we could speculate that HRD1-degradation pathway might be involved in the regulation of the ΔN-Nrf2 stability.

Even though the expression and the stability of the ΔN-Nrf2 is high in all the tested cells, comparing to the full-length Nrf2, it was not identified prior to this study. It could be due to the different migration of Nrf2 than predicated in the SDS-PAGE gel, the limited specificity of the available antibodies and difficulties in separating the isoforms in the SDS-PAGE gel.

The role of the newly identified ΔN-Nrf2 is not known yet. An important example of a transcription factors with expression of multiple protein isoforms are p53, p63 and p73. Due to the multiple splicing, alternative promoter usage and alternative translation initiation sites, *p53, p63* and *p73* genes encode for various protein isoforms that have different biological functions (224). An example of the interactions between these isoforms is the negative feedback loop between p53 and p73, where p53 and transactivating isoform p73 (TAp73) bind to the N-truncated p73 (ΔNp73) promoter to induce its transcription, while in return ΔNp73 inhibits p53 and TAp73 activity by competing for the promoter sites or directly binding the proteins (225). This is a good example of how important it is to investigate different protein isoforms and that the ratio between the expression of isoforms could be important in terms of the cell fate. In our case, the transcript levels of full length Nrf2 isoform 1 and ΔN-Nrf2 isoform 2 are similar, however, the protein expression of the two isoforms is changing between the tested cell lines. To be able to investigate if the differences come from the stability of synthesis, we could compare the expression of different Nrf2 transcripts on the polysomes. From that point on, we would be able to further explore if there is an interaction/competition between different Nrf2 isoforms, similarly to the p53 family members.

CHAPTER 4

Conclusion

4.1. Highlights

- Nrf2 depletion decreased HLA class I protein and cell surface expression, but not RNA expression
- Nrf2 is in the direct interaction with HLA class I molecules and it affects their stability
- Identification of a stable Nrf2 form (named ΔN-Nrf2) abundantly expressed in lung cells
- Stable ΔN-Nrf2 form originates from transcript variants 2 and 4, that are encoding the same protein-Nrf2 isoform 2
- The deletion of the first 16 amino acids in ΔN-Nrf2 is causing the impairment of Keap1 binding to Nrf2
- ΔN-Nrf2 is mainly localized in the cytoplasm under homeostatic conditions and upon electrophilic stress, and it is not regulated through Keap1-Cul3-E3 ubiquitin ligase system

4.2. Conclusion and future perspectives

In the first part of my PhD project, I have showed that Nrf2 has a role in the regulation of HLA class I expression, since its depletion decreased the protein and cell surface expression of HLA class I molecules, but increased their RNA expression. Further results suggested that Nrf2 can bind HLA class I molecules in lung cancer cells with different binding affinities towards different HLA class I alleles. Nrf2 bound to the HLA class I molecules, particularly HLA-A alleles, is causing their stabilization and therefore affecting their final expression on the cell surface, where they present antigens to the cytotoxic T cells.

During the first part of my PhD project, I observed the extraordinary stability of one of the forms detected with Nrf2 antibodies. That encouraged me to investigate it deeper and to try to identify the origin of the detected form. Therefore, the second part of the PhD project was focused on the detailed comparison of the full-length Nrf2 expression, that is already well-characterized, and this newly detected Nrf2 form (named ΔN-Nrf2). I have identified the form as an Nrf2 isoform 2, abundantly expressed across different lung cancer cell lines and normal lung fibroblasts. I've tracked the origin of isoform 2 using different approaches and showed that

isoform 2 is encoded by transcript variants 2 and 4. Based on the lambda-phosphatase treatment, low stability upon translation elongation inhibition (in the correlation with the literature) and responsiveness to the silencing of Keap1 expression, I have confirmed that the phosphorylated full-length Nrf2 is migrating around 130 kDa in the 8% SDS-PAGE gel, which is significantly slower than predicted. In addition, I have identified the third Nrf2 form as a dephosphorylated full-length Nrf2, migrating around 110 kDa in the 8% SDS-PAGE gel.

The newly identified ΔN-Nrf2 form is not constantly degraded under homeostatic conditions and it is not regulated through canonical Keap1-Cul3-mediated degradation pathway. Compared to the full-length Nrf2, ΔN-Nrf2 has a deletion of the first 16 amino acids causing the impairment of the Keap1 binding and inability of the Nrf2 lysine residues to be ubiquitinated, which can explain its high stability. Since the main mechanism to regulate Nrf2 activity is through its stability, the alternative Keap1-independent degradation pathway, such as one involving HRD1 protein, could have a role in the regulation of ΔN-Nrf2 expression.

The results from the first part of my project, focused on the Nrf2 role in the HLA class I expression, suggest that the novel potential role of Nrf2 is the stabilization of the HLA class I molecules. Since the most of the experiments in the first part of the project were done in the model A549 cell line, that has constitutively active Nrf2, it is not quite clear which Nrf2 isoform could regulate HLA-I expression. On the other hand, even though A549 cells have high expression of full-length Nrf2 isoform 1, that is resistant to Keap1-Cul3-E3 ubiquitin ligase system, they also have high expression and even higher stability of ΔN-Nrf2. Moreover, co-immunoprecipitation and direct interaction of Nrf2 and HLA-I was confirmed in RERF and NSCLC 1 cells, which should have constantly degraded full-length Nrf2 and more abundantly expressed ΔN-Nrf2 under homeostatic conditions. The PLA results have shown that Nrf2 and HLA-A are in the close proximity in A549 and RERF cells, in the cytoplasm and in the nucleus, suggesting that both full-length Nrf2 and ΔN-Nrf2 might interact with HLA-I molecules. It is important to mention that so far studies on Nrf2 were mostly focused on its transcriptional activity and functions as a transcription factor. Therefore, the effect of Nrf2 on the direct protein-protein level is a novel observation. Future approach is going to include the transfection of the lung cells with separate plasmids containing Nrf2 isoform 1 and Nrf2 isoform 2, based on the differences in their sequences, and mass spectrometry analysis of the Nrf2 isoform 1 and Nrf2 isoform 2 interactome. That would reveal the similarities and differences between the roles of these two Nrf2 isoforms. Moreover, based on the different stability of the Nrf2 isoforms, the pulse-chase analysis combined with the PLA with HLA-I could reveal which Nrf2 isoform interacts and stabilizes HLA-I molecules.

Bibliography

1. Moi P, Chan K, Asunis I, Cao A, Kan YW. Isolation of NF-E2-related factor 2 (Nrf2), a NF-E2-like basic leucine zipper transcriptional activator that binds to the tandem NF-E2/AP1 repeat of the beta-globin locus control region. Proceedings of the National Academy of Sciences. 1994 Oct 11;91(21):9926–30.

2. Jeong WS, Jun M, Kong ANT. Nrf2: A Potential Molecular Target for Cancer Chemoprevention by Natural Compounds. Antioxidants & Redox Signaling. 2006 Jan;8(1–2):99–106.

3. Motohashi H, Yamamoto M. Nrf2-Keap1 Defines a Physiologically Important Stress Response Mechanism. Trend Mol Med. 2004;10(11):549–57.

4. Zhang DD. Mechanistic Studies of the Nrf2-Keap1 Signaling Pathway. Drug Metab Rev. 2006;38(4):769–89.

5. Kensler TW, Wakabayashi N, Biswal S. Cell Survival Responses to Environmental Stresses Via the Keap1-Nrf2-ARE Pathway. Annual Review of Pharmacology and Toxicology. 2007;47:89–116.

6. Lau A, Villeneuve NF, Sun Z, Wong PK, Zhang DD. Dual roles of Nrf2 in cancer. Pharmacological Research. 2008;58:262–70.

7. He CH, Gong P, Hu B, Stewart D, Choi ME, Choi AMK, et al. Identification of Activating Transcription Factor 4 (ATF4) as an Nrf2-interacting Protein. Journal of Biological Chemistry. 2001 Jun;276(24):20858–65.

8. Pajares M, Cuadrado A, Rojo AI. Modulation of proteostasis by transcription factor NRF2 and impact in neurodegenerative diseases. Redox Biology. 2017 Apr;11:543–53.

9. Kwak MK, Wakabayashi N, Greenlaw JL, Yamamoto M, Kensler TW. Antioxidants Enhance Mammalian Proteasome Expression through the Keap1-Nrf2 Signaling Pathway. Molecular and Cellular Biology. 2003 Dec;23(23):8786–94.

10. Pajares M, Jiménez-Moreno N, García-Yagüe ÁJ, Escoll M, de Ceballos ML, van Leuven F, et al. Transcription factor NFE2L2/NRF2 is a regulator of macroautophagy genes. Autophagy. 2016 Oct 2;12(10):1902–16.

11. He F, Antonucci L, Karin M. NRF2 as a regulator of cell metabolism and inflammation in cancer. Carcinogenesis. 2020 Jun 17;41(4):405–16.

12. He F, Ru X, Wen T. NRF2, a transcription factor for stress response and beyond. International Journal of Molecular Sciences. 2020;21(13):1–23.

13. Jaramillo MC, Zhang DD. The emerging role of the Nrf2-Keap1 signaling pathway in cancer. Genes and Development. 2013;27(20):2179–91.

14. Sun Z, Huang Z, Zhang DD. Phosphorylation of Nrf2 at Multiple Sites by MAP Kinases Has a Limited Contribution in Modulating the Nrf2-Dependent Antioxidant Response. PLoS ONE. 2009 Aug 11;4(8):e6588.

15. Cullinan SB, Diehl JA. PERK-dependent Activation of Nrf2 Contributes to Redox Homeostasis and Cell Survival following Endoplasmic Reticulum Stress. Journal of Biological Chemistry. 2004 May;279(19):20108–17.

16. Bloom DA, Jaiswal AK. Phosphorylation of Nrf2 at Ser40 by Protein Kinase C in Response to Antioxidants Leads to the Release of Nrf2 from INrf2, but Is Not Required for Nrf2 Stabilization/Accumulation in the Nucleus and Transcriptional Activation of Antioxidant Response Element-mediated NAD(P)H:Quinone Oxidoreductase-1 Gene Expression. Journal of Biological Chemistry. 2003 Nov;278(45):44675–82.

17. Huang HC, Nguyen T, Pickett CB. Regulation of the antioxidant response element by protein kinase C-mediated phosphorylation of NF-E2-related factor 2. Proc Natl Acad Sci U S A. 2000 Nov;97(23):12475–80.

18. Huang HC, Nguyen T, Pickett CB. Phosphorylation of Nrf2 at Ser-40 by Protein Kinase C Regulates Antioxidant Response Element-mediated Transcription. Journal of Biological Chemistry. 2002 Nov;277(45):42769–74.

19. McMahon M, Thomas N, Itoh K, Yamamoto M, Hayes JD. Dimerization of Substrate Adaptors Can Facilitate Cullin-mediated Ubiquitylation of Proteins by a “Tethering” Mechanism. Journal of Biological Chemistry. 2006 Aug;281(34):24756–68.

20. Tong KI, Kobayashi A, Katsuoka F, Yamamoto M. Two-site substrate recognition model for the Keap1-Nrf2 system: a hinge and latch mechanism. Biol Chem [Internet]. 2006 Oct 1 [cited 2021 Dec 7];387(10–11):1311–20. Available from: https://pubmed.ncbi.nlm.nih.gov/17081101/

21. Zhang DD, Lo SC, Cross J v., Templeton DJ, Hannink M. Keap1 Is a Redox-Regulated Substrate Adaptor Protein for a Cul3-Dependent Ubiquitin Ligase Complex. Molecular and Cellular Biology. 2004 Dec 15;24(24):10941–53.

22. McMahon M, Thomas N, Itoh K, Yamamoto M, Hayes JD. Redox-regulated turnover of Nrf2 is determined by at least two separate protein domains, the redox-sensitive Neh2 degron and the redox-insensitive Neh6 degron. J Biol Chem [Internet]. 2004 Jul 23 [cited 2021 Dec 9];279(30):31556–67. Available from: https://pubmed.ncbi.nlm.nih.gov/15143058/

23. Rada P, Rojo AI, Chowdhry S, McMahon M, Hayes JD, Cuadrado A. SCF/ -TrCP Promotes Glycogen Synthase Kinase 3-Dependent Degradation of the Nrf2 Transcription Factor in a Keap1-Independent Manner. Molecular and Cellular Biology. 2011;31(6):1121–33.

24. Chowdhry S, Zhang Y, McMahon M, Sutherland C, Cuadrado A, Hayes JD. Nrf2 is controlled by two distinct β-TrCP recognition motifs in its Neh6 domain, one of which can be modulated by GSK-3 activity. Oncogene. 2013;32(32):3765–81.

25. Katoh Y, Itoh K, Yoshida E, Miyagishi M, Fukamizu A, Yamamoto M. Two domains of Nrf2 cooperatively bind CBP, a CREB binding protein, and synergistically activate transcription. Genes to Cells. 2001 Oct;6(10):857–68.

26. Nioi P, Nguyen T, Sherratt PJ, Pickett CB. The Carboxy-Terminal Neh3 Domain of Nrf2 Is Required for Transcriptional Activation. Molecular and Cellular Biology. 2005 Dec 15;25(24):10895–906.

27. Wang H, Liu K, Geng M, Gao P, Wu X, Hai Y, et al. RXRα Inhibits the NRF2-ARE Signaling Pathway through a Direct Interaction with the Neh7 Domain of NRF2. Cancer Research. 2013 May 15;73(10):3097–108.

28. Kopacz A, Kloska D, Forman HJ, Jozkowicz A, Grochot-Przeczek A. Beyond repression of Nrf2: An update on Keap1. Vol. 157, Free Radical Biology and Medicine. Elsevier Inc.; 2020. p. 63–74.

29. Albagli O, Dhordain P, Deweindt C, Lecocq G, Leprince D. The BTB/POZ domain: a new protein-protein interaction motif common to DNA- and actin-binding proteins. Cell Growth Differ. 1995 Sep;6(9):1193–8.

30. Cleasby A, Yon J, Day PJ, Richardson C, Tickle IJ, Williams PA, et al. Structure of the BTB Domain of Keap1 and Its Interaction with the Triterpenoid Antagonist CDDO. PLoS ONE. 2014 Jun 4;9(6):e98896.

31. Menegon S, Columbano A, Giordano S. The Dual Roles of NRF2 in Cancer. Trends in Molecular Medicine. 2016;22(7):578–93.

32. McMahon M, Lamont DJ, Beattie KA, Hayes JD. Keap1 perceives stress via three sensors for the endogenous signaling molecules nitric oxide, zinc, and alkenals. Proc Natl Acad Sci U S A. 2010 Nov 2;107(44):18838–43.

33. Sánchez-Ortega M, Carrera AC, Garrido A. Role of NRF2 in lung cancer. Vol. 10, Cells. MDPI; 2021.

34. Kobayashi A, Kang MI, Watai Y, Tong KI, Shibata T, Uchida K, et al. Oxidative and Electrophilic Stresses Activate Nrf2 through Inhibition of Ubiquitination Activity of Keap1. Molecular and Cellular Biology. 2006 Jan;26(1):221–9.

35. Shibata T, Ohta T, Tong KI, Kokubu A, Odogawa R, Tsuta K, et al. Cancer related mutations in NRF2 impair its recognition by Keap1-Cul3 E3 ligase and promote malignancy. Proc Natl Acad Sci U S A [Internet]. 2008 Sep 9 [cited 2021 May 25];105(36):13568–73. Available from: https://pubmed.ncbi.nlm.nih.gov/18757741/

36. Lee JM, Chan K, Kan YW, Johnson JA. Targeted disruption of Nrf2 causes regenerative immune-mediated hemolytic anemia. Proc Natl Acad Sci U S A. 2004;101(26):9751–6.

37. Kwak MK, Wakabayashi N, Itoh K, Motohashi H, Yamamoto M, Kensler TW. Modulation of gene expression by cancer chemopreventive dithiolethiones through the Keap1-Nrf2 pathway: Identification of novel gene clusters for cell survival. Journal of Biological Chemistry [Internet]. 2003;278(10):8135–45. Available from: http://dx.doi.org/10.1074/jbc.M211898200

38. Taniguchi K, Yamachika S, He F, Karin M. p62/SQSTM1- Dr. Jekyll and Mr. Hyde that prevents oxidative stress but promotes liver cancer. FEBS Letters. 2016;590(15):2375–97.

39. Umemura A, He F, Taniguchi K, Nakagawa H, Yamachika S, Font-Burgada J, et al. p62, upregulated during preneoplasia, induces hepatocellular carcinogenesis by maintaining survival of stressed HCC-initiating cells. Cancer Cell. 2016;29(6):935–48.

40. Komatsu M, Kurokawa H, Waguri S, Taguchi K, Kobayashi A, Ichimura Y, et al. The selective autophagy substrate p62 activates the stress responsive transcription factor Nrf2 through inactivation of Keap1. Nature Cell Biology. 2010;12:213–23.

41. Hast BE, Goldfarb D, Mulvaney KM, Hast MA, Siesser PF, Yan F, et al. Proteomic analysis of ubiquitin ligase KEAP1 reveals associated proteins that inhibit NRF2 ubiquitination. CANCER RESEARCH. 2013;73(7):2199–210.

42. Camp ND, James RG, Dawson DW, Yan F, Davison JM, Houck SA, et al. Wilms tumor gene on X chromosome (WTX) inhibits degradation of NRF2 protein through competitive binding to KEAP1 protein. Journal of Biological Chemistry. 2012;287(9):6539–50.

43. Ma J, Cai H, Wu T, Sobhian B, Huo Y, Alcivar A, et al. PALB2 Interacts with KEAP1 To Promote NRF2 Nuclear Accumulation and Function. Molecular and Cellular Biology. 2012;32(8):1506–17.

44. Ichimura Y, Waguri S, Sou Y shin, Kageyama S, Hasegawa J, Ishimura R, et al. Phosphorylation of p62 Activates the Keap1-Nrf2 Pathway during Selective Autophagy. Molecular Cell. 2013 Sep;51(5):618–31.

45. Lau A, Tian W, Whitman SA, Zhang DD. The predicted molecular weight of Nrf2: It is what it is not. Antioxidants and Redox Signaling. 2013;18(1):91–3.

46. Chen W, Sun Z, Wang XJ, Jiang T, Huang Z, Fang D, et al. Direct interaction between Nrf2 and p21Cip1/WAF1 upregulates the Nrf2-mediated antioxidant response. Mol Cell. 2009;34(6):663–73.

47. Gorrini C, Baniasadi PS, Harris IS, Silvester J, Inoue S, Snow B, et al. BRCA1 interacts with Nrf2 to regulate antioxidant signaling and cell survival. Journal of Experimental Medicine. 2013;210(8):1529–44.

48. Ganner A, Pfeiffer ZC, Wingendorf L, Kreis S, Klein M, Walz G, et al. The acetyltransferase p300 regulates NRF2 stability and localization. Biochemical and Biophysical Research Communications [Internet]. 2020;524(4):895–902. Available from: https://doi.org/10.1016/j.bbrc.2020.02.006

49. Hayes JD, Chowdhry S, Dinkova-Kostova AT, Sutherland C. Dual regulation of transcription factor Nrf2 by Keap1 and by the combined actions of β-TrCP and GSK-3. Biochem Soc Trans. 2015;43(4):611–20.

50. Lo JY, Spatola BN, Curran SP. WDR23 regulates NRF2 independently of KEAP1. PLoS Genetics. 2017;13(4):1–26.

51. Taguchi K, Yamamoto M. The KEAP1–NRF2 System in Cancer. Frontiers in Oncology [Internet]. 2017;7(May):1–11. Available from: http://journal.frontiersin.org/article/10.3389/fonc.2017.00085/full

52. Wu T, Zhao F, Gao B, Tan C, Yagishita N, Nakajima T, et al. Hrd1 suppresses Nrf2-mediated cellular protection during liver cirrhosis. Genes and Development. 2014 Apr 1;28(7):708–22.

53. Goldstein LD, Lee J, Gnad F, Klijn C, Schaub A, Reeder J, et al. Recurrent Loss of NFE2L2 Exon 2 Is a Mechanism for Nrf2 Pathway Activation in Human Cancers. Cell Reports [Internet]. 2016;16(10):2605–17. Available from: http://dx.doi.org/10.1016/j.celrep.2016.08.010

54. Singh A, Misra V, Thimmulappa RK, Lee H, Ames S, Hoque MO, et al. Dysfunctional KEAP1-NRF2 interaction in non-small-cell lung cancer. PLoS Medicine. 2006;3(10):1865–76.

55. Padmanabhan B, Tong KI, Ohta T, Nakamura Y, Scharlock M, Ohtsuji M, et al. Structural Basis for Defects of Keap1 Activity Provoked by Its Point Mutations in Lung Cancer. Molecular Cell. 2006 Mar;21(5):689–700.

56. Ohta T, Iijima K, Miyamoto M, Nakahara I, Tanaka H, Ohtsuji M, et al. Loss of Keap1 Function Activates Nrf2 and Provides Advantages for Lung Cancer Cell Growth. Cancer Research. 2008 Mar 1;68(5):1303–9.

57. Fukutomi T, Takagi K, Mizushima T, Ohuchi N, Yamamoto M. Kinetic, Thermodynamic, and Structural Characterizations of the Association between Nrf2-DLGex Degron and Keap1. Molecular and Cellular Biology. 2014 Mar;34(5):832–46.

58. Tung MC, Lin PL, Wang YC, He TY, Lee MC, Yeh SD, et al. Mutant p53 confers chemoresistance in non-small cell lung cancer by upregulating Nrf2 [Internet]. Vol. 6. 2015. Available from: www.impactjournals.com/oncotarget

59. Scheffler M, Bos M, Gardizi M, König K, Michels S, Fassunke J, et al. PIK3CA mutations in non-small cell lung cancer (NSCLC): Genetic heterogeneity, prognostic impact and incidence of prior malignancies [Internet]. Vol. 6, Oncotarget. 2014. Available from: www.impactjournals.com/oncotarget/

60. Best SA, Ding S, Kersbergen A, Dong X, Song JY, Xie Y, et al. Distinct initiating events underpin the immune and metabolic heterogeneity of KRAS-mutant lung adenocarcinoma. Nature Communications. 2019 Dec 1;10(1).

61. Arbour KC, Jordan E, Kim HR, Dienstag J, Yu HA, Sanchez-Vega F, et al. Effects of co-occurring genomic alterations on outcomes in patients with KRAS-mutant non-small cell lung cancer. Clinical Cancer Research. 2018 Jan 15;24(2):334–40.

62. Joo MS, Kim WD, Lee KY, Kim JH, Koo JH, Kim SG. AMPK Facilitates Nuclear Accumulation of Nrf2 by Phosphorylating at Serine 550. Molecular and Cellular Biology. 2016 Jul 15;36(14):1931–42.

63. Rada P, Rojo AI, Evrard-Todeschi N, Innamorato NG, Cotte A, Jaworski T, et al. Structural and Functional Characterization of Nrf2 Degradation by the Glycogen Synthase Kinase 3/β-TrCP Axis. Molecular and Cellular Biology. 2012 Sep;32(17):3486–99.

64. Jain AK, Jaiswal AK. GSK-3β Acts Upstream of Fyn Kinase in Regulation of Nuclear Export and Degradation of NF-E2 Related Factor 2. Journal of Biological Chemistry. 2007 Jun;282(22):16502–10.

65. Cullinan SB, Zhang D, Hannink M, Arvisais E, Kaufman RJ, Diehl JA. Nrf2 Is a Direct PERK Substrate and Effector of PERK-Dependent Cell Survival. Molecular and Cellular Biology. 2003 Oct 15;23(20):7198–209.

66. Nguyen T, Sherratt PJ, Huang HC, Yang CS, Pickett CB. Increased Protein Stability as a Mechanism That Enhances Nrf2-mediated Transcriptional Activation of the Antioxidant Response Element. Journal of Biological Chemistry. 2003 Feb;278(7):4536–41.

67. Kang KW, Ryu JH, Kim SG. The Essential Role of Phosphatidylinositol 3-Kinase and of p38 Mitogen-Activated Protein Kinase Activation in the Antioxidant Response Element-Mediated rGSTA2 Induction by Decreased Glutathione in H4IIE Hepatoma Cells. Molecular Pharmacology. 2000 Nov 1;58(5):1017–25.

68. Sun Z, Chin YE, Zhang DD. Acetylation of Nrf2 by p300/CBP Augments Promoter-Specific DNA Binding of Nrf2 during the Antioxidant Response. Molecular and Cellular Biology. 2009 May 15;29(10):2658–72.

69. Kawai Y, Garduño L, Theodore M, Yang J, Arinze IJ. Acetylation-Deacetylation of the Transcription Factor Nrf2 (Nuclear Factor Erythroid 2-related Factor 2) Regulates Its Transcriptional Activity and Nucleocytoplasmic Localization. Journal of Biological Chemistry. 2011 Mar;286(9):7629–40.

70. Wu KC, Cui JY, Klaassen CD. Effect of Graded Nrf2 Activation on Phase-I and -II Drug Metabolizing Enzymes and Transporters in Mouse Liver. PLoS ONE. 2012 Jul 12;7(7):e39006.

71. Hayes JD, Dinkova-Kostova AT. The Nrf2 regulatory network provides an interface between redox and intermediary metabolism. Trends in Biochemical Sciences. 2014 Apr;39(4):199–218.

72. Tonelli C, Chio IIC, Tuveson DA. Transcriptional Regulation by Nrf2. Antioxidants and Redox Signaling. 2018;29(17):1727–45.

73. Jayaraj GG, Hipp MS, Hartl FU. Functional Modules of the Proteostasis Network. Cold Spring Harbor Perspectives in Biology. 2020 Jan;12(1):a033951.

74. Hetz C. The unfolded protein response: controlling cell fate decisions under ER stress and beyond. Nature Reviews Molecular Cell Biology. 2012 Feb 18;13(2):89–102.

75. Jiang T, Harder B, Rojo de la Vega M, Wong PK, Chapman E, Zhang DD. p62 links autophagy and Nrf2 signaling. Free Radical Biology and Medicine. 2015 Nov;88:199–204.

76. Münz C. Enhancing Immunity Through Autophagy. Annual Review of Immunology. 2009 Apr 1;27(1):423–49.

77. Mizushima N, Levine B, Cuervo AM, Klionsky DJ. Autophagy fights disease through cellular self-digestion. Nature. 2008 Feb;451(7182):1069–75.

78. Degenhardt K, Mathew R, Beaudoin B, Bray K, Anderson D, Chen G, et al. Autophagy promotes tumor cell survival and restricts necrosis, inflammation, and tumorigenesis. Cancer Cell. 2006 Jul;10(1):51–64.

79. Cuadrado A, Rojo AI, Wells G, Hayes JD, Cousin SP, Rumsey WL, et al. Therapeutic targeting of the NRF2 and KEAP1 partnership in chronic diseases. Nature Reviews Drug Discovery. 2019 Apr 4;18(4):295–317.

80. Holmström KM, Kostov R v., Dinkova-Kostova AT. The multifaceted role of Nrf2 in mitochondrial function. Current Opinion in Toxicology. 2016 Dec;1:80–91.

81. Hu Q, Ren J, Li G, Wu J, Wu X, Wang G, et al. The mitochondrially targeted antioxidant MitoQ protects the intestinal barrier by ameliorating mitochondrial DNA damage via the Nrf2/ARE signaling pathway. Cell Death & Disease. 2018 Mar 14;9(3):403.

82. Piantadosi CA, Carraway MS, Babiker A, Suliman HB. Heme Oxygenase-1 Regulates Cardiac Mitochondrial Biogenesis via Nrf2-Mediated Transcriptional Control of Nuclear Respiratory Factor-1. Circulation Research. 2008 Nov 21;103(11):1232–40.

83. Gureev AP, Shaforostova EA, Popov VN. Regulation of Mitochondrial Biogenesis as a Way for Active Longevity: Interaction Between the Nrf2 and PGC-1α Signaling Pathways. Frontiers in Genetics. 2019 May 14;10.

84. Wang XJ, Sun Z, Villeneuve NF, Zhang S, Zhao F, Li Y, et al. Nrf2 enhances resistance of cancer cells to chemotherapeutic drugs, the dark side of Nrf2. Carcinogenesis. 2008;29(6):1235–43.

85. Jiang T, Chen N, Zhao F, Wang XJ, Kong B, Zheng W, et al. High levels of Nrf2 determine chemoresistance in type II endometrial cancer. Cancer Research. 2010;70(13):5486–96.

86. Mitsuishi Y, Taguchi K, Kawatani Y, Shibata T, Nukiwa T, Aburatani H, et al. Nrf2 Redirects Glucose and Glutamine into Anabolic Pathways in Metabolic Reprogramming. Cancer Cell. 2012;22(1):66–79.

87. Mitsuishi Y, Motohashi H, Yamamoto M. The Keap1–Nrf2 system in cancers: stress response and anabolic metabolism. Frontiers in Oncology. 2012;2(December):1–13.

88. Kitamura H, Motohashi H. NRF2 addiction in cancer cells. Cancer Science. 2018;109(4):900–11.

89. Kobayashi A, Kang MI, Okawa H, Ohtsuji M, Zenke Y, Chiba T, et al. Oxidative Stress Sensor Keap1 Functions as an Adaptor for Cul3-Based E3 Ligase To Regulate Proteasomal Degradation of Nrf2. Molecular and Cellular Biology. 2004;24(16):7130–9.

90. Kemmerer ZA, Ader NR, Mulroy SS, Eggler AL. Comparison of human Nrf2 antibodies: A tale of two proteins. Toxicology Letters. 2015 Oct;238(2):83–9.

91. Shibata T, Kokubu A, Gotoh M, Ojima H, Ohta T, Yamamoto M, et al. Genetic Alteration of Keap1 Confers Constitutive Nrf2 Activation and Resistance to Chemotherapy in Gallbladder Cancer. Gastroenterology. 2008;135(4):1358–68.

92. Sasaki H, Suzuki A, Shitara M, Hikosaka Y, Okuda K, Moriyama S, et al. Genotype analysis of the NRF2 gene mutation in lung cancer. International Journal of Molecular Medicine. 2013;31(5):1135–8.

93. Solis LM, Behrens C, Dong W, Suraokar M, Ozburn C. N, Moran CA, et al. Nrf2 and Keap1 Abnormalities in Non-Small Cell Lung Carcinoma and Association with Clinicopathologic Features. Clin Cancer Res. 2010;16(14):3743–53.

94. Toth R, Warfel N. Strange Bedfellows: Nuclear Factor, Erythroid 2-Like 2 (Nrf2) and Hypoxia-Inducible Factor 1 (HIF-1) in Tumor Hypoxia. Antioxidants. 2017;6(2):27.

95. You A, Nam C won, Wakabayashi N, Yamamoto M, Kensler TW, Kwak MK. Transcription factor Nrf2 maintains the basal expression of Mdm2: An implication of the regulation of p53 signaling by Nrf2. Archives of Biochemistry and Biophysics. 2011 Mar;507(2):356–64.

96. Rojo de la Vega M, Chapman E, Zhang DD. NRF2 and the Hallmarks of Cancer. Cancer Cell. 2018;34(1):21–43.

97. Best SA, Sutherland KD. “Keaping” a lid on lung cancer: the Keap1-Nrf2 pathway. Vol. 17, Cell Cycle. Taylor and Francis Inc.; 2018. p. 1696–707.

98. Smolková K, Mikó E, Kovács T, Leguina-Ruzzi A, Sipos A, Bai P. Nuclear factor erythroid 2-related factor 2 in regulating cancer metabolism. Vol. 33, Antioxidants and Redox Signaling. Mary Ann Liebert Inc.; 2020. p. 966–97.

99. Robertson H, Dinkova-Kostova AT, Hayes JD. NRF2 and the Ambiguous Consequences of Its Activation during Initiation and the Subsequent Stages of Tumourigenesis. Cancers (Basel). 2020 Dec 2;12(12).

100. Adam J, Hatipoglu E, O’Flaherty L, Ternette N, Sahgal N, Lockstone H, et al. Renal cyst formation in Fh1-deficient mice is independent of the Hif/Phd pathway: roles for fumarate in KEAP1 succination and Nrf2 signaling. Cancer Cell. 2011 Oct 18;20(4):524–37.

101. Kang JS, Nam LB, Yoo OK, Keum YS. Molecular mechanisms and systemic targeting of NRF2 dysregulation in cancer. Biochemical Pharmacology. 2020;177:114002.

102. Bhattacharjee S, Dashwood RH. Epigenetic regulation of NRF2/KEAP1 by phytochemicals. Vol. 9, Antioxidants. MDPI; 2020. p. 1–22.

103. Zhang D, Rennhack J, Andrechek ER, Rockwell CE, Liby KT. Identification of an Unfavorable Immune Signature in Advanced Lung Tumors from Nrf2-Deficient Mice. Antioxidants & Redox Signaling. 2018;29(16):1535–52.

104. Yarosz EL, Chang CH. The Role of Reactive Oxygen Species in Regulating T Cell-mediated Immunity and Disease. Immune Network. 2018;18(1).

105. Rockwell CE, Zhang M, Fields PE, Klaassen CD. Th2 Skewing by Activation of Nrf2 in CD4 $^{+}$ T Cells. The Journal of Immunology. 2012 Feb 15;188(4):1630–7.

106. Saddawi-Konefka R, Seelige R, Gross ETE, Levy E, Searles SC, Washington A, et al. Nrf2 Induces IL-17D to Mediate Tumor and Virus Surveillance. Cell Reports. 2016 Aug;16(9):2348–58.

107. Yeang HXA, Hamdam JM, Al-Huseini LMA, Sethu S, Djouhri L, Walsh J, et al. Loss of Transcription Factor Nuclear Factor-Erythroid 2 (NF-E2) p45-related Factor-2 (Nrf2) Leads to Dysregulation of Immune Functions, Redox Homeostasis, and Intracellular Signaling in Dendritic Cells. Journal of Biological Chemistry. 2012 Mar;287(13):10556–64.

108. Zhao M, Chen H, Ding Q, Xu X, Yu B, Huang Z. Nuclear Factor Erythroid 2-related Factor 2 Deficiency Exacerbates Lupus Nephritis in B6/lpr mice by Regulating Th17 Cell Function. Scientific Reports. 2016 Dec 12;6(1):38619.

109. Kobayashi EH, Suzuki T, Funayama R, Nagashima T, Hayashi M, Sekine H, et al. Nrf2 suppresses macrophage inflammatory response by blocking proinflammatory cytokine transcription. Nature Communications. 2016 Sep 23;7(1):11624.

110. Johnson DA, Amirahmadi S, Ward C, Fabry Z, Johnson JA. The Absence of the Pro-antioxidant Transcription Factor Nrf2 Exacerbates Experimental Autoimmune Encephalomyelitis. Toxicological Sciences. 2010 Apr;114(2):237–46.

111. Sutton C, Brereton C, Keogh B, Mills KHG, Lavelle EC. A crucial role for interleukin (IL)-1 in the induction of IL-17–producing T cells that mediate autoimmune encephalomyelitis. Journal of Experimental Medicine. 2006 Jul 10;203(7):1685–91.

112. Okuda Y. IL-6-deficient mice are resistant to the induction of experimental autoimmune encephalomyelitis provoked by myelin oligodendrocyte glycoprotein. International Immunology. 1998 May 1;10(5):703–8.

113. Gold R, Kappos L, Arnold DL, Bar-Or A, Giovannoni G, Selmaj K, et al. Placebo-Controlled Phase 3 Study of Oral BG-12 for Relapsing Multiple Sclerosis. New England Journal of Medicine. 2012 Sep 20;367(12):1098–107.

114. Pareek TK, Belkadi A, Kesavapany S, Zaremba A, Loh SL, Bai L, et al. Triterpenoid modulation of IL-17 and Nrf-2 expression ameliorates neuroinflammation and promotes remyelination in autoimmune encephalomyelitis. Scientific Reports. 2011 Dec 19;1(1):201.

115. Saha S, Buttari B, Panieri E, Profumo E, Saso L. An Overview of Nrf2 Signaling Pathway and Its Role in Inflammation. Molecules. 2020 Nov 23;25(22):5474.

116. Olagnier D, Farahani E, Thyrsted J, Blay-Cadanet J, Herengt A, Idorn M, et al. SARS-CoV2-mediated suppression of NRF2-signaling reveals potent antiviral and anti-inflammatory activity of 4-octyl-itaconate and dimethyl fumarate. Nature Communications. 2020 Dec 2;11(1):4938.

117. Ramezani A, Nahad MP, Faghihloo E. The role of Nrf2 transcription factor in viral infection. Journal of Cellular Biochemistry. 2018 Aug 8;119(8):6366–82.

118. Olagnier D, Brandtoft AM, Gunderstofte C, Villadsen NL, Krapp C, Thielke AL, et al. Nrf2 negatively regulates STING indicating a link between antiviral sensing and metabolic reprogramming. Nature Communications. 2018 Dec 29;9(1):3506.

119. Horton R, Gibson R, Coggill P, Miretti M, Allcock RJ, Almeida J, et al. Variation analysis and gene annotation of eight MHC haplotypes: The MHC Haplotype Project. Immunogenetics. 2008;60(1):1–18.

120. Shiina T, Inoko H, Kulski JK. An update of the HLA genomic region, locus information and disease associations: 2004. Tissue Antigens. 2004;64(6):631–49.

121. Sznarkowska A, Mikac S, Pilch M. MHC Class I Regulation: The Origin Perspective. Cancers (Basel). 2020;12(5):E1155.

122. Shiina T, Hosomichi K, Inoko H, Kulski JK. The HLA Genomic Loci Map: Expression, Interaction, Diversity and Disease. J Hum Genet. 2009;54(1):15–39.

123. Blais ME, Dong T, Rowland-Jones S. HLA-C as a mediator of natural killer and T-cell activation: Spectator or key player? Immunology. 2011;133(1):1–7.

124. Goadsby PJ, Kurth T, Pressman A. Present Yourself! By MHC Class I and MHC Class II Molecules. Trends in Immunology. 2016;35(14):1252–60.

125. Yewdell JW. DRiPs Solidify: Progress in Understanding Endogenous MHC Class I Antigen Processing. Trends in Immunology. 2011;32(11):548–58.

126. Garrido F, Aptsiauri N, Doorduijn EM, Garcia Lora AM, van Hall T. The urgent need to recover MHC class I in cancers for effective immunotherapy. Curr Opin Immunol. 2016;39:44–51.

127. Campoli M, Ferrone S. HLA antigen changes in malignant cells: Epigenetic mechanisms and biologic significance. Oncogene. 2008;27(45):5869–85.

128. Kitamura H, Onodera Y, Murakami S, Suzuki T, Motohashi H. IL-11 contribution to tumorigenesis in an NRF2 addiction cancer model. Oncogene [Internet]. 2017;36(45):6315–24. Available from: http://dx.doi.org/10.1038/onc.2017.236

129. Telkoparan-Akillilar P, Panieri E, Cevik D, Suzen S, Saso L. Therapeutic targeting of the NRF2 signaling pathway in Cancer. Molecules. 2021 Mar 1;26(5).

130. Kensler TW, Curphey TJ, Maxiutenko Y, Roebuck BD. Chemoprotection by Organosulfur Inducers of Phase 2 Enzymes: Dithiolethiones and Dithiins. Drug Metabolism and Drug Interactions. 2000 Jan;17(1–4).

131. Conaway CC, Wang CX, Pittman B, Yang YM, Schwartz JE, Tian D, et al. Phenethyl Isothiocyanate and Sulforaphane and their *N* -Acetylcysteine Conjugates Inhibit Malignant Progression of Lung Adenomas Induced by Tobacco Carcinogens in A/J Mice. Cancer Research. 2005 Sep 15;65(18):8548–57.

132. Joseph MA, Moysich KB, Freudenheim JL, Shields PG, Bowman ED, Zhang Y, et al. Cruciferous Vegetables, Genetic Polymorphisms in Glutathione S-Transferases M1 and T1, and Prostate Cancer Risk. Nutrition and Cancer. 2004 Nov;50(2):206–13.

133. Ambrosone CB, McCann SE, Freudenheim JL, Marshall JR, Zhang Y, Shields PG. Breast Cancer Risk in Premenopausal Women Is Inversely Associated with Consumption of Broccoli, a Source of Isothiocyanates, but Is Not Modified by GST Genotype. The Journal of Nutrition. 2004 Oct 1;134(5):1134–8.

134. Seow A. Dietary isothiocyanates, glutathione S-transferase polymorphisms and colorectal cancer risk in the Singapore Chinese Health Study. Carcinogenesis. 2002 Dec 1;23(12):2055–61.

135. Spitz MR, Duphorne CM, Detry MA, Pillow PC, Amos CI, Lei L, et al. Dietary intake of isothiocyanates: evidence of a joint effect with glutathione S-transferase polymorphisms in lung cancer risk. Cancer Epidemiol Biomarkers Prev. 2000 Oct;9(10):1017–20.

136. Chen X, Jiang Z, Zhou C, Chen K, Li X, Wang Z, et al. Activation of Nrf2 by Sulforaphane Inhibits High Glucose-Induced Progression of Pancreatic Cancer via AMPK Dependent Signaling. Cellular Physiology and Biochemistry. 2018;50(3):1201–15.

137. Kong B, Qia C, Erkan M, Kleeff J, Michalski CW. Overview on how oncogenic Kras promotes pancreatic carcinogenesis by inducing low intracellular ROS levels. Frontiers in Physiology. 2013;4.

138. Thimmulappa R, Rangasamy T, Alam J, Biswal S. Dibenzoylmethane Activates Nrf2-Dependent Detoxification Pathway and Inhibits Benzo(a)pyrene Induced DNA Adducts in Lungs. Medicinal Chemistry. 2008 Sep 1;4(5):473–81.

139. Garg R, Gupta S, Maru GB. Dietary curcumin modulates transcriptional regulators of phase I and phase II enzymes in benzo[a]pyrene-treated mice: mechanism of its anti-initiating action. Carcinogenesis. 2008 May;29(5):1022–32.

140. Wakabayashi N, Dinkova-Kostova AT, Holtzclaw WD, Kang MI, Kobayashi A, Yamamoto M, et al. Protection against electrophile and oxidant stress by induction of the phase 2 response: Fate of cysteines of the Keap1 sensor modified by inducers. Proceedings of the National Academy of Sciences. 2004 Feb 17;101(7):2040–5.

141. Phillips J, Fox R. BG-12 in Multiple Sclerosis. Seminars in Neurology. 2013 May 25;33(01):056–65.

142. Ren D, Villeneuve NF, Jiang T, Wu T, Lau A, Toppin HA, et al. Brusatol enhances the efficacy of chemotherapy by inhibiting the Nrf2-mediated defense mechanism. Proceedings of the National Academy of Sciences. 2011 Jan 25;108(4):1433–8.

143. Gao AM, Zhang XY, Ke ZP. Apigenin sensitizes BEL-7402/ADM cells to doxorubicin through inhibiting miR-101/Nrf2 pathway. Oncotarget. 2017 Oct 10;8(47):82085–91.

144. Gambardella V, Gimeno-Valiente F, Tarazona N, Ciarpaglini CM, Roda D, Fleitas T, et al. NRF2 through RPS6 Activation Is Related to Anti-HER2 Drug Resistance in *HER2* -Amplified Gastric Cancer. Clinical Cancer Research. 2019 Mar 1;25(5):1639–49.

145. El-Naggar AM, Somasekharan SP, Wang Y, Cheng H, Negri GL, Pan M, et al. Class I <scp>HDAC</scp> inhibitors enhance <scp>YB</scp> -1 acetylation and oxidative stress to block sarcoma metastasis. EMBO Rep. 2019 Dec 5;20(12).

146. DUONG HQ, YI YW, KANG HJ, HONG Y bin, TANG W, WANG A, et al. Inhibition of NRF2 by PIK-75 augments sensitivity of pancreatic cancer cells to gemcitabine. International Journal of Oncology. 2014 Mar;44(3):959–69.

147. Lee J, Kang JS, Nam LB, Yoo OK, Keum YS. Suppression of NRF2/ARE by convallatoxin sensitises A549 cells to 5-FU-mediated apoptosis. Free Radical Research. 2018 Dec 2;52(11–12):1416–23.

148. Tang X, Wang H, Fan L, Wu X, Xin A, Ren H, et al. Luteolin inhibits Nrf2 leading to negative regulation of the Nrf2/ARE pathway and sensitization of human lung carcinoma A549 cells to therapeutic drugs. Free Radical Biology and Medicine. 2011 Jun;50(11):1599–609.

149. Singh A, Venkannagari S, Oh KH, Zhang YQ, Rohde JM, Liu L, et al. Small Molecule Inhibitor of NRF2 Selectively Intervenes Therapeutic Resistance in KEAP1-Deficient NSCLC Tumors. ACS Chemical Biology. 2016 Nov 18;11(11):3214–25.

150. Wang XJ, Hayes JD, Henderson CJ, Wolf CR. Identification of retinoic acid as an inhibitor of transcription factor Nrf2 through activation of retinoic acid receptor alpha. Proceedings of the National Academy of Sciences. 2007 Dec 4;104(49):19589–94.

151. Valenzuela M, Glorieux C, Stockis J, Sid B, Sandoval JM, Felipe KB, et al. Retinoic acid synergizes ATO-mediated cytotoxicity by precluding Nrf2 activity in AML cells. British Journal of Cancer. 2014;111(5):874–82.

152. Suzuki K, Bose P, Leong-Quong RY, Fujita DJ, Riabowol K. REAP: A two minute cell fractionation method. BMC Research Notes. 2010 Dec 10;3(1):294.

153. Bolger AM, Lohse M, Usadel B. Trimmomatic: A flexible trimmer for Illumina sequence data. Bioinformatics [Internet]. 2014 Aug 1 [cited 2021 May 4];30(15):2114–20. Available from: https://pubmed.ncbi.nlm.nih.gov/24695404/

154. Law WD, Warren RL, McCallion AS. Establishment of an eHAP1 human haploid cell line hybrid reference genome assembled from short and long reads. Genomics. 2020 May 1;112(3):2379–84.

155. Kim D, Paggi JM, Park C, Bennett C, Salzberg SL. Graph-based genome alignment and genotyping with HISAT2 and HISAT-genotype. Nature Biotechnology [Internet]. 2019 Aug 1 [cited 2021 May 4];37(8):907–15. Available from: https://pubmed.ncbi.nlm.nih.gov/31375807/

156. Li H, Handsaker B, Wysoker A, Fennell T, Ruan J, Homer N, et al. The Sequence Alignment/Map format and SAMtools. Bioinformatics [Internet]. 2009 Aug 15 [cited 2021 May 4];25(16):2078–9. Available from: https://academic.oup.com/bioinformatics/article-lookup/doi/10.1093/bioinformatics/btp352

157. R Core Team (2020). — European Environment Agency [Internet]. [cited 2021 May 4]. Available from: https://www.eea.europa.eu/data-and-maps/indicators/oxygen-consuming-substances-in-rivers/r-development-core-team-2006

158. Pertea M, Kim D, Pertea GM, Leek JT, Salzberg SL. Transcript-level expression analysis of RNA-seq experiments with HISAT, StringTie and Ballgown. Nature Protocols [Internet]. 2016 Sep 1 [cited 2021 May 4];11(9):1650–67. Available from: https://www.nature.com/articles/nprot.2016.095

159. Thorvaldsdóttir H, Robinson JT, Mesirov JP. Integrative Genomics Viewer (IGV): High-performance genomics data visualization and exploration. Briefings in Bioinformatics [Internet]. 2013 Mar [cited 2021 May 4];14(2):178–92. Available from: https://pubmed.ncbi.nlm.nih.gov/22517427/

160. Vidal-Petiot E, Cheval L, Faugeroux J, Malard T, Doucet A, Jeunemaitre X, et al. A New Methodology for Quantification of Alternatively Spliced Exons Reveals a Highly Tissue-Specific Expression Pattern of WNK1 Isoforms. PLoS ONE. 2012 May 31;7(5):e37751.

161. Yang J, Yan R, Roy A, Xu D, Poisson J, Zhang Y. The I-TASSER Suite: protein structure and function prediction. Nature Methods. 2015 Jan 30;12(1):7–8.

162. Zheng W, Li Y, Zhang C, Pearce R, Mortuza SM, Zhang Y. Deep-learning contact-map guided protein structure prediction in CASP13. Proteins: Structure, Function, and Bioinformatics. 2019 Dec 14;87(12):1149–64.

163. Vos SM, Farnung L, Linden A, Urlaub H, Cramer P. Structure of complete Pol II–DSIF–PAF–SPT6 transcription complex reveals RTF1 allosteric activation. Nature Structural & Molecular Biology. 2020 Jul 15;27(7):668–77.

164. Brooks BR, Brooks CL, Mackerell AD, Nilsson L, Petrella RJ, Roux B, et al. CHARMM: The biomolecular simulation program. Journal of Computational Chemistry. 2009 Jul 30;30(10):1545–614.

165. Chemical Computing Group. Molecular Operating Environment (MOE) 2011.10. Montreal, Quebec, Canada; 2011.

166. Lo SC, Li X, Henzl MT, Beamer LJ, Hannink M. Structure of the Keap1:Nrf2 interface provides mechanistic insight into Nrf2 signaling. The EMBO Journal. 2006 Aug 9;25(15):3605–17.

167. Hörer S, Reinert D, Ostmann K, Hoevels Y, Nar H. Crystal-contact engineering to obtain a crystal form of the Kelch domain of human Keap1 suitable for ligand-soaking experiments. Acta Crystallographica Section F Structural Biology and Crystallization Communications. 2013 Jun 1;69(6):592–6.

168. Pronk S, Páll S, Schulz R, Larsson P, Bjelkmar P, Apostolov R, et al. GROMACS 4.5: a high-throughput and highly parallel open source molecular simulation toolkit. Bioinformatics. 2013 Apr 1;29(7):845–54.

169. Bjelkmar P, Larsson P, Cuendet MA, Hess B, Lindahl E. Implementation of the CHARMM Force Field in GROMACS: Analysis of Protein Stability Effects from Correction Maps, Virtual Interaction Sites, and Water Models. Journal of Chemical Theory and Computation. 2010 Feb 9;6(2):459–66.

170. Padariya M, Fahraeus R, Hupp T, Kalathiya U. Molecular Determinants and Specificity of mRNA with Alternatively-Spliced UPF1 Isoforms, Influenced by an Insertion in the 'Regulatory Loop.' International Journal of Molecular Sciences. 2021 Nov 25;22(23):12744.

171. Berendsen HJC, Postma JPM, van Gunsteren WF, Hermans J. Interaction Models for Water in Relation to Protein Hydration. In 1981. p. 331–42.

172. Darden T, York D, Pedersen L. Particle mesh Ewald: An *N* ·log(*N*) method for Ewald sums in large systems. The Journal of Chemical Physics. 1993 Jun 15;98(12):10089–92.

173. Bussi G, Donadio D, Parrinello M. Canonical sampling through velocity rescaling. The Journal of Chemical Physics. 2007 Jan 7;126(1):014101.

174. Parrinello M, Rahman A. Polymorphic transitions in single crystals: A new molecular dynamics method. Journal of Applied Physics. 1981 Dec;52(12):7182–90.

175. van Gunsteren WF, Berendsen HJC. A Leap-frog Algorithm for Stochastic Dynamics. Molecular Simulation. 1988 Mar 3;1(3):173–85.

176. Humphrey W, Dalke A, Schulten K. VMD: Visual molecular dynamics. Journal of Molecular Graphics. 1996 Feb;14(1):33–8.

177. Chaikovsky AC, Sage J. Beyond the cell cycle: Enhancing the immune surveillance of tumors via CDK4/6 inhibition. Molecular Cancer Research. 2018;16(10):1454–7.

178. Goel S, Decristo MJ, Watt AC, Brinjones H, Sceneay J, Li BB, et al. CDK4/6 inhibition triggers anti-tumour immunity. Nature [Internet]. 2017;548(7668):471–5. Available from: http://dx.doi.org/10.1038/nature23465

179. Peng KJ, Wang JH, Su WT, Wang XC, Yang FT, Nie WH. Characterization of two human lung adenocarcinoma cell lines by reciprocal chromosome painting. Dong wu xue yan jiu = Zoological research / “Dong wu xue yan jiu” bian ji wei yuan hui bian ji. 2010 Apr;31(2):113–21.

180. Bialk P, Wang Y, Banas K, Kmiec EB. Functional Gene Knockout of NRF2 Increases Chemosensitivity of Human Lung Cancer A549 Cells in Vitro and in a Xenograft Mouse Model. Molecular Therapy - Oncolytics. 2018;11(December):75–89.

181. Homma S, Ishii Y, Morishima Y, Yamadori T, Matsuno Y, Haraguchi N, et al. Nrf2 Enhances Cell Proliferation and Resistance to Anticancer Drugs in Human Lung Cancer. Clinical Cancer Research. 2009 May 15;15(10):3423–32.

182. Makhadiyeva D, Lam L, Moatari M, Vallance J, Zheng Y, Campbell EC, et al. MHC class I dimer formation by alteration of the cellular redox environment and induction of apoptosis. Immunology. 2012 Feb 11;135(2):133–9.

183. Carlini F, Ferreira V, Buhler S, Tous A, Eliaou JF, René C, et al. Association of HLA-A and Non-Classical HLA Class I Alleles. PLOS ONE. 2016 Oct 4;11(10):e0163570.

184. Bardi MS, Jarduli LR, Jorge AJ, Camargo RBOG, Carneiro FP, Gelinski JR, et al. HLA-A, B and DRB1 allele and haplotype frequencies in volunteer bone marrow donors from the north of Parana State. Revista Brasileira de Hematologia e Hemoterapia. 2011;34(1):25–30.

185. Kwak MK, Itoh K, Yamamoto M, Kensler TW. Enhanced Expression of the Transcription Factor Nrf2 by Cancer Chemopreventive Agents: Role of Antioxidant Response Element-Like Sequences in the *nrf2* Promoter. Molecular and Cellular Biology. 2002 May;22(9):2883–92.

186. Wijdeven RH, van Luijn MM, Wierenga-Wolf AF, Akkermans JJ, van den Elsen PJ, Hintzen RQ, et al. Chemical and genetic control of IFNγ-induced MHCII expression. EMBO Rep. 2018;19(9):e45553.

187. Wong W, Bai X chen, Brown A, Fernandez IS, Hanssen E, Condron M, et al. Cryo-EM structure of the Plasmodium falciparum 80S ribosome bound to the anti-protozoan drug emetine. Elife. 2014 Jun 9;3.

188. Chan C, Martin P, Liptrott NJ, Siccardi M, Almond L, Owen A. Incompatibility of chemical protein synthesis inhibitors with accurate measurement of extended protein degradation rates. Pharmacology Research & Perspectives. 2017 Oct;5(5):e00359.

189. Akinboye ES, Bakare O. Biological Activities of Emetine. The Open Natural Products Journal. 2011.

190. HU VW, HEIKKA DS. Radiolabeling revisited: metabolic labeling with ^{35} S-methionine inhibits cell cycle progression, proliferation, and survival. The FASEB Journal. 2000 Mar;14(3):448–54.

191. Hu VW, Heikka DS, Dieffenbach PB, Ha U. Metabolic radiolabeling: experimental tool or Trojan horse? ^{35} S-Methionine induces DNA fragmentation and p53-dependent ROS production. The FASEB Journal. 2001 Jul;15(9):1562–8.

192. Morey TM, Esmaeili MA, Duennwald ML, Rylett RJ. SPAAC Pulse-Chase: A Novel Click Chemistry-Based Method to Determine the Half-Life of Cellular Proteins. Frontiers in Cell and Developmental Biology. 2021 Sep 7;9.

193. Dieterich DC, Link AJ, Graumann J, Tirrell DA, Schuman EM. Selective identification of newly synthesized proteins in mammalian cells using bioorthogonal noncanonical amino acid tagging (BONCAT). Proceedings of the National Academy of Sciences. 2006 Jun 20;103(25):9482–7.

194. Cane G, Leuchowius K, Soderberg O, Kamali-Moghaddam M, Jarvius M, Helbing I, et al. Protein Diagnostics by Proximity Ligation: Combining Multiple Recognition and DNA Amplification for Improved Protein Analyses. In: Molecular Diagnostics (Third Edition). 2017. p. 219–31.

195. Alam MS. Proximity Ligation Assay (PLA). Current Protocols in Immunology. 2018 Nov;123(1):e58.

196. Aier I, Varadwaj PK, Raj U. Structural insights into conformational stability of both wild-type and mutant EZH2 receptor. Scientific Reports. 2016 Dec 7;6(1):34984.

197. Pi J, Bai Y, Reece JM, Williams J, Liu D, Freeman ML, et al. Molecular mechanism of human Nrf2 activation and degradation: Role of sequential phosphorylation by protein kinase CK2. Free Radical Biology and Medicine. 2007 Jun;42(12):1797–806.

198. Apopa PL, He X, Ma Q. Phosphorylation of Nrf2 in the transcription activation domain by casein kinase 2 (CK2) is critical for the nuclear translocation and transcription activation function of Nrf2 in IMR-32 neuroblastoma cells. Journal of Biochemical and Molecular Toxicology. 2008;22(1):63–76.

199. Torrente L, Sanchez C, Moreno R, Chowdhry S, Cabello P, Isono K, et al. Crosstalk between NRF2 and HIPK2 shapes cytoprotective responses. Oncogene. 2017 Nov 10;36(44):6204–12.

200. Mikac S, Rychłowski M, Dziadosz A, Szabelska-beresewicz A, Fahraeus R, Hupp T, et al. Identification of a Stable , Non-Canonically Regulated Nrf2 Form in Lung Cancer Cells. 2021;

201. Ozaki S. Hybridomas, T Cell. In: Encyclopedia of Immunology. Elsevier; 1998. p. 1152–4.

202. Itoh K, Wakabayashi N, Katoh Y, Ishii T, O'Connor T, Yamamoto M. Keap1 regulates both cytoplasmic-nuclear shuttling and degradation of Nrf2 in response to electrophiles. Genes to Cells. 2003;8(4):379–91.

203. McMahon M, Itoh K, Yamamoto M, Hayes JD. Keap1-dependent proteasomal degradation of transcription factor Nrf2 contributes to the negative regulation of antioxidant response element-driven gene expression. Journal of Biological Chemistry [Internet]. 2003;278(24):21592–600. Available from: http://dx.doi.org/10.1074/jbc.M300931200

204. Stewart D, Killeen E, Naquin R, Alam S, Alam J. Degradation of transcription factor Nrf2 via the ubiquitin-proteasome pathway and stabilization by cadmium. Journal of Biological Chemistry [Internet]. 2003;278(4):2396–402. Available from: http://dx.doi.org/10.1074/jbc.M209195200

205. Sanghvi VR, Leibold J, Mina M, Mohan P, Berishaj M, Li Z, et al. The Oncogenic Action of NRF2 Depends on De-glycation by Fructosamine-3-Kinase. Cell. 2019 Aug;178(4):807-819.e21.

206. Otsuki A, Okamura Y, Aoki Y, Ishida N, Kumada K, Minegishi N, et al. Identification of Dominant Transcripts in Oxidative Stress Response by a Full-Length Transcriptome Analysis. Molecular and Cellular Biology. 2021 Jan 25;41(2).

207. Kalsotra A, Cooper TA. Functional consequences of developmentally regulated alternative splicing. Nature Reviews Genetics. 2011 Oct 16;12(10):715–29.

208. Minegishi N, Ohta J, Suwabe N, Nakauchi H, Ishihara H, Hayashi N, et al. Alternative Promoters Regulate Transcription of the Mouse GATA-2 Gene. Journal of Biological Chemistry. 1998 Feb;273(6):3625–34.

209. Ito E, Toki T, Ishihara H, Ohtani H, Gu L, Yokoyama M, et al. Erythroid transcription factor GATA-1 is abundantly transcribed in mouse testis. Nature. 1993 Apr;362(6419):466–8.

210. Frankish A, Diekhans M, Ferreira AM, Johnson R, Jungreis I, Loveland J, et al. GENCODE reference annotation for the human and mouse genomes. Nucleic Acids Research. 2019 Jan 8;47(D1):D766–73.

211. Wang ET, Sandberg R, Luo S, Khrebtukova I, Zhang L, Mayr C, et al. Alternative isoform regulation in human tissue transcriptomes. Nature. 2008 Nov 27;456(7221):470–6.

212. Carninci P, Sandelin A, Lenhard B, Katayama S, Shimokawa K, Ponjavic J, et al. Genome-wide analysis of mammalian promoter architecture and evolution. Nature Genetics. 2006 Jun 1;38(6):626–35.

213. An integrated encyclopedia of DNA elements in the human genome. Nature. 2012 Sep 5;489(7414):57–74.

214. Lan H, Tang Z, Jin H, Sun Y. Neddylation inhibitor MLN4924 suppresses growth and migration of human gastric cancer cells. Scientific Reports. 2016;6:1–12.

215. Tong S, Si Y, Yu H, Zhang L, Xie P, Jiang W. MLN4924 (Pevonedistat), a protein neddylation inhibitor, suppresses proliferation and migration of human clear cell renal cell carcinoma. Scientific Reports. 2017;7(1):1–9.

216. Imhoff BR, Hansen JM. Tert-butylhydroquinone induces mitochondrial oxidative stress causing Nrf2 activation. Cell Biology and Toxicology. 2010 Dec;26(6):541–51.

217. Kobayashi M, Li L, Iwamoto N, Nakajima-Takagi Y, Kaneko H, Nakayama Y, et al. The Antioxidant Defense System Keap1-Nrf2 Comprises a Multiple Sensing Mechanism for Responding to a Wide Range of Chemical Compounds. Molecular and Cellular Biology. 2009 Jan 15;29(2):493–502.

218. Ahlgren-Beckendorf JA, Reising AM, Schander MA, Herdler JW, Johnson JA. Coordinate regulation of NAD(P)H:Quinone oxidoreductase and glutathione-S-transferases in primary cultures of rat neurons and glia: Role of the antioxidant/electrophile responsive element. Glia. 1999 Jan 15;25(2):131–42.

219. Li W, Jain MR, Chen C, Yue X, Hebbar V, Zhou R, et al. Nrf2 Possesses a Redox-insensitive Nuclear Export Signal Overlapping with the Leucine Zipper Motif. Journal of Biological Chemistry. 2005 Aug;280(31):28430–8.

220. Theodore M, Kawai Y, Yang J, Kleshchenko Y, Reddy SP, Villalta F, et al. Multiple Nuclear Localization Signals Function in the Nuclear Import of the Transcription Factor Nrf2. Journal of Biological Chemistry. 2008 Apr;283(14):8984–94.

221. Yamasaki S, Yagishita N, Sasaki T, Nakazawa M, Kato Y, Yamadera T, et al. Cytoplasmic destruction of p53 by the endoplasmic reticulum-resident ubiquitin ligase 'Synoviolin.' The EMBO Journal. 2007 Jan 10;26(1):113–22.

222. Gao B, Lee S, Chen A, Zhang J, Zhang DD, Kannan K, et al. Synoviolin promotes IRE1 ubiquitination and degradation in synovial fibroblasts from mice with collagen-induced arthritis. EMBO Rep. 2008 May 28;9(5):480–5.

223. Tsuchiya Y, Morita T, Kim M, Iemura S ichiro, Natsume T, Yamamoto M, et al. Dual Regulation of the Transcriptional Activity of Nrf1 by β-TrCP- and Hrd1-Dependent Degradation Mechanisms. Molecular and Cellular Biology. 2011 Nov 15;31(22):4500–12.

224. Murray-Zmijewski F, Lane DP, Bourdon JC. p53/p63/p73 isoforms: an orchestra of isoforms to harmonise cell differentiation and response to stress. Cell Death & Differentiation. 2006 Jun 7;13(6):962–72.

225. Grob TJ, Novak U, Maisse C, Barcaroli D, Lüthi AU, Pirnia F, et al. Human ΔNp73 regulates a dominant negative feedback loop for TAp73 and p53. Cell Death & Differentiation. 2001 Dec 6;8(12):1213–23.

Appendices

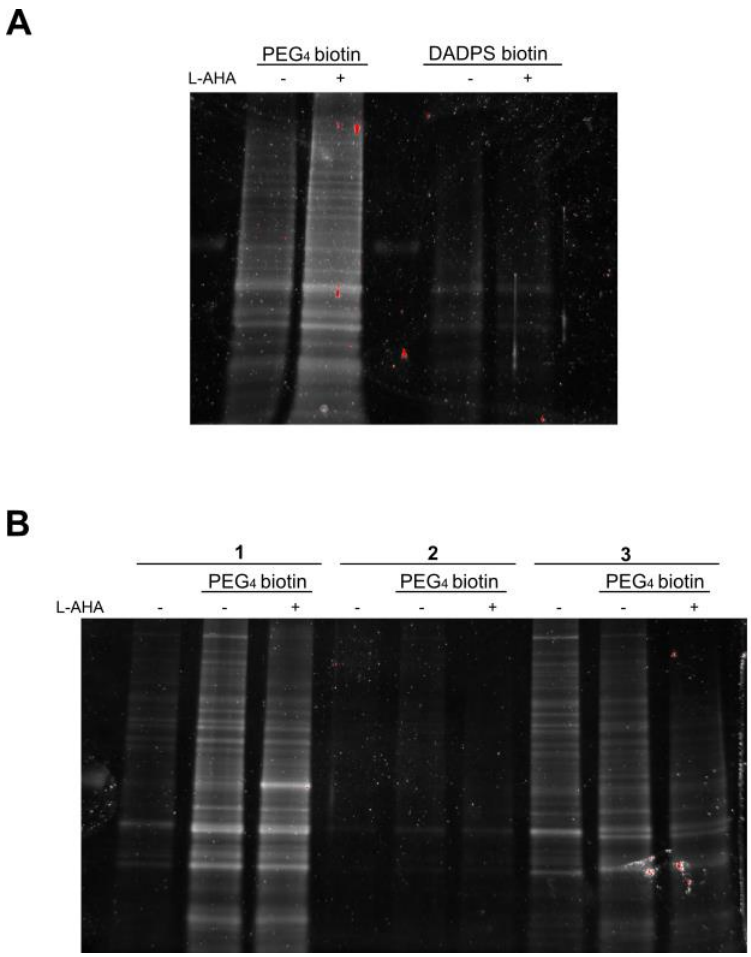

Figure S1. **Click-iT labeling of newly synthesized proteins with biotin and pull-down with streptavidin magnetic beads.** (A) L-AHA (50 µM, 1 hour) was added to the A549 living cells. After 1 hours of incubation, cells were lysed and biotin was added to the samples, together with the components of Click-it labeling kit (Thermo Fisher Scientific). We used two types of biotin: 1) Acetylene-PEG_4-biotin (500 µM) and 2) DADPS biotin - with cleavable DADPS linker (300 µM). After protein precipitation, streptavidin pull-down of biotin-labeled proteins was performed, proteins were eluted, stained with Flamingo stain and and visualized by UV fluorescence. Control sample was only biotin added to the samples containing cells that did not have incorporated L-AHA. (B) L-AHA (50 µM, 1 hour) was added to the A549 living cells. After 1 hours of incubation, cells were lysed and PEG_4 biotin was added to the samples, together with the components of Click-it labeling kit (Thermo Fisher Scientific). After protein precipitation, streptavidin pull-down of biotin-labeled proteins was performed with three different washing procedures: 1) 2 times wash with 0.1% SDS in PBS and 1 wash with 6 M urea; 2) all three times wash with 1% SDS in PBS; 3) all three times wash with 0.1% SDS in PBS + 150 mM NaCl. Next, proteins were eluted, stained with Flamingo stain and visualized by UV fluorescence.

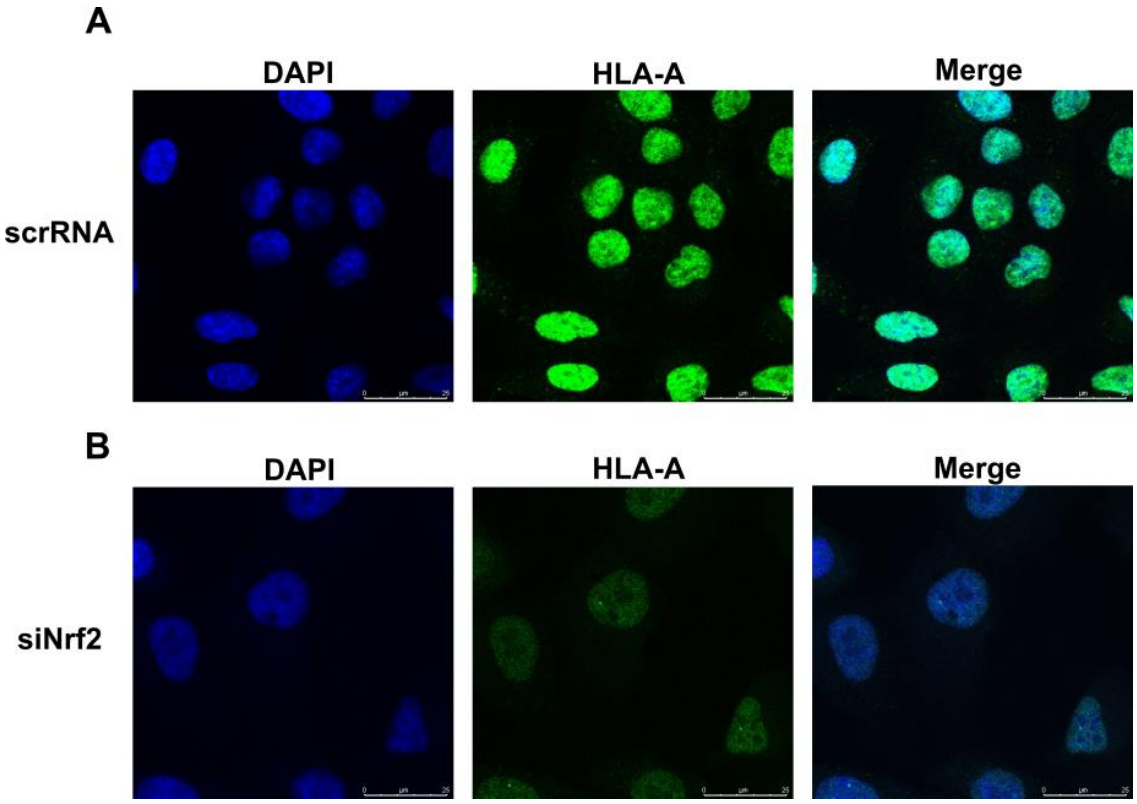

Figure S2. **HLA-A is mainly localized in the nucleus in A549 cell line.** (A) Immunofluorescent staining after transfection of A549 cells with scrRNA (10 nM) for 48 hours, used as a control for transfection. HLA-A was detected with anti-HLA-A (cat. no. ab52922; Abcam) antibodies. Nuclei were stained with DAPI. (B) Immunofluorescent staining after HLA-A knockdown with the HLA-A siRNA (10 nM) for 48 hours in A549 cells. HLA-A was detected with anti-HLA-A (cat. no. ab52922; Abcam) antibodies. Nuclei were stained with DAPI. Specimens were visualized by confocal microscope.

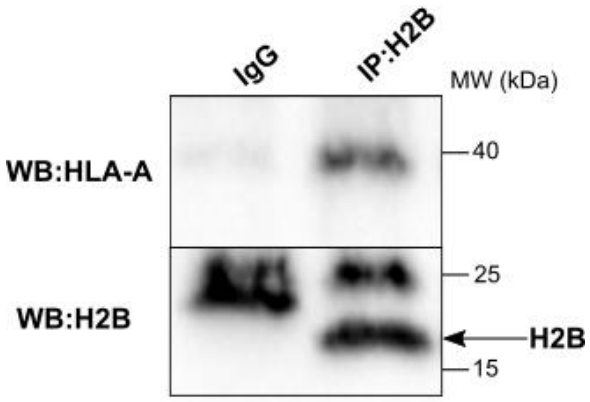

Figure S3**. HLA-A and histone H2B are co-immunoprecipitating in RERF-LC-AI cell line.** Co-immunoprecipitation of histone (H2B) and western blot detection of HLA-A in RERF-LC-AI cell line. IgG

mouse was used as a control. The light chains of IgG are detected at molecular weight around 25 kDa. Arrow indicates precipitated H2B.

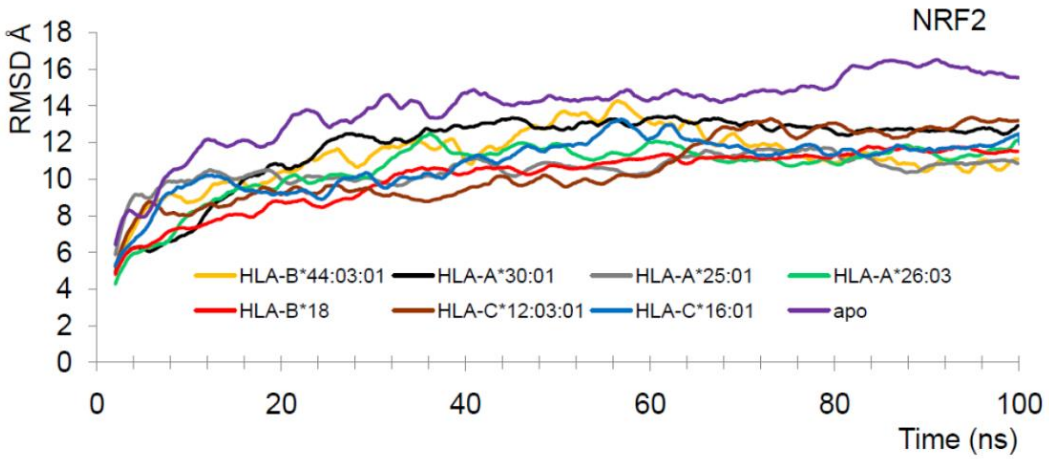

Figure S4. **Stability check for Nrf2 with/without HLA class I molecules.** In order to check the stability of Nrf2 with/without HLA molecules, the RMSDs (root-mean-square deviations) were computed. RMSD calculations are usually used for measuring the difference between the backbones of a protein from its initial structural conformation to its final position. The stability of the protein relative to its conformation can be determined by the deviations produced during the course of its simulation. A RMSD value is expressed in Ångström (Å) which is equal to 10^{-10} m. Nrf2 apo-form is found to be highly flexible and destabilized, while the presence of HLA class I molecules stabilizes Nrf2 protein.

Table S1. Expression of Nrf2 isoform and loading control (β actin) in H1299 cell line after treatment with translation elongation inhibitor, emetine dihydrochloride (20 μM), at different time points (15 min, 2 and 4 hours).

Time points [h]	Nrf2 isoform signal	Loading control signal	Normalization (sample/loading control)	Normalization (sample/control sample)
0	8321.104	10283.25	0.8092	1
0.25	7008.054	7940.004	0.8826	1.0908
2	9036.004	15087.22	0.5989	0.7401
4	0	18733.02	0	0

Half-life of Nrf2 isoform (best-fit value): 2.067 hours

Table S2. Expression of Nrf2 isoform and loading control (β actin) in NSCLC 1[1] after treatment with translation elongation inhibitor, emetine dihydrochloride (20 μM), at different time points (15 min, 2 and 4 hours).

Time points [h]	Nrf2 isoform signal	Loading control signal	Normalization (sample/loading control)	Normalization (sample/control sample)
0	9476.347	17315.116	0.5473	1
0.25	6238.69	21434.551	0.2911	0.5318
2	4603.861	21916.622	0.2101	0.3838
4	5730.418	23930.986	0.2395	0.4375

Half-life of Nrf2 isoform (best-fit value): 1.936 hours

Table S3. Expression of Nrf2 isoform and loading control (β actin) in NSCLC 2[2] after treatment with translation elongation inhibitor, emetine dihydrochloride (20 μM), at different time points (15 min, 2 and 4 hours).

Time points [h]	Nrf2 isoform signal	Loading control signal	Normalization (sample/loading control)	Normalization (sample/control sample)
0	11203.52	12061	0.9289	1
0.25	5413.104	13628.49	0.3972	0.4276
2	3536.276	14047.49	0.2517	0.2710
4	4129.154	23391.89	0.1765	0.1900

Half-life of Nrf2 isoform (best-fit value): 0.2075 hours

[1] Cells derived from patient (1) with non-small cell lung cancer.
[2] Cells derived from patient (2) with non-small cell lung cancer.

Scientific accomplishments

Publications

Mikac S., Rychłowski M., Dziadosz A., Szabelska-Beresewicz A., Fahraeus R., Hupp T., Sznarkowska A. Identification of a Stable, Non-Canonically Regulated Nrf2 Form in Lung Cancer Cells. Antioxidants 2021; 10(5): 786.

Mikac S., Dziadosz A., Padariya M., Kalathiya U., Fahraeus R., Marek-Trzonkowska N., Chruściel E., Urban-Wójciuk Z., Papak I., Arcimowicz Ł., Marjanski T., Rzyman W., Sznarkowska A. Keap1-resistant ΔN-Nrf2 isoform does not translocate to the nucleus upon electrophilic stress (submitted; preprint https://doi.org/10.1101/2022.06.10.495609)

Padariya M., Sznarkowska A., Kote S., Gómez-Herranz M., **Mikac S.**, Pilch M., Alfaro J., Fahraeus R., Hupp T., Kalathiya U. Functional Interfaces, Biological Pathways, and Regulations of Interferon-Related DNA Damage Resistance Signature (IRDS) Genes. Biomolecules 2021; 11(5): 622.

Padariya M., Kalathiya U., **Mikac S.**, Dziubek K., Tovar Fernandez MC., Sroka E., Fahraeus R., Sznarkowska A. Viruses, cancer and non-self recognition. Open Biology 2021; 11(3): 200348.

Sznarkowska A., **Mikac S.**, Pilch M. MHC Class I Regulation: The Origin Perspective. Cancers 2020; 12(5): 1155-1178.

Conferences

Mikac S., Fahraeus R., Sznarkowska A. Nrf2 role in immune surveillance. 9th Intercollegiate Biotechnology Symposium "Symbioza", Warsaw University of Technology, 2021 (oral presentation)

Mikac S., Sznarkowska A., Fahraeus R. MHC class I regulation in response to dsRNA stress. EMBO Workshop-Antigen Processing and Presentation (APP 10), Paris, France, 2019 (poster presentation)

Sznarkowska A., **Mikac S.**, Fahraeus R. Nrf2 in non-small cell lung cancer: potential role in immune surveillance. 11th International Conference of Contemporary Oncology, Poznan, Poland, 2019 (poster presentation)

Mikac S., Sznarkowska A., Fahraeus R. Nrf2 role in immune surveillance. ScanBalt Forum-Molecular Biology and Immunology of Cancer-R&D Perspectives, Gdansk, Poland, 2019 (poster presentation)